SLIDING MODE CONTROLLER – OBSERVER FOR UNCERTAIN DYNAMICAL SYSTEMS

A Thesis submitted to

Savitribai Phule Pune University
(formerly University of Pune)

for the award of Degree of

DOCTOR OF PHILOSOPHY (Ph.D)
in the Faculty of Engineering
(Instrumentation & Control Engg.)

Submitted by

Prasheel V. Suryawanshi
(MIS No. : 131109003)

Under the Guidance of

Prof. Pramod D. Shendge

Department of Instrumentation & Control Engg.
College of Engineering, Pune (COEP)
(An Autonomous Institute of Govt. of Maharashtra)

December 2015

Certificate

This is to certify that the thesis entitled **"Sliding Mode Controller – Observer for Uncertain Dynamical Systems"** is a bonafide record of the research work carried out by **Prasheel V. Suryawanshi** (MIS No. 131109003), at Department of Instrumentation & Control Engineering, College of Engineering, Pune (COEP) under the supervision and guidance of **Prof. Pramod D. Shendge**.

The results embodied in this thesis have not been submitted to any other institute or university for the award of any degree or diploma.

The thesis is submitted in partial fulfilment of the requirements for the award of degree of Doctor of Philosophy (PhD) in Instrumentation & Control Engineering of Savitribai Phule Pune University (formerly University of Pune).

Prof. Pramod D. Shendge
Research Guide

Prof. C. Y. Patil
Head of Department

Prof. B. B. Ahuja
Officiating Director

Certificate of Guide

This is to certify that the work incorporated in this thesis, entitled **“Sliding Mode Controller – Observer for Uncertain Dynamical Systems”** submitted by **Prasheel V. Suryawanshi** (MIS No. 131109003), is carried out by the candidate at Advanced Control Lab. of Department of Instrumentation & Control Engg., College of Engineering, Pune (COEP), under my supervision and guidance.

Such material as has been obtained from other sources has been acknowledged duly in this thesis.

Prof. Pramod D. Shendge
Research Guide

Declaration

This is to declare that the thesis entitled **"Sliding Mode Controller – Observer for Uncertain Dynamical Systems"** submitted by me for the award of degree of Doctor of Philosophy (PhD) in Instrumentation & Control Engineering; is the record of work carried out by me at College of Engineering, Pune (COEP).

The said work is carried out during the period 30/09/2011 to 31/08/2015 under the guidance of **Prof. Pramod D. Shendge** and has not formed the basis for the award of any degree, diploma, associateship, fellowship, titles in this or any other university or other institution of higher learning.

I further declare that the material obtained from other sources has been duly acknowledged in the thesis.

Prasheel V. Suryawanshi
(MIS No. 131109003)

Abstract

The control of systems with uncertainties and disturbances is an interesting and challenging problem in control engineering. The problem is further complicated when uncertainties and disturbances are mismatched i.e. act in channels where there is no control input. Further all states of the system are not available for measurement. Modern controllers are implemented using discrete hardware for which, it is necessary to design discrete controllers.

Sliding mode control is an elegant technique for controlling systems, affected by the matched uncertainties and disturbances. The control action in conventional sliding mode is discontinuous, which affects the performance adversely. Further, the control also requires full state vector for implementation. This thesis proposes a combination of sliding mode control with uncertainty estimation techniques to reduce the magnitude of discontinuous component. This enables mitigation of unfavorable effects of chatter, excitation of unmodeled dynamics, and wear and tear of actuators. A sliding mode control with observer to estimate states and uncertainties is designed for linear, nonlinear, matched and unmatched systems.

The estimation techniques used here are the uncertainty and disturbance estimator, the equivalent input disturbance and the disturbance observer. An uncertainty and disturbance estimator is combined with sliding mode control for ameliorating the effects of chatter in conventional sliding mode control. The control scheme uses uncertainty and disturbance estimator based control for a smooth approximation inside the boundary layer. A robust sliding mode control strategy for a class of uncertain system, where control appears through a nonlinear function is proposed for the first time. The control is synthesized by estimating states and uncertainties using uncertainty and disturbance estimation techniques.

A method called as equivalent input disturbance is proposed in the literature for mismatched systems. The control logic in this approach usually employs integral action bringing in also its disadvantages. The problem is resolved in this work by combining equivalent input disturbance with sliding mode control. The capability of conventional equivalent input disturbance is extended so as to estimate the derivatives of equivalent input disturbance. Such an equivalent input disturbance with a higher-order filter combined with sliding mode control is proposed here for the first time. The theory is generalized to a filter of arbitrary order. The equivalent input disturbance method is further extended for use with disturbance observer for estimation. This theory is also generalized for disturbance observer of any order.

The sliding mode control reported in the literature is designed and analyzed in continuous-time domain. The actual implementation of control strategies on the other hand, is invariably realized using digital hardware like microcontrollers or DSPs . The discrete implementation of sliding mode control requires complete redesign of the controller. A discrete-time unified sliding mode control using UDE is proposed in this thesis for uncertain systems. The proposed observer-controller combination reduces the quasi-sliding band for a given sampling period. It also mitigates the degradation in performance caused by moderate increase in the sampling period.

The proposed control strategies are validated for varied applications in simulation. The applications used are a flexible joint, an inverted pendulum, an anti-lock braking, active steering and motion control. All the applications are assessed and tested for a variety of cases like road friction, mass uncertainties, road gradients, inertia changes, among others.

This thesis has taken a few concrete steps in solving the problems associated with the conventional sliding mode control and proved the viability of proposed techniques for applications in motion control and automotive control.

Contents

List of Figures

List of Tables

List of Acronyms

ABS	Anti-lock Braking System
DLC	Double Lane Change
DO	Disturbance Observer
DSMC	Discrete Sliding Mode Control
DSP	Digital Signal Processor
EID	Equivalent Input Disturbance
ESO	Extended State Observer
GESO	Generalized State Observer
IB	Integrator Backstepping
MIMO	Multi-input multi-output
PID	Proportional Integral Derivative
RMS	Root Mean Square
SISO	Single-input single-output
SLC	Single Lane Change
SMC	Sliding Mode Control
TDC	Time Delay Control
UDE	Uncertainty and Disturbance Estimator
VSC	Variable Structure Control
VSS	Variable Structure System

Chapter 1

Introduction

The recent years have seen an increased interest in control of uncertain systems. Sliding mode control (SMC) has evolved into an effective strategy for controlling plants with significant uncertainties and unmeasurable disturbances. The intent is to find a methodology that is in line with the practicality of actual plants.

1.1 Overview

Sliding Mode Control (SMC) is a special class of variable structure systems (VSS) that alters the dynamics of a system with a switching control (*Emelyanov*, 1970). The theory of sliding mode is based on the concept of changing the structure of controller in response to the changing state of system, to achieve a desired response (*Itkis*, 1976). The closed loop system can thus be made insensitive to system uncertainties and external disturbances. The increased interest is a result of robustness becoming an important requirement in modern control applications.

The invariance and robustness properties has resulted in SMC maturing into an effective strategy for controlling systems in the presence of uncertainties, external disturbances, and plant parameter variations (*Fridman et al.*, 2011). SMC has now been developed into a general design method and extended to a wide spectrum of system types; predominantly in motion control (*Sabanovic*, 2011).

The conventional SMC, however employs discontinuous control that results in undesirable chatter. This chatter causes excessive wear and tear of actuators and may excite unmodeled dynamics. Furthermore, the control can be designed only if bounds of uncertainty and disturbances are known. The conventional SMC is insensitive to only matched disturbances (*Drazenovic*, 1969), and also requires full state vector for implementation.

SMC has found a variety of applications in robotics, aerospace vehicles, electrical drives and automotive industry to name a few. There are however applications where; uncertainties and disturbances act in channels in which, a control input is not present. The magnetic levitation, under-actuated mechanical systems, systems having actuators in cascade, are all examples of such mismatched systems. When conventional SMC is applied to such systems, the controlled output is affected by uncertainties and disturbances even when the system is in sliding mode.

A control design using simultaneous estimation of states along with uncertainties and disturbances can effectively alleviate the problem. In this design, the effect of uncertainties is compensated by augmenting the controller designed for nominal system with the estimates. There are several techniques reported for uncertainty estimation like time delay control (TDC) (*Youcef-Toumi and Ito*, 1990), disturbance observer (DO) (*Chen*, 2004), extended state observer (ESO) (*Han*, 2009). The ESO enables estimation of states, with disturbances as an extended state. The uncertainty and disturbance estimator (UDE) (*Zhong and Rees*, 2004) is an effective technique for estimating slow varying uncertainties. The equivalent input disturbance (EID) method (*She et al.*, 2008) is a recent addition to the literature.

The characteristics of discrete-SMC are different from continuous-SMC in that, they can undergo only quasi-sliding motion i.e. the state of the system can approach the switching surface but cannot generally stay on it. This is due to the fact that the control action can only be activated at sampling instants and control effort is constant over each sampling period (*Misawa*, 1997a). The δ operator can be used to formulate an unified design thereby resolving the dichotomy between results in continuous and discrete time control law; especially with regard to limiting properties as sampling time $T_s \to 0$ (*Middleton and Goodwin*, 1990). The δ operator is used for unification of sliding condition in (*Ginoya et al.*, 2015b).

A new control method for uncertain dynamical systems is proposed and is shown in Fig. 1.1. It is based on a unique disturbance rejection concept leveraging the benefits of uncertainty and disturbance estimation. The proposed robust control scheme consists of an *Estimator* for estimating the uncertainty and disturbance, *Observer* for estimating the states, and *Control law* based on *Sliding Mode Control*. The proposed approach can be used for tracking as well as regulation problem.

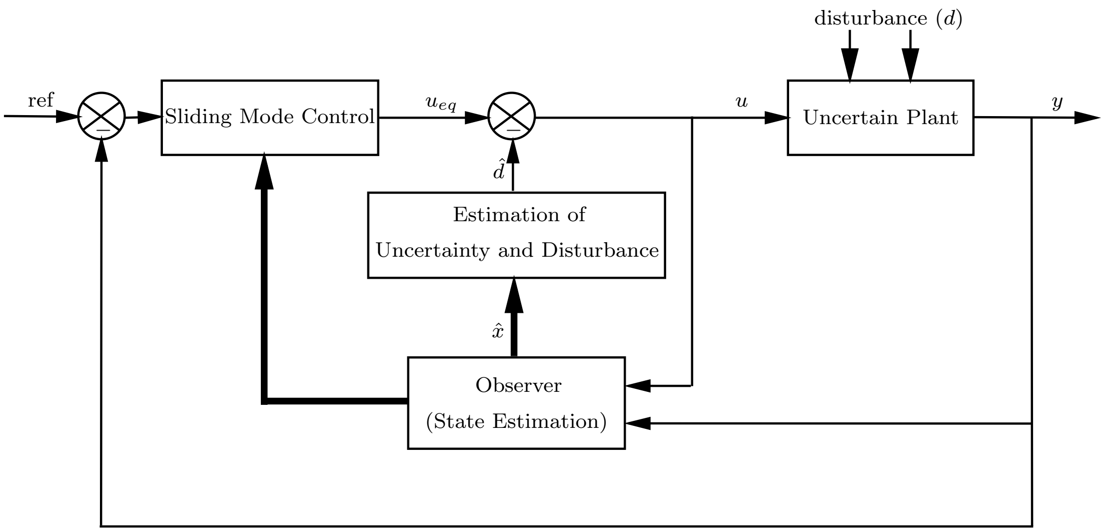

Figure 1.1: Configuration of proposed control

This is motivated by the requirements of practical plant; since most plants and systems encountered in practice possess significant uncertainty and are subjected to varied disturbances. The robust control law is designed for both matched as well as mismatched uncertainties and the sliding surface is designed to preclude large initial control. The designed control laws are tested for representative plant configurations and validated for varied applications in motion and automotive control. The same is demonstrated through simulation, frequency response analysis and hardware tests for handling set-point changes, inertia and friction variations, plant uncertainties and external disturbances.

This work attempts to propose conceptual solutions to address the fundamental limitations in existing framework. It is envisaged that the proposed method lends itself well; in providing innovative solutions to practical problems. The central theme is to develop robust control algorithms for uncertain dynamical systems.

1.2 Concept of Sliding Mode Control

Consider a second-order system with a feedback control u,

$$\left.\begin{aligned} \ddot{x} &= a\dot{x} + u \quad a > 0 \\ u &= -kx \end{aligned}\right\} \tag{1.1}$$

The eigen-values of the closed-loop are,

$$\lambda_{1,2} = (-a \pm \sqrt{a^2 - 4k})/2 \tag{1.2}$$

If $|k| = b$ and $b > a^2/4$, there are 2 structures corresponding to $k < 0$ or $k > 0$:

1. If $k = b$, Fig. 1.2(a) shows the phase portrait of this structure.
2. If $k = -b$, the phase portrait of the system is shown in Fig. 1.2(b).

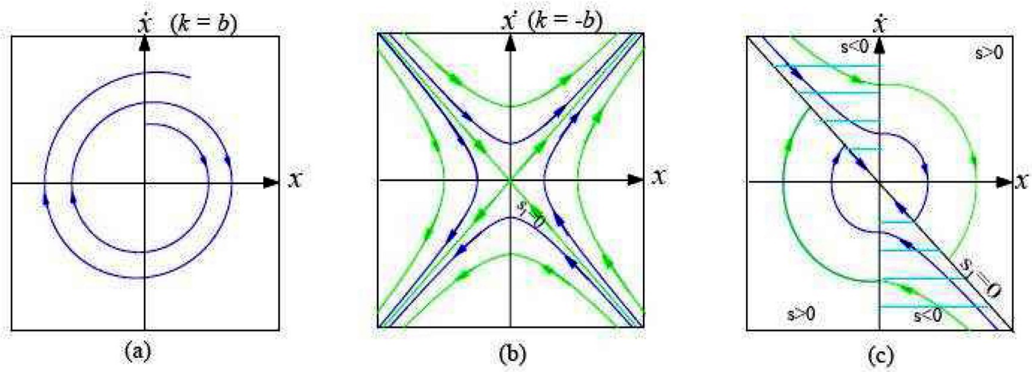

Figure 1.2: Asymptotically stable VSS consisting of two unstable structures

Both these structures are unstable. However, note that in the second structure, there is a motion along the line corresponding to stable eigen value $(\dot{x} - \lambda_2 x = 0)$, i.e. a motion which tends to the origin. Therefore, defining a switching function,

$$s = \dot{x} + \lambda x \tag{1.3}$$

and let the system switch on lines $x = 0$ and $\sigma = 0$; according to switching law,

$$k = \begin{cases} b & \text{if } s > 0 \\ -b & \text{if } s < 0 \end{cases} \tag{1.4}$$

the resulting phase trajectory is shown in Fig. 1.2(c).

The two unstable structures replace each other on the line, hence all the trajectories are oriented towards the line and then asymptotically converge to origin. The motion along the line, which is not a trajectory of any structures is called sliding mode. The concept of SMC is illustrated in Fig. 1.3.

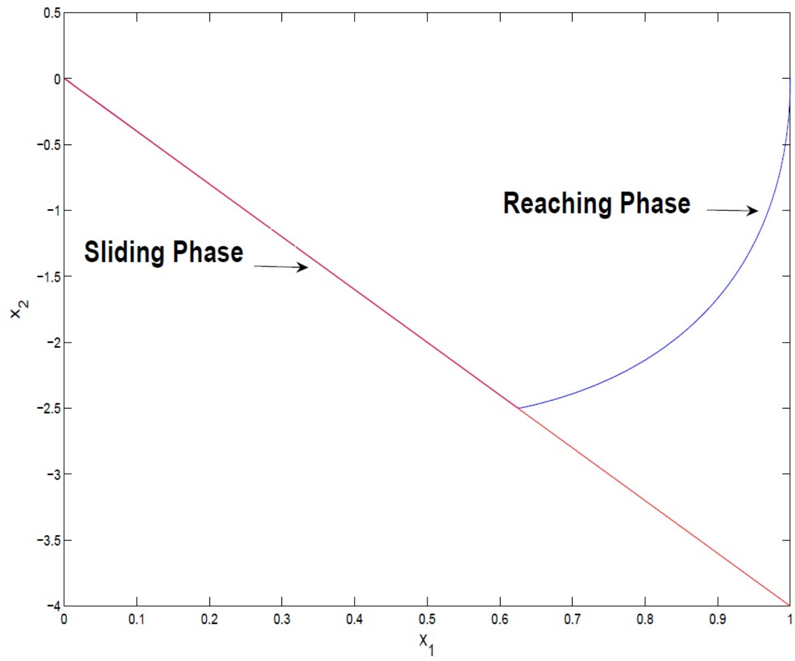

Figure 1.3: Sliding mode concept

The problem of SMC design involves selecting the parameters of each of the structures and define the switching logic. The motion of a SMC system includes two phases; the reaching phase and the sliding phase as shown in Fig. 1.3. During the reaching phase, the system state is pushed towards the switching surfaces. During this phase, the system response is sensitive to parameter uncertainties and disturbances. Thus, one would ideally like to shorten the duration or even eliminate the reaching phase.

One easy way to minimize the reaching phase and hence reaching time is to employ a larger control input (*Utkin*, 1992; *Edwards and Spurgeon*, 1999). This however, may cause extreme system sensitivity to unmodeled dynamics, actuator saturation and higher chattering as well. The robustness of the SMC can be improved by shortening the reaching phase or may be guaranteed during whole intervals of control action by eliminating the reaching phase (*Ackermann and Utkin*, 1998).

1.3 Uncertainty Estimation

There are several interesting techniques available for estimation of uncertainty. The uncertainty and disturbance estimator (UDE), disturbance observer (DO), and equivalent input disturbance (EID) are briefed in this section.

A generic uncertain plant can be described as,

$$\left.\begin{aligned} \dot{x}(t) &= Ax(t) + Bu(t) + B_d e(x,u,t) \\ y(t) &= Cx(t) \end{aligned}\right\} \tag{1.5}$$

where, $x(t)$ is the state vector, $u(t)$ is the control input, $y(t)$ is the output of plant and $e(x,u,t)$ is the lumped uncertainty.

$$e(x,u,t) = \Delta Ax(t) + \Delta Bu(t) + \upsilon(t) + \zeta(x,t) \tag{1.6}$$

where, ΔA is uncertainty in plant, ΔB is uncertainty in input, $\upsilon(t)$ is external disturbance and $\zeta(x,t)$ represent nonlinearities in the plant

1.3.1 Uncertainty and Disturbance Estimator (UDE)

The key idea in UDE based control is, to use a filter of appropriate band-width to estimate the lumped uncertainty; and to use the opposite of estimate in control to negate the effect of uncertainty (*Zhong and Rees*, 2004; *Talole and Phadke*, 2008). This method is based on an idea similar to TDC (*Youcef-Toumi and Ito*, 1990), but does not require derivative of system state and does not use time delayed signals. The lumped uncertainty (e) can be estimated as,

$$\hat{e} = G_f(s)\, e \tag{1.7}$$

where $G_f(s)$ is a filter with sufficiently large bandwidth, of the form,

$$G_f(s) = \frac{1}{1+\tau s} \tag{1.8}$$

where τ is a small positive constant.

The accuracy of estimation can be improved with a higher-order filter.

1.3.2 Disturbance Observer (DO)

Disturbance observer is an estimation scheme that utilizes an auxiliary dynamical system to estimate the uncertainties and disturbances acting on the system. The disturbance estimates are then used in the control law to compensate the effect of uncertainty.

$$\left.\begin{aligned} \hat{e} &= p + lx \\ \dot{p} &= -l(Ax + Bu + B_d\,\hat{e}) \end{aligned}\right\} \tag{1.9}$$

where p is an auxiliary variable and l is user chosen constant.

The accuracy of estimation can be improved by estimating the uncertainties and its derivatives with a higher-order DO.

1.3.3 Equivalent Input Disturbance (EID)

The EID is a disturbance on the control input channel that produces the same effect on controlled output as actual disturbances (*She et al.*, 2008).

Consider a uncertain plant as,

$$\left.\begin{aligned} \dot{x}_1 &= x_2 + d_1 \\ \dot{x}_2 &= x_3 + d_2 \\ \dot{x}_3 &= u \end{aligned}\right\} \tag{1.10}$$

The plant with EID can be written as,

$$\left.\begin{aligned} \dot{x}_1 &= x_2 \\ \dot{x}_2 &= x_3 \\ \dot{x}_3 &= u + d_e \end{aligned}\right\} \tag{1.11}$$

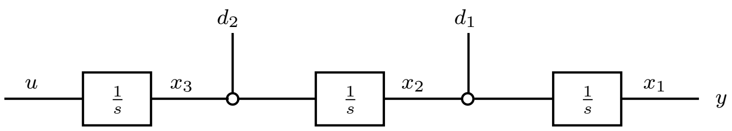

Figure 1.4: General uncertain plant

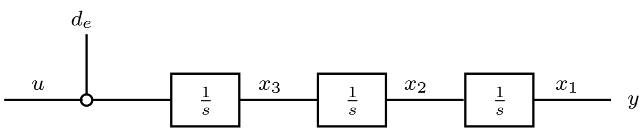

Figure 1.5: General plant with EID

Consider $u = \sin\omega_u t, \quad d_1 = \sin\omega_{d_1} t \quad$ and $\quad d_2 = \sin\omega_{d_2} t$

Therefore, for the original plant (equation (1.10), Fig. 1.4),

$$\left.\begin{aligned}
u &= \sin\omega_u t \\
x_3 &= \frac{\cos\omega_u t}{\omega_u} \\
x_3 + d_2 &= \frac{\cos\omega_u t}{\omega_u} + \sin\omega_{d_2} t \\
x_2 &= -\frac{\sin\omega_u t}{\omega_u^2} + \frac{\cos\omega_{d_2} t}{\omega_{d_2}} \\
x_2 + d_1 &= -\frac{\sin\omega_u t}{\omega_u^2} + \frac{\cos\omega_{d_2} t}{\omega_{d_2}} + \sin\omega_{d_1} t \\
x_1 &= -\frac{\cos\omega_u t}{\omega_u^3} - \frac{\sin\omega_{d_2} t}{\omega_{d_2}^2} + \frac{\cos\omega_{d_1} t}{\omega_{d_1}} \\
y &= -\frac{\cos\omega_u t}{\omega_u^3} + \frac{\cos\omega_{d_1} t}{\omega_{d_1}} - \frac{\sin\omega_{d_2} t}{\omega_{d_2}^2}
\end{aligned}\right\} \tag{1.12}$$

The output for the plant with EID (equation (1.11), Fig. 1.5) can be derived as,

$$\left.\begin{aligned}
u &= \sin\omega_u t \\
d_e &= \ddot{d}_1 + \dot{d}_2 \\
&= -\omega_{d_1}^2 \sin\omega_{d_1} t + \omega_{d_2} \sin\omega_{d_2} t \\
u + d_e &= \sin\omega_u t - \omega_{d_1}^2 \sin\omega_{d_1} t + \omega_{d_2} \sin\omega_{d_2} t \\
x_3 &= \frac{\cos\omega_u t}{\omega_u} - \omega_{d_1} \cos\omega_{d_1} t + \sin\omega_{d_2} t \\
x_2 &= -\frac{\sin\omega_u t}{\omega_u^2} + \sin\omega_{d_1} t + \frac{\cos\omega_{d_2} t}{\omega_{d_2}} \\
x_1 &= -\frac{\cos\omega_u t}{\omega_u^3} + \frac{\cos\omega_{d_1} t}{\omega_{d_1}} - \frac{\sin\omega_{d_2} t}{\omega_{d_2}^2} \\
y &= -\frac{\cos\omega_u t}{\omega_u^3} + \frac{\cos\omega_{d_1} t}{\omega_{d_1}} - \frac{\sin\omega_{d_2} t}{\omega_{d_2}^2}
\end{aligned}\right\} \tag{1.13}$$

The equations (1.12) and (1.13) clearly depict that the output in both the cases is same. This implies that instead of estimating d_1 and d_2, the EID (d_e) can be estimated to compensate the effect of d_1 and d_2 on the output. The analysis also demonstrates that a full-order observer is necessary for estimation of EID.

1.4 Literature Review

Variable structure control (VSC) with sliding mode first made its appearance in early sixties in the erstwhile Soviet Union (*Emelyanov*, 1970; *Itkis*, 1976). Since then, significant interest on variable structure systems and sliding mode control has been generated in the control community. Early utilization of this SMC approach can be found in (*Utkin*, 1977; *Decarlo et al.*, 1988; *Hung et al.*, 1993). One of the most interesting aspects of sliding mode is the discontinuous nature of control action. The primary function of each of the nonlinear feedback channels is to switch between two distinctively different system structures, so that a new type of motion called *Sliding Mode* exists in a manifold (*Young et al.*, 1999). A SMC system may be regarded as a combination of subsystems, each with fixed structure and each operating in a specified region of state space. With the help of SMC, it is possible to combine the useful properties of each of the structures. A SMC would then possess new properties not present in any of the subsystems used; e.g. an asymptotically stable system may consist of two structures neither of which is asymptotically stable (*Utkin*, 1977). This results in a system performance which is robust to parameter variations and disturbances.

The motion of a SMC system include two phases; the reaching phase and sliding phase. During the reaching phase, the system states move towards the switching plane. The robustness of the SMC can be improved by shortening the reaching phase or may be guaranteed during whole intervals of control action by eliminating the reaching phase (*Ackermann and Utkin*, 1998). The concept of SMC has been extended to discrete case in (*Gao et al.*, 1995; *Misawa*, 1997a) and the δ-operator has been introduced in (*Middleton and Goodwin*, 1990).

VSC systems are switching feedback control systems known to be insensitive to matched uncertainties (*Drazenovic*, 1969). The high frequency switching results in chattering phenomenon (*Utkin and Lee*, 2006), which is due to presence of finite time delays for control computation and limitations of physical elements like actuators. The chatter can be mitigated by using a smooth approximation of discontinuous function (*Slotine and Sastry*, 1983; *Burton and Zinobar*, 1986), and boundary layer control with continuous control inside the boundary.

The conventional SMC also requires full state vector for implementation and as such, an observer to estimate the states becomes imperative. There has been considerable interest in developing robust observers for uncertain dynamical systems. The classical *Luenberger* observer fails when the output is sensed in presence of model uncertainties and/or sensor noise. As such, observer designs in the presence of disturbances, dynamic uncertainties and nonlinearities pose great challenges in practical applications.

Slotine designed observer using sliding surfaces and proved that sliding-mode observers offer advantages similar to sliding controllers (*Slotine et al.*, 1987). A related approach applied to a more restricted class of problem is taken by Zak and Walcott. A lyapunov based approach is used for system with matched and bounded uncertainties (*Walcott and Zak*, 1988). An observer based on TDC is proposed in (*Chang et al.*, 1997). A combined state and perturbation observer using the time delay observer (*Kwon and Chung*, 2003) and proportional integral observer (*Chang*, 2006) are available. A SMC design using state and extended disturbance observer (*Ginoya et al.*, 2015a) for mismatched uncertain systems is an interesting addition to the literature.

The conventional SMC can be designed only if bounds of uncertainty and disturbances are known, however they are not easy to find. The bounds can be determined adaptively (*Slotine and Coetsee*, 1986; *Yoo and Chung*, 1992b), however it is limited to only structured uncertainties. An alternative approach could be estimation of uncertainty and disturbances, which relaxes the requirement of knowing the bounds. The UDE (*Zhong and Rees*, 2004) is one such technique that uses a low-pass filter of appropriate order and band-width for estimation. This method is based on an idea similar to the TDC (*Youcef-Toumi and Ito*, 1990), but does not require the derivative of system states and does not use time delayed signals. The SMC using UDE enforces sliding mode without using discontinuous control, and without requiring the knowledge of uncertainties or their bounds. The UDE has been applied to SMC of linear systems (*Talole and Phadke*, 2008), systems with state delays (*Stobart et al.*, 2011; *Kuperman and Zhong*, 2011) and input-output linearization (*Talole and Phadke*, 2009). A variety of applications using UDE are reported as in (*Phadke and Talole*, 2012; *Kolhe et al.*, 2013).

The problem of matching conditions can be solved for a certain class of systems using the back-stepping technique (*Krstic et al.*, 1995). A technique called as multiple-sliding surface control (*Huang and Chen*, 2004) handles the problem in a similar way. The issue of mismatched uncertainty in nonlinear systems is also handled using robust estimation techniques like DO (*Yang et al.*, 2011a, 2012a) and generalized ESO (*Li et al.*, 2012). A SMC design employing DO to compensate mismatched uncertainties and its higher order derivatives is an interesting solution. The design uses a novel sliding surface, which includes the estimate of unmatched disturbances (*Ginoya et al.*, 2014). The strategy substantially alleviates the problem of chatter in control; in addition to counteracting the effect of mismatched uncertainties. Several other techniques like adaptive control, dynamic sliding surface based control, and integral SMC are also available for compensating mismatched uncertainties.

The Equivalent Input Disturbance (EID) approach is an interesting way to tackle mismatched systems. An EID is a disturbance on the control input channel that produces the same effect on controlled output as actual disturbances do. An EID always exists for a controllable and observable plant with no zeros on imaginary axis (*She et al.*, 2008). Several extensions of EID to MIMO (*She and Xin*, 2007), under-actuated (*She et al.*, 2012), systems; as also applications in motion control, power systems (*Hu et al.*, 2013), automotive control systems (*She et al.*, 2007), mechatronics (*She et al.*, 2011), etc have been reported. However the technique merits additional investigation especially in the context of higher-order filter. The body of work in the literature on EID, also does not include SMC based control, DO based estimation or uncertainty in plant parameters.

The robust sliding mode control (SMC) design augmented by estimates of uncertainty and disturbance can be employed in a variety of applications like motion control, robotics, magnetic levitation (*Yang et al.*, 2011b; *Lin et al.*, 2007b), active steering control (*Ding and Taheri*, 2010; *Rajamani*, 2011; *Zhang and Wang*, 2015), anti-lock braking systems (*Mirzaeinejad and Mirzaei*, 2010; *Rajamani et al.*, 2012; *Pasillas-Lépine et al.*, 2012).

The state-of-the-art gives an overview of the body of work in the literature and gives insights into what more needs to be done for interesting solutions.

1.5 Motivation

SMC is an effective strategy for controlling systems with significant uncertainties and unmeasurable disturbances. However there are certain issues, concerns and restrictions that merit attention.

- The control is discontinuous, which results in undesirable chatter. The chatter causes excessive wear and tear of actuators and may excite unmodeled dynamics.
- The sliding mode can be enforced only if bounds of uncertainty and disturbances are known. However, the bounds are not always easy to find. The rate of change of uncertainty is also a concern.
- The conventional SMC design has capabilities to compensate disturbances of only matched type, i.e. the disturbance entering the same channel as input. This poses severe limitations on the applicability of SMC.
- A majority of SMC strategies are based on state feedback. However, it is of common knowledge that though most practical systems are observable, all the system states are seldom measurable. Therefore, the sliding mode control algorithms may not be implementable in many cases. The problem is further compounded in the presence of uncertainties and disturbances.
- An accurate mathematical model may not be always available in case of most of the plants, i.e. uncertainty, un-modeled dynamics and external disturbances exist. As such, uncertainty estimation is imperative for disturbance rejection.

This work aims at designing robust sliding mode control strategy that mitigates the restrictions imposed in the existing design. The problem of nonlinear systems with matched as well as mismatched uncertainty is considered. The objective is to have simultaneous state and uncertainty estimation. The estimation methods used are UDE, DO and EID. The thesis also aims at validating the designs in motion and automotive control application.

1.6 Objectives

The central theme is to develop robust control algorithms for uncertain dynamical systems in varied domains.

- Design a boundary layer SMC law using UDE for mitigating chatter.
- Design a SMC law for nonlinear systems by estimating the states and
  - matched uncertainties using UDE.
  - matched and mismatched uncertainties using EID and filter.
  - matched and mismatched uncertainties using EID and DO.
- Design a discrete SMC algorithm with estimation of states and uncertainties.

1.7 Methodology

The core aspects of this work is divided into five distinct phases, which broadly encapsulate the stages of;

- Redefining the control problem
- Convergence and robustness analysis
- Stability analysis
- Performance evaluation
- Application validation

The objectives are realized using a approach comprising of,

- Theoretical Formulation
  Derivation of control law, Derivation of stability proof and stability analysis, Convergence and Robustness analysis
- Numerical Simulation
- Application Validation

1.8 Main Contributions

The algorithms proposed in this treatise may be summarized as,

- A new boundary layer sliding mode control strategy is designed for chatter reduction. The control scheme uses a discontinuous control outside the boundary layer and switches over to uncertainty and disturbance estimator (UDE) based control inside. The problem of large initial control underlying the method of UDE, is also addressed with a modified sliding surface. The overall stability of the system is proved and the results are verified on an illustrative example and application to flexible joint system. The results show that the proposed method exhibits much better control performance than the baseline SMC using *'sat'* function, for reduced chattering.

- A robust sliding mode control (SMC) strategy for an uncertain nonlinear system subjected to time varying disturbance is proposed. The class of system considered includes state dependent nonlinearity in the input vector (in addition to the plant matrix). The control scheme uses uncertainty and disturbance estimator (UDE) to estimate the lumped uncertainty and the accuracy of estimation is improved with a higher-order filter. The control law is made implementable by estimating the states as well, to give a robust observer. The proposed control enforces sliding without using discontinuous control and without requiring the knowledge of uncertainties or their bounds. The overall boundedness is proved. The effectiveness of the proposed strategy is verified for model following and robust performance; and validated for an inverted pendulum system.

- A SMC strategy for nonlinear systems with mismatched uncertainties is proposed. A nonlinear model of the plant is considered with state-dependent uncertainty. The mismatched uncertainties are estimated using EID method. An observer is designed for estimation of EID. The effect of higher-order filter for improving the accuracy of estimation; by estimating disturbance and its derivatives is proved. The theory is generalized to a $k^{th}-$order filter. The conventional sliding surface is modified to improve system performance without causing a large increase in initial control; mitigating the effects of chatter.

The overall stability is proved using Lyapunov theory. The results of designed strategy are verified by application to an anti-lock braking systems (ABS) control case-study. The ABS is considered to include actuator dynamics and the slip regulation is ensured for different friction models.

- A robust control strategy for systems with matched and mismatched uncertainties using EID approach is proposed. A nonlinear model of the plant is considered with state-dependent uncertainty. The SMC law is augmented with estimate of EID and the same is obtained using a DO. As earlier, the observed states are used for estimation. The design of extended DO to accommodate a large class of mismatched disturbances is also shown, which estimates disturbance and its derivatives. The overall stability is proved using Lyapunov theory. The results are verified by application to an active steering control problem.

- The concept of discrete sliding mode using δ-operator is introduced. The δ-operator is used to formulate an unified design thereby resolving the dichotomy between results in continuous and discrete time control law. The design is robustified by designing a discrete observer that estimates states, uncertainty and disturbance. The analysis with a 2^{nd} order filter is shown to prove the improvement in estimation. The overall stability is proved in the usual way and the results are verified for an industrial motion case-study.

The core idea underlying all the aforementioned work is the estimation of states, uncertainty and disturbance for robust sliding mode control. The system considered are all nonlinear with matched as well as mismatched uncertainty. The various designs proposed, address the limitations of the conventional SMC design. The sliding variable (σ), estimation error ($\tilde{e}$) and state estimation error ($\tilde{x}$) are ultimately bounded in all cases in the sense of *Corless and Leitmann* (1981).

The simplicity of control design supplemented by estimation capability of methods like UDE, DO and EID makes this approach an attractive proposition. The applicability of designed control to a wide range of systems (as demonstrated in the work), leads the author to believe that uncertainty estimation based sliding mode control techniques shall be a major topic of interest in robust control.

1.9 Organization of Thesis

The thesis is divided into seven chapters. Chapter 1 gives a road-map of the thesis and answers the fundamental questions of what, why and how. A brief review of literature is also included. The issues and concerns in conventional SMC are then addressed in successive chapters.

Chapter 2 deals with the design and validation of boundary-layer SMC law using UDE, for chatter mitigation. The UDE is further used to synthesize a observer-controller structure for nonlinear uncertain systems in chapter 3. The class of system considered includes state dependent nonlinearity in the input vector as well as plant matrix and also external disturbance. Chapter 4 is concerned with SMC of mismatched uncertain systems using EID method. The effect of higher-order filter for improving the accuracy of estimation is proved.

The work is further extended for robust control of systems with matched and mismatched uncertainties in Chapter 5. The EID is estimated using DO and this estimate is supplemented in the control law. The estimation is generalized to a $n^{th}-$order DO. The results of both these EID approaches are verified for automotive applications. Chapter 6 introduces the concept of discrete sliding mode control using δ-operator. The control law is made implementable by designing a discrete observer that estimates states, uncertainty and disturbance.

Throughout chapter 2 to 6, some essential results of other researchers are briefly introduced, discussed and referenced. The conclusions and recommendations for future work are presented in the final chapter of the thesis.

Chapter 2

Boundary Layer SMC using UDE

The chapter explains design and validation of a new boundary-layer sliding mode control design for chatter mitigation. The control scheme employs discontinuous control outside the boundary layer and switches over to uncertainty and disturbance estimator (UDE) based control inside.

The chapter starts with an introduction in section 2.1 covering the state-of-art, followed by problem formulation in section 2.2. Section 2.3 describes discontinuous SMC design. A control based on UDE is explained in Section 2.4 and the proposed control in section 2.5. Section 2.6 gives the stability analysis. The performance is illustrated by an example in section 2.7 followed by application to flexible joint system in section 2.8. The chapter concludes with a summary in section 2.9.

2.1 Introduction

SMC is a discontinuous control for controlling uncertain systems (*Utkin*, 1977; *Hung et al.*, 1993; *Young et al.*, 1999; *Sabanovic*, 2011). The discontinuous control leads to chatter that is undesirable, because it causes excessive wear and tear of components and can excite fast unmodelled dynamics. The chatter in control and states is thus a major concern in the practical implementation of sliding mode control (*Utkin and Lee*, 2006; *Boiko*, 2011).

The most popular method for chatter control is the boundary layer control (*Slotine and Sastry*, 1983; *Burton and Zinobar*, 1986) in which, the control is discontinuous outside a boundary layer, but is continuous inside. The method tries to strike a trade off between invariance of system trajectories and smoothness of control.

Lee and Utkin (*Lee and Utkin*, 2007) use state-dependent or equivalent-control-dependent, magnitude of the discontinuous control for suppression of chatter. A variety of strategies like filtering of control signal (*Lei and Chen*, 2010), euler time-discretization method (*Acary and Brogliato*, 2010), time varying feedback gain method (*Xu*, 2008; *Potluri*, 2012), integration of control signal (*Chen et al.*, 2007), fuzzy logic (*Liu and Sun*, 2006), neural network (*Fang and Chow*, 1998), have been proposed in literature to address the problem of chattering. The methods related to higher order sliding modes can be found in (*Levant*, 2003).

A combination of SMC with estimates of uncertainty and disturbance enables the reduction of discontinuous component of control, thereby suppressing the chatter significantly. The UDE (*Zhong and Rees*, 2004) is one such strategy for estimating slow varying uncertainties. This method has been applied to SMC of uncertain linear systems (*Talole and Phadke*, 2008) and in applications like load frequency controller (*Shendge and Patre*, 2007), robotic control (*Kolhe et al.*, 2013) to name a few. The focus in these papers is on estimation accuracy rather than chatter; and sliding surface used has the shortcoming of resulting in large initial control. The afore-said issues are addressed in this work.

A strategy for chatter control based on UDE is proposed in this work. The UDE is used to estimate the lumped uncertainty comprising of uncertainty in plant as well as input matrix and unknown disturbance. The class of disturbances considered here is significantly larger. The uncertainties and disturbances are assumed to be bounded, however no knowledge of bounds is required. The method of UDE results in a large initial control for systems with non-zero initial conditions. The sliding surface is modified to circumvent the problem of this large initial control. The stability of system inside the boundary layer is proved. The ultimate boundedness of estimation error ($\tilde{e}$) and sliding variable (σ) is guaranteed inside the boundary layer. The theoretically expected results are verified by computer simulation in MATLAB SIMULINK environment.

2.2 Problem Formulation

Consider a single input single output (SISO) uncertain system as,

$$\dot{x} = Ax + bu + \Delta Ax + \Delta bu + d(x,t) \tag{2.1}$$

where x is the state vector, u is the control input, A and b are known constant matrices, ΔA and Δb are uncertainties and $d(x,t)$ is the unknown, unmeasurable disturbance.

Assumption 2.1 *The uncertainties $\Delta A, \Delta b$ and disturbance $d(x,t)$ satisfy matching conditions given by,*

$$\Delta A = bD, \quad \Delta b = bE, \quad d(x,t) = bv(x,t) \tag{2.2}$$

where D and E are unknown matrices of appropriate dimensions and $v(x,t)$ is an unknown function.

The equation (2.2) is the well-known matching condition required to guarantee invariance and is an explicit statement of structural constraint (*Drazenovic*, 1969). The system (2.1) can now be written as,

$$\dot{x} = Ax + bu + bDx + bEu + bv(x,t) \tag{2.3}$$

$$\dot{x} = Ax + bu + be(x,t) \tag{2.4}$$

where $e(x,t) = Dx + Eu + v(x,t)$ is the lumped uncertainty comprising of uncertainties in A and b as well as external disturbance.

Assumption 2.2 *The lumped uncertainty $e(x,t)$ is bounded by a known function,*

$$|e(x,t)| = \rho(x,t) \tag{2.5}$$

where $\rho(x,t)$ is a known positive scalar function.

The objective is to design sliding mode control law for a SISO plant comprising uncertainties and disturbances. The control law is expected to minimize the discontinuous component, thereby mitigating chatter.

2.3 Discontinuous Control

Consider a sliding surface,

$$\sigma = s\,x \tag{2.6}$$

Differentiating (2.6) and using (2.4),

$$\dot{\sigma} = sAx + sbu + sbe \tag{2.7}$$

Let the control that ensures sliding be given by,

$$u = u_{eq} + u_n \tag{2.8}$$

where u_{eq} caters to the known terms and u_n takes care of uncertainties

Using (2.8) in (2.7),

$$\dot{\sigma} = sAx + sbu_{eq} + sbu_n + sbe \tag{2.9}$$

$$u_{eq} = -(sb)^{-1}(sAx + k\sigma) \qquad k > 0 \tag{2.10}$$

Therefore,

$$\dot{\sigma} = sbu_n + sbe - k\sigma \tag{2.11}$$

Designing u_n such that $\sigma\dot{\sigma} < 0$,

$$\sigma\dot{\sigma} = \sigma sbu_n + \sigma sbe - k\sigma^2 \tag{2.12}$$

With some simple mathematics,

$$u_n = -\rho(x,t)\,\mathrm{sgn}(\sigma sb) \tag{2.13}$$

The control given by (2.13) is discontinuous. Since discontinuous control is objectionable, a commonly used smooth approximation of u_n is given by,

$$u_n = \begin{cases} -\rho(x,t)\,\mathrm{sgn}(\sigma sb), & |\sigma sb| > \epsilon \\ \frac{-\rho(x,t)}{\epsilon}, & |\sigma sb| \le \epsilon \end{cases} \tag{2.14}$$

where ϵ is a small positive number.

The well known drawbacks of the smooth approximation are that; a small ϵ retains invariance but may result in chatter, while large ϵ suppresses chatter but results in significant loss of invariance.

2.4 A New Smooth Control

A smoothing approach using UDE is used for chatter suppression. The key idea in UDE based control is to approximate and estimate the uncertainty using a filter of right bandwidth. The opposite of estimate is then used in control to negate the effect of uncertainty (*Zhong and Rees*, 2004; *Talole and Phadke*, 2008). The following assumption is needed to ensure that $\tilde{e}$ (i.e. $e - \hat{e}$) is bounded.

Assumption 2.3 *The lumped uncertainty $e(x,t)$ is continuous and satisfies,*

$$\left|\frac{d^{(j)}e(x,t)}{dt^{(j)}}\right| \leq \mu \qquad \textit{for } j = 0, 1, 2, \ldots, r \tag{2.15}$$

where μ is a small positive number.

The lumped uncertainty $e(x,t)$ can be estimated as,

$$\hat{e} = e\, G_f(s) \tag{2.16}$$

where $G_f(s)$ is a strictly proper low-pass filter with unity steady state gain and sufficiently large bandwidth.

Using (2.4) and (2.6)

$$\dot{\sigma} = sAx + sbu + sbe \tag{2.17}$$

Using (2.8) and (2.10) in (2.17)

$$\dot{\sigma} = sbu_n + sbe - k\sigma \tag{2.18}$$

$$e = (sb)^{-1}(\dot{\sigma} + k\sigma) - u_n \tag{2.19}$$

The control strategy in UDE is to estimate lumped uncertainty e as $\hat{e}$ and use $-\hat{e}$ as a component in control; to cancel the effect of e. Let,

$$u_n = -\hat{e} \tag{2.20}$$

Using (2.16), (2.19) and (2.20),

$$u_n = -(sb)^{-1}(\dot{\sigma} + k\sigma)\frac{G_f(s)}{1 - G_f(s)} \tag{2.21}$$

Specially for a choice of $G_f(s)$ given by,

$$G_f(s) = \frac{1}{1+\tau s} \qquad \text{(first order filter)} \tag{2.22}$$

where τ is a small positive constant,

$$u_n = -(sb)^{-1}\frac{1}{\tau}\left(\sigma + k\int\sigma\right) \tag{2.23}$$

From equations (2.16) and (2.22)

$$\dot{\tilde{e}} = -\frac{1}{\tau}\tilde{e} + \dot{e} \tag{2.24}$$

From equations (2.18) and (2.20)

$$\dot{\sigma} = -k\,\sigma + s\,b\,\tilde{e} \tag{2.25}$$

Remark 2.1 *If $\dot{e} = 0$, $\tilde{e}$ goes to zero asymptotically; otherwise it is ultimately bounded. As a consequence $\sigma \to 0$, if $k > 0$ and $\tau > 0$. If $\dot{e}$ is not small, but $\ddot{e}$ is small, i.e $j = 2$ in* (2.15)*, then the accuracy of estimation can be improved by estimating e as well as $\dot{e}$.*

The ultimate boundedness of $\tilde{e}$ and calculation of bound is discussed in section 2.6. The improvement obtained using an higher order filter is derived in subsection 2.4.3 and shown in the results. The proposed estimator does not need any knowledge of the size of uncertainty. It can estimate slow varying lumped uncertainties accurately, if τ is chosen to be a small constant. However a small τ results in a large control u_n at $t = 0$, since $\sigma(0)$ may not be a small number in general. To circumvent this problem, a modified sliding surface is proposed.

2.4.1 Modified Sliding Surface

The conventional sliding surface is modified as,

$$\sigma^* = \sigma - \sigma(0)\,e^{-\alpha t} \tag{2.26}$$

where α is a user chosen positive constant.

It may be noted that at $t = 0$, the modified sliding variable $\sigma^*(0) = 0$ for any $\sigma(0)$ and $\sigma^* \to \sigma$ as $t \to \infty$.

2.4.2 Design of Control

Using (2.4), (2.6) and (2.26),

$$\dot{\sigma}^* = sAx + sbu + sbe + \sigma(0)\alpha e^{-\alpha t} \tag{2.27}$$

selecting control,

$$u = u_{eq} + u_n \tag{2.28}$$

$$\dot{\sigma}^* = sAx + sbu_{eq} + sbu_n + sbe + \sigma(0)\alpha e^{-\alpha t} \tag{2.29}$$

$$u_{eq} = -(sb)^{-1}(sAx + \sigma(0)\alpha e^{-\alpha t} + k\sigma^*) \tag{2.30}$$

Working on lines similar to Section 2.4, it is straightforward to obtain,

$$u_n = -(sb)^{-1}\frac{1}{\tau}\left[\sigma^* + k\int \sigma^*\right] \tag{2.31}$$

Remark 2.2 *The equation* (2.31) *implies that even for small* τ*,* u_n *is not large, since* σ^* *is small for all* $t \geq 0$*. It may be noted that* u *is continuous for all* $t \geq 0$ *and therefore the control is chatter free.*

Remark 2.3 *The control developed in this section is different from the one developed in Shendge and Patre (2007). The definition of sliding variable is different and while the control in Shendge and Patre (2007) requires real time integration to find the values of sliding variable, the proposed control does not require such an integration.*

2.4.3 Control using second order UDE

With reference to Remark 2.1, the accuracy of estimation can be improved by using a second order UDE. The uncertainty (e) and its derivative ($\dot{e}$) can be estimated by using a second order filter of the form,

$$G_f(s) = \frac{1 + 2\tau s}{\tau^2 s^2 + 2\tau s + 1} \tag{2.32}$$

where τ is a small positive constant.

Using (2.27), (2.28) and (2.30)

$$\dot{\sigma}^* = sbu_n + sbe - k\sigma^* \tag{2.33}$$

$$e = (sb)^{-1}(\dot{\sigma}^* + k\sigma^*) - u_n \tag{2.34}$$

Using (2.16), (2.20) and (2.34),

$$u_n = -(sb)^{-1}(\dot{\sigma}^* + k\sigma^*)\frac{G_f(s)}{1 - G_f(s)} \tag{2.35}$$

With $G_f(s)$ as in (2.32),

$$u_n = -(sb)^{-1}\left(\frac{2}{\tau}\sigma^* + \frac{2\tau k + 1}{\tau^2}\int_0^t \sigma^* + \frac{k}{\tau^2}\int_0^t\int_0^t \sigma^*\right) \tag{2.36}$$

It is worth noting that, the design can be easily extended to any n^{th} order filter to improve the estimation accuracy and thereby mitigate chatter.

2.5 Proposed Control

The proposed boundary layer sliding mode control for chatter reduction can be written as,

1. for 1st order UDE,

$$u_{eq} = -(sb)^{-1}(sAx + \sigma(0)\alpha e^{-\alpha t} + k\sigma^*) \tag{2.37}$$

$$u_n = \begin{cases} -\rho\,\mathrm{sgn}(\sigma sb), & |\sigma sb| > \epsilon \\ -(sb)^{-1}\dfrac{1}{\tau}\left(\sigma^* + k\displaystyle\int \sigma^*\right), & |\sigma sb| \le \epsilon \end{cases} \tag{2.38}$$

2. for 2nd order UDE,

$$u_{eq} = -(sb)^{-1}(sAx + \sigma(0)\alpha e^{-\alpha t} + k\sigma^*) \tag{2.39}$$

$$u_n = \begin{cases} -\rho\,\mathrm{sgn}(\sigma sb), & |\sigma sb| > \epsilon \\ -(sb)^{-1}\left(\dfrac{2}{\tau}\sigma^* + \dfrac{2\tau k + 1}{\tau^2}\displaystyle\int_0^t \sigma^* + \dfrac{k}{\tau^2}\int_0^t\int_0^t \sigma^*\right), & |\sigma sb| \le \epsilon \end{cases} \tag{2.40}$$

2.6 Stability

The estimation error $\tilde{e}$ and sliding variable σ are ultimately bounded. Here the general case when $j = 1$ in (2.15) is considered. The bounds on $\tilde{e}$ and σ are found by considering the Lyapunov function as,

$$V(\sigma, \tilde{e}) = \frac{1}{2}\sigma^2 + \frac{1}{2}\tilde{e}^2 \tag{2.41}$$

Taking derivative of $V(\sigma, \tilde{e})$ along (2.24) and (2.25),

$$\begin{aligned} \dot{V}(\sigma, \tilde{e}) &= -k\sigma^2 + s\, b\, \sigma\, \tilde{e} - \frac{1}{\tau}\tilde{e}^2 + \tilde{e}\, \dot{e} && (2.42) \\ &\leq -k\sigma^2 + |sb|\, |\sigma|\, \|\tilde{e}\| - \frac{1}{\tau}\|\tilde{e}\|^2 + \|\tilde{e}\|\, \mu && (2.43) \end{aligned}$$

Using Young's inequality (*Trench*, 2003),

$$ab \leq \frac{a^2 + b^2}{2}$$

for any real a and b, one can obtain,

$$\dot{V}(\sigma, \tilde{e}) \leq -k\sigma^2 + \frac{|sb|}{2}\left(|\sigma|^2 + \|\tilde{e}\|^2\right) - \frac{1}{\tau}\|\tilde{e}\|^2 + \|\tilde{e}\|\, \mu \tag{2.44}$$

$$\dot{V}(\sigma, \tilde{e}) \leq -|\sigma|^2 \left(k - \frac{|sb|}{2}\right) - \|\tilde{e}\|^2 \left(\frac{1}{\tau} - \frac{|sb|}{2}\right) + \|\tilde{e}\|\, \mu \tag{2.45}$$

$$\dot{V}(\sigma, \tilde{e}) \leq -|\sigma|^2 \left(k - \frac{|sb|}{2}\right) - \|\tilde{e}\| \left[\|\tilde{e}\| \left(\frac{1}{\tau} - \frac{|sb|}{2}\right) - \mu\right] \tag{2.46}$$

With $\left(k - \frac{|sb|}{2}\right) > 0$ and $\left(\frac{1}{\tau} - \frac{|sb|}{2}\right) > 0$, the system will be ultimately bounded. Using (2.46), the bound on $\tilde{e}$ works out to be,

$$\|\tilde{e}\| \leq \frac{\mu}{\left(\frac{1}{\tau} - \frac{|sb|}{2}\right)} \tag{2.47}$$

Similarly the bound on σ works out to be,

$$|\sigma| \leq \frac{|sb|\mu}{k\left(\frac{1}{\tau} - \frac{|sb|}{2}\right)} \tag{2.48}$$

Thus $\|\tilde{e}\|$ and $|\sigma|$ are ultimately bounded and the bounds can be lowered using control parameters k and τ.

2.7 Numerical Example

Consider an uncertain plant,

$$\dot{x} = Ax + bu + \Delta Ax + \Delta bu + d(t) \tag{2.49}$$

with,

$$A = \begin{bmatrix} 0 & 1 \\ -2 & -3 \end{bmatrix} \quad b = \begin{bmatrix} 0 \\ 1 \end{bmatrix} \quad \Delta A = \begin{bmatrix} 0 & 0 \\ -1 & -2 \end{bmatrix} \quad \Delta b = \begin{bmatrix} 0 \\ -0.4 \end{bmatrix}$$

where ΔA and Δb are the uncertainties in the plant.

The disturbances considered are sinusoidal and sawtooth as shown in Fig. 2.1

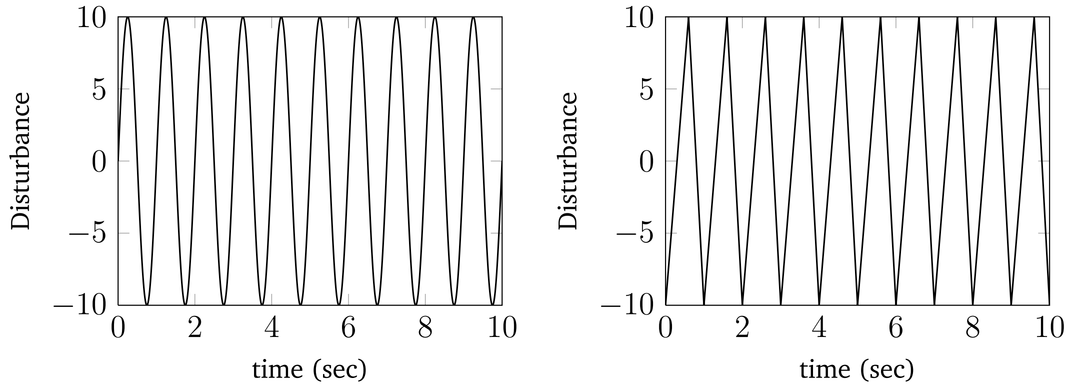

(a) sinusoidal (b) triangular

Figure 2.1: Disturbances considered

The initial conditions for the plant are $x_0 = [1 \quad 0]^T$. The sliding plane used is $\sigma = 4x_1 + x_2$ and control gain is $k = 5$.

The control proposed in section 2.5 is tested on the illustrative example described. The results are verified for three different cases. The discontinuous control is approximated with continuous approximation inside the boundary layer.

The approximations used are, *sat* function, first order UDE and second order UDE. The well known trade-off between smoothing and invariance is verified. The effect of smoothing functions on chatter mitigation is validated.

Case 1 : *sat* function inside boundary layer

The control performance is illustrated in Fig. 2.2 for a sinusoidal disturbance and boundary layer width of $\epsilon = 0.02$. The control scheme uses *sat* function inside the boundary layer.

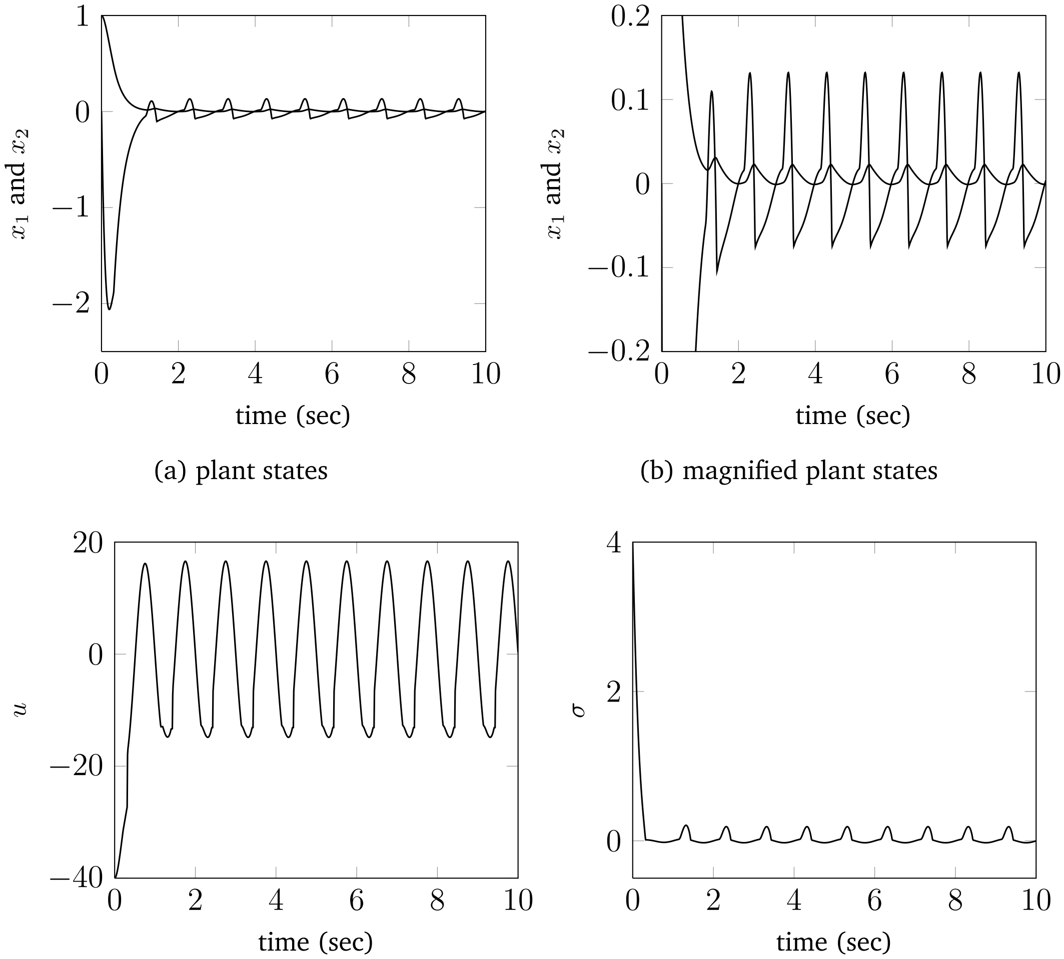

(a) plant states (b) magnified plant states

(c) control (d) sliding variable

Figure 2.2: Control performance with *sat* function

The states are shown in Fig. 2.2(a), while a magnified view of the same graph is shown in Fig. 2.2(b). It can be seen that, evolution of states inside the boundary layer depends on the disturbance acting. The control is shown in Fig. 2.2(c) and the sliding variable is shown in Fig. 2.2(d). The chattering is evident in Fig. 2.2(d). The results are similar for triangular disturbance as well.

The trade-off between smoothing and invariance is verified for varying values of ϵ; for both sinusoidal as well as sawtooth disturbance. It is clearly evident that, the chatter is dependent on value of ϵ. The RMS values of σ for different values of ϵ are tabulated in Table 2.1.

Table 2.1: Variation in σ for different values of ϵ

Boundary layer width – ϵ	RMS value of σ	
	for sinusoidal	for sawtooth
0.02	0.0004524	0.02545
0.2	0.03646	0.1908
2	0.5244	0.4639

Case 2 : first order UDE inside boundary layer

The *sat* function is replaced by a first order UDE with time constant τ. The sliding plane is modified as $\sigma^* = \sigma - \sigma(0)\, e^{-\alpha t}$ so that initial control is within limits. The Fig. 2.3 shows that, the modified sliding variable ($\sigma^* = \sigma - \sigma(0)\, e^{-\alpha t}$) significantly reduces the initial control as compared to conventional sliding plane ($\sigma = sx$).

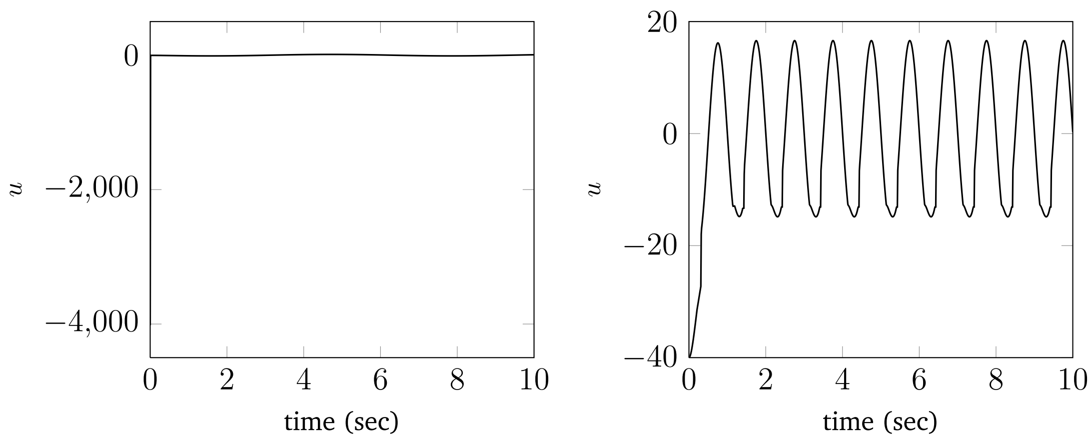

(a) Conventional sliding plane

(b) Modified sliding plane

Figure 2.3: Comparison of control

The control performance with a first order UDE inside the boundary layer is illustrated in Fig. 2.4 for a sinusoidal disturbance. The filter time-constant $\tau = 0.001$ s and boundary layer width is $\epsilon = 0.02$.

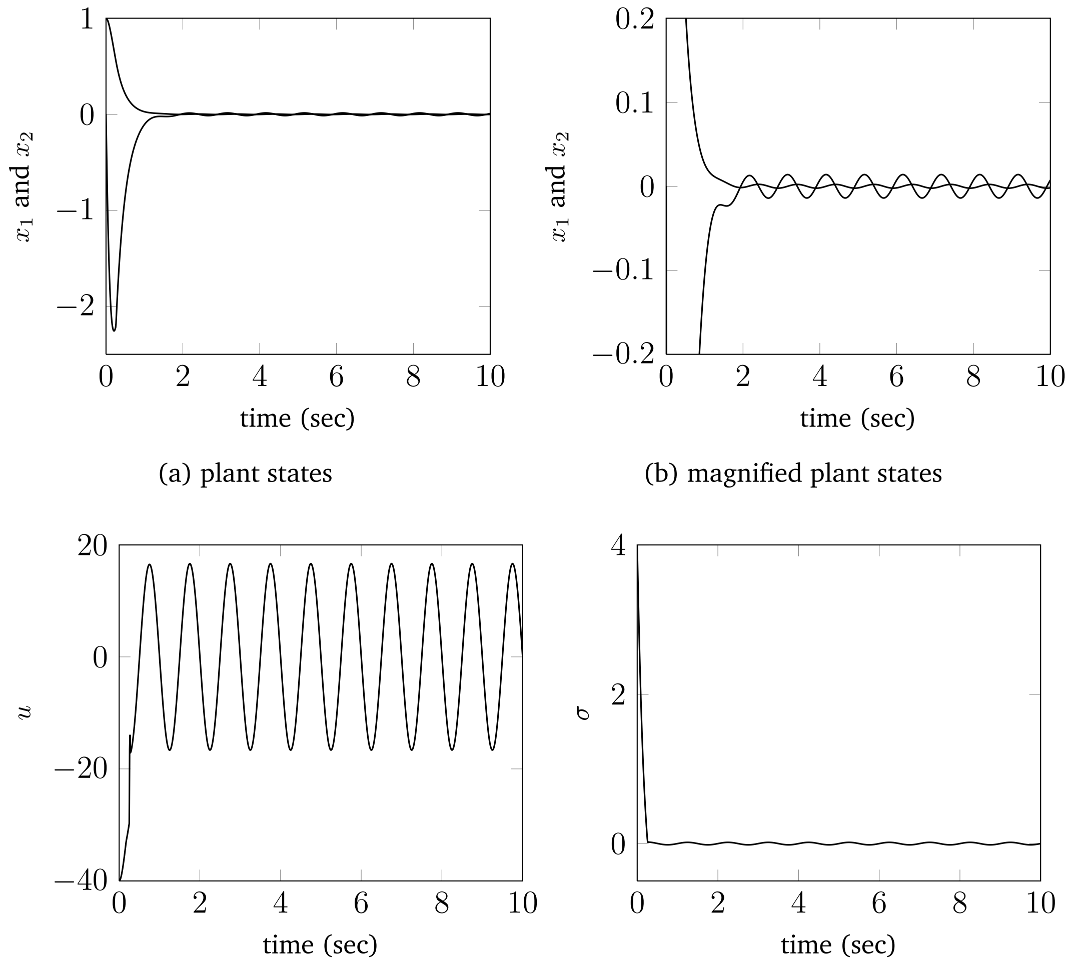

(a) plant states (b) magnified plant states

(c) control (d) sliding variable

Figure 2.4: Control performance with *first order UDE*

The states are shown in Fig. 2.4(a), while a magnified view of the same graph is shown in Fig. 2.4(b). The control is shown in Fig. 2.4(c) and the sliding variable is shown in Fig. 2.4(d). It can be seen that, evolution of states inside the boundary layer depends on the disturbance. The results clearly demonstrate that, use of first order UDE in comparison to *sat* function reduces the chatter by a substantial amount. The results are similar for triangular disturbance as well.

The RMS values of σ with modified sliding plane and first order UDE, for $\epsilon = 0.02$ in Table 2.2 validates the same.

Table 2.2: Variation in σ with first order UDE

Time constant	RMS value of σ	
τ	for sinusoidal	for sawtooth
0.001	0.0001926	0.01641
0.01	0.01697	0.1434
0.1	0.4947	0.5625

The value of τ has a direct effect on chatter mitigation, for a given boundary layer width ϵ. The value of τ directly affects the accuracy of uncertainty estimation and consequently decides the achievable chatter reduction. The same is demonstrated in Fig. 2.5.

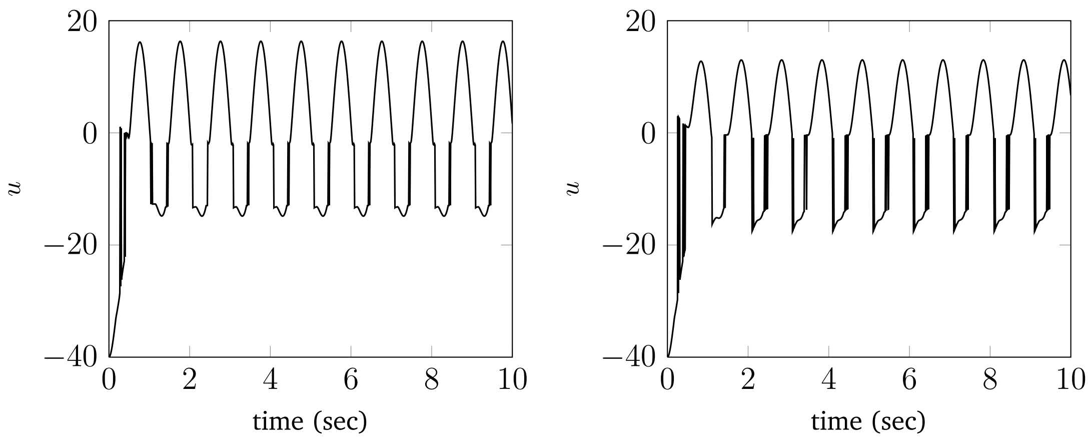

(a) first order UDE ($\tau = 0.01\,s$) (b) first order UDE ($\tau = 0.1\,s$)

Figure 2.5: Effect of τ (first order filter) on chatter mitigation

The Fig. 2.5 shows control signal for 2-different values of τ. It is evident from Fig. 2.5(a) and Fig. 2.5(b) that, the chatter is reduced as filter time-constant (τ) is changed from 0.1 to 0.01 s.

Case 3 : second order UDE inside boundary layer

The results with a second order filter for $\tau = 0.001$ s are shown in Fig. 2.6. The filter time-constant $\tau = 0.001$ s and boundary layer width is $\epsilon = 0.02$.

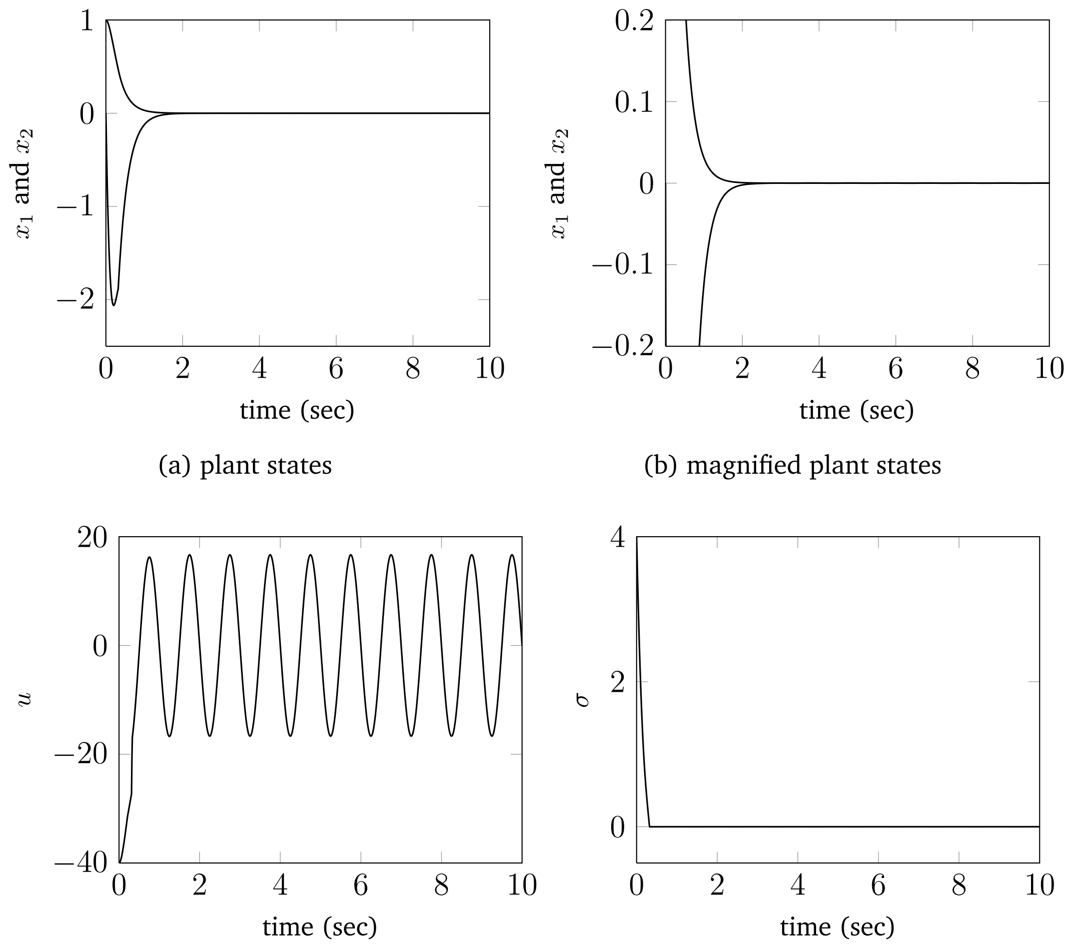

(a) plant states

(b) magnified plant states

(c) control

(d) sliding variable

Figure 2.6: Control performance with *second order UDE*

The states are shown in Fig. 2.6(a), while a magnified view of the same graph is shown in Fig. 2.6(b). The control is shown in Fig. 2.6(c) and the sliding variable is shown in Fig. 2.6(d). It can be seen that, evolution of states inside the boundary layer depends on the disturbance. The results clearly demonstrate that, use of second order UDE in comparison to first order UDE reduces the chatter by a substantial amount. The results are similar for triangular disturbance as well.

It is evident from Fig. 2.4(d) and Fig. 2.6(d), that chattering is significantly reduced. The disturbance considered in these results is sinusoidal. The same results are observed for constant as well as sawtooth disturbance.

The value of τ and order of filter directly affect the accuracy of uncertainty estimation and consequently affect the achievable chatter reduction. The same can be seen in Fig. 2.7.

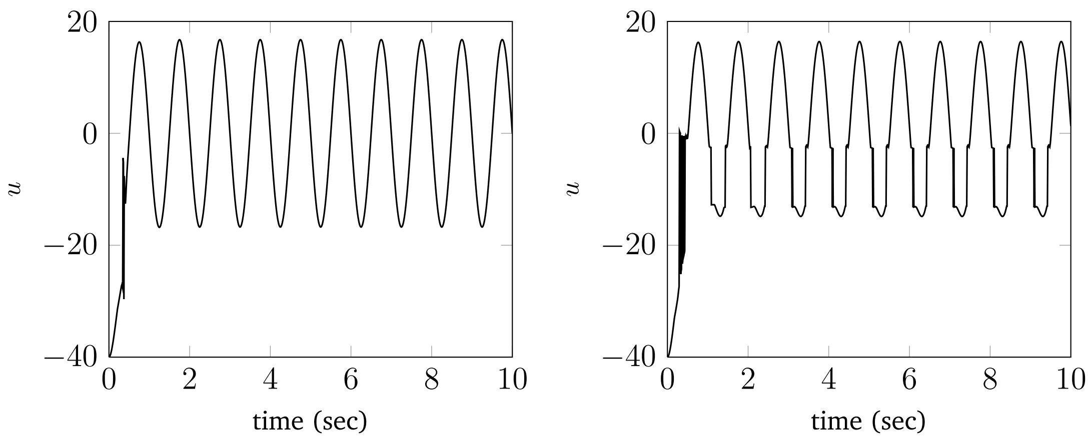

(a) second order UDE ($\tau = 0.01\,s$) (b) second order UDE ($\tau = 0.1\,s$)

Figure 2.7: Effect of τ and filter order on chatter mitigation

The RMS values of σ with $\epsilon = 0.02$ clearly demonstrates that, UDE scores in comparison with *sat* function. The chatter is reduced as the order of UDE is increased. The value of $\tau = 0.001\,s$ and sinusoidal disturbance is considered.

Table 2.3: Variation in σ with different approximations

Approximation	RMS value of σ
sat function	4.524×10^{-4}
first order UDE	1.926×10^{-4}
second order UDE	6.475×10^{-5}

2.8 Application: Flexible Joint System

The problem of joint flexibility is very crucial in manipulator design. This joint flexibility is typically on account of gear elasticity, shaft windup, etc., and is important in the derivation of control law. Unwanted oscillations due to joint flexibility impose bandwidth limitations on all algorithm designs based on rigid robots, and may create stability problems for feedback controls that neglect joint flexibility. A ESO based control for trajectory tracking of a flexible joint robotic system is proposed in (*Talole et al.*, 2010a). Controller design based on adaptation (*Ghorbel et al.*, 1989), adaptive sliding mode (*Farooq et al.*, 2008) and back-stepping (*Oh and Lee*, 1997) are some other approaches reported.

The present assignment deals with a model following SMC for control of flexible joint manipulator with uncertainty and disturbance. A nonlinear disturbance is considered here and the plant model is controlled to follow the desired states. The UDE is used to estimate uncertainty and disturbance.

The dynamic equations of motion for Quanser's Flexible Joint module as given in (*Quanser*, 2008) are,

$$\left.\begin{array}{rcl} \ddot{\theta} + F_1\dot{\theta} - \dfrac{K_{\text{stiff}}}{J_{\text{eq}}}\alpha & = & F_2 V_m \\ \ddot{\theta} - F_1\dot{\theta} + \dfrac{K_{\text{stiff}}(J_{\text{eq}} + J_{\text{arm}})}{J_{\text{eq}}J_{\text{arm}}}\alpha & = & -F_2 V_m \end{array}\right\} \tag{2.50}$$

where,

$$F_1 \triangleq \frac{\eta_m \eta_g K_t K_m K_g^2 + B_{\text{eq}} R_m}{J_{\text{eq}} R_m} \quad \text{and}$$

$$F_2 \triangleq \frac{\eta_m \eta_g K_t K_m}{J_{\text{eq}} R_m}$$

The parameters are : θ is motor load angle, α is link joint deflection, η_m is motor efficiency, η_g is gearbox efficiency, K_t is motor torque constant, K_m is back EMF constant, K_g is gearbox ratio, B_{eq} is viscous damping coefficient, R_m is armature resistance, J_{eq} is gear inertia, K_{stiff} is spring stiffness, J_{arm} is link inertia, and V_m is motor control voltage.

Considering the output of system as $y = \theta + \alpha$, the dynamics (2.50) can be rewritten in terms of y and θ as,

$$\ddot{y} = \frac{K_{\text{stiff}}}{J_{\text{eq}}} F_3 y - \frac{K_{\text{stiff}}}{J_{\text{eq}}} F_3 \theta \tag{2.51}$$

$$\ddot{\theta} = \frac{K_{\text{stiff}}}{J_{\text{eq}}} y - \frac{K_{\text{stiff}}}{J_{\text{eq}}} \theta - F_1 \dot{\theta} + F_2 V_m \tag{2.52}$$

where $F_3 \triangleq \left(1 - \frac{J_{\text{eq}} + J_{\text{arm}}}{J_{\text{arm}}}\right)$.

Defining the state variables as, $x_1 = y$, $x_2 = \dot{y} = \dot{x}_1$, $x_3 = \theta$, $x_4 = \dot{\theta} = \dot{x}_3$, the dynamics (2.51)–(2.52) become,

$$\left.\begin{aligned}
\dot{x}_1 &= x_2 \\
\dot{x}_2 &= \frac{K_{\text{stiff}}}{J_{\text{eq}}} F_3 (x_1 - x_3) \\
\dot{x}_3 &= x_4 \\
\dot{x}_4 &= \frac{K_{\text{stiff}}}{J_{\text{eq}}} (x_1 - x_3) - F_1 x_4 + F_2 V_m
\end{aligned}\right\} \tag{2.53}$$

The state space form for (2.53) can be written as,

$$\dot{x} = A\,x + B\,V_m \tag{2.54}$$

where, $\dot{x} = [\dot{x}_1 \quad \dot{x}_2 \quad \dot{x}_3 \quad \dot{x}_4]^T$

$$A = \begin{bmatrix} 0 & 1 & 0 & 0 \\ \frac{K_{\text{stiff}}}{J_{\text{eq}}} F_3 & 0 & -\frac{K_{\text{stiff}}}{J_{\text{eq}}} F_3 & 0 \\ 0 & 0 & 0 & 1 \\ \frac{K_{\text{stiff}}}{J_{\text{eq}}} F_3 & 0 & -\frac{K_{\text{stiff}}}{J_{\text{eq}}} F_3 & -F_1 \end{bmatrix} \qquad B = \begin{bmatrix} 0 \\ 0 \\ 0 \\ F_2 \end{bmatrix}$$

The relative output y is differentiated to get desired output. The system (2.54) is converted to phase variable form, to satisfy the model-following condition.

Using the transformation,

$$Z = Tx$$

Then the Eq. (2.54) can be written as in (*Talole et al.*, 2010a),

$$\dot{z} = A\,z + B\,V_m \tag{2.55}$$

where, $\dot{z} = [\dot{z}_1 \quad \dot{z}_2 \quad \dot{z}_3 \quad \dot{z}_4]^T$

$$A = \begin{bmatrix} 0 & 1 & 0 & 0 \\ 0 & 0 & 1 & 0 \\ 0 & 0 & 0 & 1 \\ 0 & -\dfrac{K_{\text{stiff}}F_1}{J_{\text{arm}}} & -\dfrac{K_{\text{stiff}}(J_{\text{eq}}+J_{\text{arm}})}{J_{\text{eq}}J_{\text{arm}}} & -F_1 \end{bmatrix} \qquad B = \begin{bmatrix} 0 \\ 0 \\ 0 \\ \dfrac{K_{\text{stiff}}F_2}{J_{\text{arm}}} \end{bmatrix}$$

The nominal values of various parameters of flex-joint are from (*Quanser*, 2008) as: K_{stiff}=1.248 Nm/rad, η_m=0.69, η_g=0.9, K_t=0.00767 Nm, $K_g = 70$, R_m=2.6 Ω, J_{eq}=0.00258 kgm^2, J_{arm}=0.00352 kgm^2.

$$\begin{bmatrix} \dot{x}_1 \\ \dot{x}_2 \\ \dot{x}_3 \\ \dot{x}_4 \end{bmatrix} = \begin{bmatrix} 0 & 1 & 0 & 0 \\ 0 & 0 & 1 & 0 \\ 0 & 0 & 0 & 1 \\ 0 & -10007 & -837 & -28 \end{bmatrix} \begin{bmatrix} x_1 \\ x_2 \\ x_3 \\ x_4 \end{bmatrix} + \begin{bmatrix} 0 \\ 0 \\ 0 \\ 10007 \end{bmatrix} V_m \tag{2.56}$$

The model to be followed is assumed as;

$$\begin{bmatrix} \dot{x}_{m_1} \\ \dot{x}_{m_2} \\ \dot{x}_{m_3} \\ \dot{x}_{m_4} \end{bmatrix} = \begin{bmatrix} 0 & 1 & 0 & 0 \\ 0 & 0 & 1 & 0 \\ 0 & 0 & 0 & 1 \\ 0 & -560 & -320 & -85 \end{bmatrix} \begin{bmatrix} x_{m_1} \\ x_{m_2} \\ x_{m_3} \\ x_{m_4} \end{bmatrix} + \begin{bmatrix} 0 \\ 0 \\ 0 \\ 160 \end{bmatrix} V_m \tag{2.57}$$

The initial conditions of plant are $x(0) = [0 \quad 0 \quad 0 \quad 0]$ and initial conditions of model are $x_m(0) = [0 \quad 0 \quad 0 \quad 0]$. The disturbance $d(t) = 2\sin(t)$, and uncertainty in the plant is 40%.

The simulation results are shown in Fig. 2.8 – Fig. 2.9 for $\tau = 10\,ms$ and $\tau = 1\,ms$ respectively. The value of $k = 5$ is considered.

Fig. 2.8(a)–2.8(d) and Fig. 2.9(a)–2.9(d) depict the plant and model states i.e. displacement, velocity, acceleration and jerk. The control torque required and sliding variable (σ) are also shown.

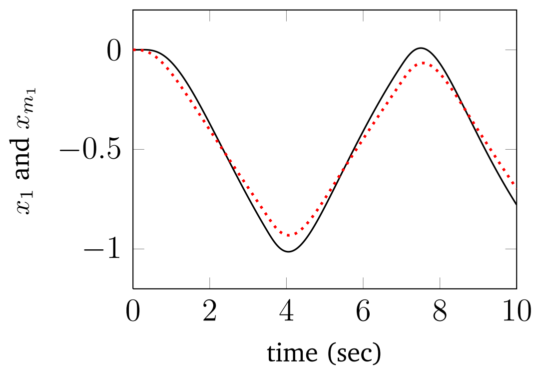

(a) plant (-) and model (...) state x_1

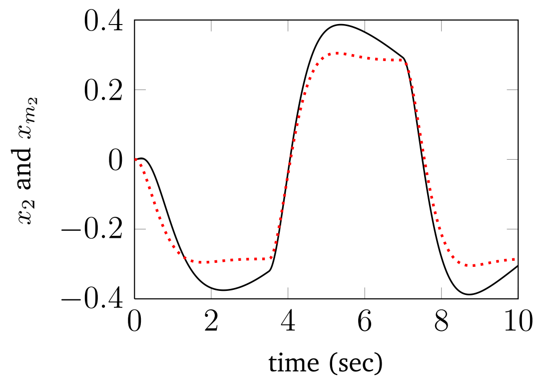

(b) plant (-) and model (...) state x_2

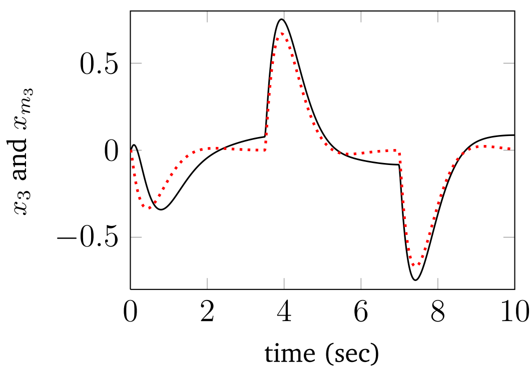

(c) plant (-) and model (...) state x_3

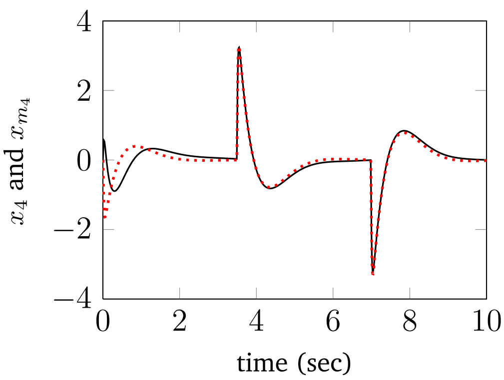

(d) plant (-) and model (...) state x_4

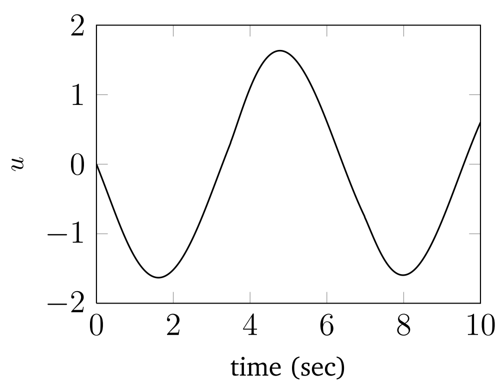

(e) control

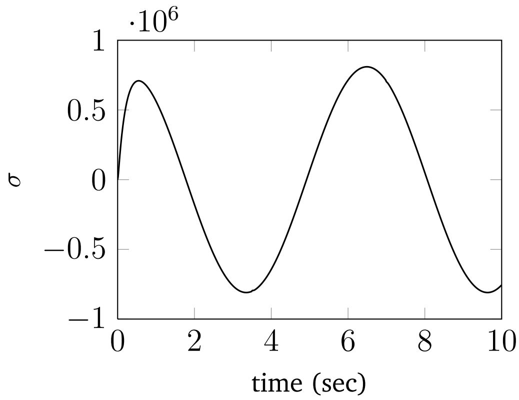

(f) sliding variable

Figure 2.8: Tracking performance with τ=10 ms

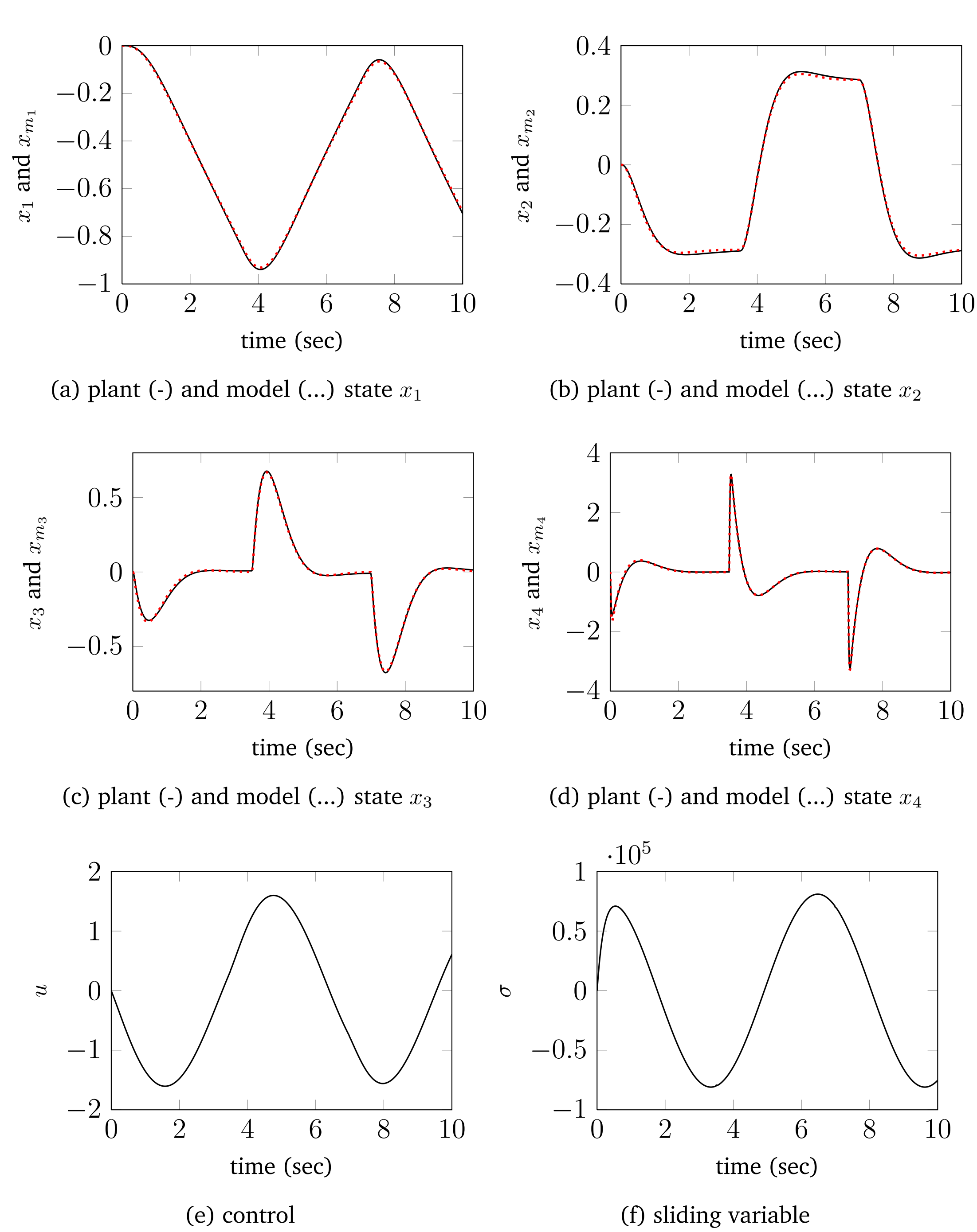

(a) plant (-) and model (...) state x_1

(b) plant (-) and model (...) state x_2

(c) plant (-) and model (...) state x_3

(d) plant (-) and model (...) state x_4

(e) control

(f) sliding variable

Figure 2.9: Tracking performance with τ=1 ms

The figures reveal ability of control, to drive the system to follow the reference model. It is easily observed that system is robust even in presence of parameter variations and external disturbance. The tracking and robustness is improved as τ is decreased from 10 ms to 1 ms.

2.9 Summary

A new boundary layer sliding mode control design for mitigation of chatter is proposed. The control scheme uses a discontinuous control outside the boundary layer and switches over to UDE based control inside. The use of UDE gives a better trade-off inside the boundary layer and this trade-off is improved by using a higher order UDE. The initial control is ensured within limits, irrespective of the uncertainty. The results show improvement to the tune of 20% to 40% over the conventional chatter control method using *'sat'* function inside boundary layer.

It is proved that the ultimate boundedness of uncertainty estimation error and sliding variable inside the boundary layer is guaranteed, and that the bounds can be lowered by appropriate choice of design parameters. The results are verified by computer simulation on an illustrative example. The efficacy of the design is also confirmed on an application to flexible joint system in robotic control.

Chapter 3

SMC for a Class of Nonlinear System using UDE

The chapter details design and validation of a robust SMC strategy for a class of uncertain system; where control appears through a nonlinear function. The control law is synthesized by estimating the states and uncertainties using UDE.

The motivation and idea is introduced in section 3.1. Section 3.2 describes the problem formulation with necessary assumptions. The design of model-following control is elaborated in section 3.3 followed by uncertainty estimation in section 3.4. The design of observer is explained next in section 3.5. Section 3.6 elaborates the Lyapunov stability analysis. The performance is illustrated by a numerical example in section 3.7 followed by application to inverted pendulum system in section 3.8. The chapter concludes with a summary in Section 3.9.

3.1 Introduction

The current sliding-mode strategies are concerned mostly with uncertain systems that are linear in the input. This formulation restricts the application potential of SMC. The systems with an input nonlinearity are usually approached by introducing a coordinate transformation (*Decarlo et al.*, 1988; *Gutierrez and Rio*, 1998) or exact linearization (*Molero et al.*, 2008). The robustness is a concern and may result in performance degradation and in some cases even to instability. A modified sliding condition combined with equivalent control (*Gutierrez and Rio*, 2005) can improve robustness. A finite-time controller (*Aghababa and Aghababa*, 2012) is introduced for synchronization of two different uncertain chaotic systems with input nonlinearities. The control however is discontinuous and requires the bounds of uncertainty.

The parametric uncertainties (*Slotine and Coetsee*, 1986) or the bounds of uncertainties (*Yoo and Chung*, 1992a) can be estimated adaptively and combined with SMC for robust performance. The uncertainties can be adaptively estimated using fuzzy and neural network (*Lin et al.*, 2007a; *Buckner*, 2002; *Fei and Ding*, 2012). The adaptive estimation algorithms can effectively take care of structured uncertainties; however sensor error or accumulation of numerical error may lead the system towards instability (*Wheeler et al.*, 1998).

A control design augmented by the estimates of uncertainties and disturbances can effectively alleviate the problem. In this design, the effect of uncertainties is compensated by augmenting the controller designed for nominal system with the estimates. The UDE (*Zhong and Rees*, 2004) is an effective technique for estimating slow varying uncertainties. This method has been applied to linear and nonlinear systems with state delays (*Stobart et al.*, 2011; *Kuperman and Zhong*, 2011) and input-output linearisation (*Talole and Phadke*, 2009).

In this work, SMC combined with UDE is extended to an uncertain system with control appearing through a nonlinear function as in (*Gutierrez and Rio*, 2005; *Han and Chen*, 1995). This formulation appears in many applications like motion control (*Sabanovic*, 2011), magnetic levitation (*Lin et al.*, 2007a; *Molero et al.*, 2008) underwater vehicles (*Cheng et al.*, 2007), vehicle control (*Canale et al.*, 2008), underactuated systems (*Almutaitri and Zribi*, 2010). The robustness is assured through UDE, that estimates the lumped uncertainty comprising of uncertainty in plant as well as input matrix and unknown disturbance. The developed strategy is applied to a representative nonlinear example as in (*Chang and Lee*, 1994) and a benchmark inverted pendulum problem (*Slotine and Li*, 1991). The system considered here covers a large class of practical applications.

3.2 Problem Formulation

Consider a non-linear single input, single output uncertain system given by,

$$\dot{x} = f(x,t) + g(x,t)u + \Delta f(x,t) + \Delta g(x,t)u + d(x,t) \tag{3.1}$$

where
$x \,\epsilon\, \mathbb{R}^n$ is the state vector and $u \,\epsilon\, \mathbb{R}^1$ is the control input
$f(x,t)$ and $g(x,t)$ is known nonlinear system and input vector respectively
$\Delta f(x,t)$ & $\Delta g(x,t)$ are uncertainties in plant and input vector respectively
$d(x,t) \,\epsilon\, \mathbb{R}^n$ is unmeasurable disturbance

Assumption 3.1 *The uncertainties $\Delta f(x,t), \Delta g(x,t)$ and disturbance $d(x,t)$ satisfy the matching conditions given by,*

$$\left.\begin{array}{rcl} \Delta f(x,t) & = & g(x,t) \cdot e_f(x,t) \\ \Delta g(x,t) & = & g(x,t) \cdot e_g(x,t) \\ d(x,t) & = & g(x,t) \cdot e_d(x,t) \end{array}\right\} \tag{3.2}$$

where e_f, e_g and e_d are unknown.

The equation (3.2) is the well known matching condition required for guaranteeing invariance. It is an explicit statement of the structural constraint stated in (*Drazenovic*, 1969).

Using the Assumption 3.1, the uncertainty and disturbances can be combined into a lumped uncertainty term $e(x,u,t) \,\epsilon\, \mathbb{R}^1$ and is given as,

$$e(x,u,t) = e_f(x,t) + e_g(x,t)u + e_d(x,t) \tag{3.3}$$

The system (3.1) can now be rewritten as,

$$\dot{x} = f(x,t) + g(x,t)u + g(x,t)e_f(x,t) + g(x,t)e_g(x,t)u + g(x,t)e_d(x,t) \tag{3.4}$$

Therefore,

$$\dot{x} = f(x,t) + g(x,t)u + g(x,t) \cdot e(x,u,t) \tag{3.5}$$

Assumption 3.2 *The lumped uncertainty $e(x, u, t)$ is continuous and satisfies,*

$$\left|\frac{d^{(j)}e(x,u,t)}{dt^{(j)}}\right| \leq \mu \qquad \textit{for } j = 0, 1, 2, \ldots, r \tag{3.6}$$

where μ is a small positive number.

Remark 3.1 *The Assumption 3.2 implies that the uncertainty $e(x, u, t)$ and its derivatives up to some finite order (r) be bounded but the bound is not required to be known. The assumption includes a fairly large class of uncertainties and disturbances that can be estimated by UDE described in Section 3.4.*

A model following control is to be designed for the uncertain plant (3.5), such that it follows the desired model given by,

$$\dot{x_m} = A_m x_m + b_m u_m \tag{3.7}$$

where $x_m \,\epsilon\, \mathbb{R}^n$ is the model state, $u_m \,\epsilon\, \mathbb{R}^1$ is the reference input and A_m, b_m are user selected matrix of suitable dimensions such that (3.7) gives the desired response. The following assumption is needed on the structure of the model to ensure perfect model following.

Assumption 3.3

$$\left.\begin{array}{lcl} f(x,t) - A_m x & = & g(x,t) \cdot L \\ b_m & = & g(x,t) \cdot M \end{array}\right\} \tag{3.8}$$

where L and M are suitable known matrices of appropriate dimensions.

The objective is to design a control u such that, the uncertain plant (3.5) follows the desired model (3.7) inspite of uncertainties and disturbances represented by $e(x, u, t)$. The control is expected to ensure robust performance for varying cases.

The control is to be designed initially, by assuming that the plant states x are available. However, the issue of non-availability of states is also expected to be addressed. An observer to estimate states in the presence of parametric uncertainties and disturbances is required; and UDE is to be utilized for estimation of states and disturbances. The estimated states and disturbances are to be employed to synthesize a robust observer-controller structure.

3.3 Design of Control

A model following control is designed, based on the sliding surface of Ackermann (*Ackermann and Utkin*, 1998). The control is designed to ensure sliding; and the choice of sliding surface ensures that, plant follows the desired model. The control is initially designed, by assuming that the plant states x are available.

3.3.1 Sliding Surface

The sliding surface is defined as,

$$\sigma = b^T x + z, \qquad z(0) = -b^T x(0) \tag{3.9}$$

where $b = [0 \quad 1]^T$. The auxiliary variable z is defined as,

$$\dot{z} = -b^T A_m x - b^T b_m u_m \tag{3.10}$$

A sliding surface of (3.9) gives full order sliding and eliminates reaching phase (*Ackermann and Utkin*, 1998). It can be easily verified that, with this sliding surface and auxiliary variable dynamics (3.10), when σ goes to 0, the plant follows the desired model. The implication of this is,

$$\dot{\sigma} = b^T(\dot{x} - A_m x - b_m u_m) \tag{3.11}$$

Therefore,

$$\dot{x} = A_m x + b_m u_m \tag{3.12}$$

3.3.2 Model Following Control

A control is designed such that, the sliding condition is satisfied and the plant follows the desired model. The control u, is designed as $u = u_{eq} + u_n$ with u_{eq} catering to the nominal (known) terms and u_n to take care of uncertainty in (3.15). Differentiating (3.9) and using (3.5) and (3.10),

$$\begin{aligned} \dot{\sigma} \quad &= \quad b^T\left[f(x,t) + g(x,t)u + g(x,t)e(x,u,t)\right] \\ &\quad -b^T A_m x - b^T b_m u_m \end{aligned} \tag{3.13}$$

Using (3.8) in (3.13) and writing a simplified representation,

$$\begin{aligned} \dot{\sigma} &= b^T(f - A_m x) + b^T g u + b^T g e - b^T b_m u_m \quad (3.14) \\ &= b^T g L + b^T g u + b^T g e - b^T g M u_m \quad (3.15) \end{aligned}$$

Let the control u be expressed as,

$$u = u_{eq} + u_n \quad (3.16)$$

Therefore,

$$\dot{\sigma} = b^T g L + b^T g u_{eq} + b^T g u_n + b^T g e - b^T g M u_m \quad (3.17)$$

$$\dot{\sigma} = b^T g(L + u_{eq} + u_n + e - M u_m) \quad (3.18)$$

Selecting,

$$u_{eq} = -L + M u_m - (b^T g)^{-1} k\sigma \quad (3.19)$$

where k is a positive constant.

Using (3.16) and (3.19) in (3.15),

$$\dot{\sigma} = b^T g u_n + b^T g e(x, u, t) - k\sigma \quad (3.20)$$

The control strategy is to estimate $e(x, u, t)$ as $\hat{e}(x, u, t)$ (3.24) using UDE and use $-\hat{e}(x, u, t)$ as a component in control; to cancel the effect of $e(x, u, t)$.

Therefore, let,

$$u_n = -\hat{e}(x, u, t) \quad (3.21)$$

Using (3.21) in (3.20),

$$\dot{\sigma} = -k\sigma + b^T g\tilde{e}(x, u, t) \quad (3.22)$$

with

$$\tilde{e}(x, u, t) = e(x, u, t) - \hat{e}(x, u, t) \quad (3.23)$$

Remark 3.2 *It is seen from* (3.22) *that, as* $\tilde{e} \to 0$*, i.e.* $\hat{e}(x, u, t) \approx e(x, u, t)$*, sliding condition is satisfied and* σ *will asymptotically approach 0, if* $k > 0$*. This implies that the uncertain plant follows the desired model i.e.* $\dot{x} = A_m x + b_m u_m$

It may be noted that, such a control u_n can be designed, only if a good estimate of e is available. The estimation of lumped disturbance using the method of UDE is utilized. The estimate ($\hat{e}$) is obtained by passing lumped uncertainty (e) through an inertial filter $G_f(s)$ and the same is described in next section.

3.4 Estimation of Uncertainty

The UDE algorithm is based on the assumption that a signal can be approximated and estimated using a filter with the right bandwidth. The opposite of estimate is used in control to negate the effect of the uncertainty (*Talole and Phadke*, 2008). The lumped uncertainty $e(x, u, t)$ can be estimated as,

$$\hat{e}(x, u, t) = G_f(s)\, e(x, u, t) \tag{3.24}$$

where $G_f(s)$ is a strictly proper low-pass filter with unity steady state gain and sufficiently large bandwidth.

Using (3.20) and (3.21),

$$e(x, u, t) = (b^T g)^{-1}(\dot{\sigma} + k\sigma) + \hat{e}(x, u, t) \tag{3.25}$$

Using (3.25) in (3.24),

$$\hat{e}(x, u, t) = G_f(s)\, \left\{(b^T g)^{-1}(\dot{\sigma} + k\sigma) + \hat{e}(x, u, t)\right\} \tag{3.26}$$

Specially for a choice of $G_f(s)$ given by,

$$G_f(s) = \frac{1}{1 + \tau s} \qquad \text{(first order filter)} \tag{3.27}$$

where τ is a small positive constant. The equation (3.26) can be written as,

$$\tau\dot{\hat{e}}(x, u, t) + \hat{e}(x, u, t) = (b^T g)^{-1}(\dot{\sigma} + k\sigma) + \hat{e}(x, u, t) \tag{3.28}$$

Therefore, with a first order low pass filter (i.e. 1st order UDE),

$$\hat{e}(x, u, t) = \frac{(b^T g)^{-1}}{\tau}\left(\sigma + k\int_0^t \sigma\right) \tag{3.29}$$

From equations (3.23), (3.24) and (3.27),

$$\dot{\tilde{e}}(x, u, t) = -\frac{1}{\tau}\tilde{e}(x, u, t) + \dot{e}(x, u, t) \tag{3.30}$$

Remark 3.3 *If $\dot{e} = 0$, $\tilde{e}$ goes to zero asymptotically, otherwise it is ultimately bounded. If $\dot{e}$ is not small, but $\ddot{e}$ is small, i.e $j = 2$ in (3.6), then the accuracy of estimation can be improved by estimating e as well as $\dot{e}$.*

3.4.1 Improvement in Estimation – 2^{nd} order UDE

The uncertainty (e) and its derivative ($\dot{e}$) can be estimated using a second order filter of the form,

$$G_f(s) = \frac{1+2\tau s}{\tau^2 s^2 + 2\tau s + 1} \qquad (2^{\text{nd}} \text{ order UDE}) \tag{3.31}$$

where τ is a small positive constant

Let $\hat{e}_1$ be the estimate of $e(x,u,t)$ and $\hat{e}_2 = \dot{\hat{e}}_1$ be the estimate of $\dot{e}(x,u,t)$. The estimation errors are derived using (3.23),

$$\tilde{e}_1 = e - \hat{e}_1 \tag{3.32}$$

$$\tilde{e}_2 = \dot{e} - \hat{e}_2 \tag{3.33}$$

Using (3.24) and (3.31),

$$\hat{e}_1 = \left(\frac{1+2\tau s}{\tau^2 s^2 + 2\tau s + 1}\right) e \tag{3.34}$$

$$\tau^2 \ddot{\hat{e}}_1 + 2\tau \dot{\hat{e}}_1 + \hat{e}_1 = 2\tau \dot{e} + e$$

$$\tau^2 \ddot{\hat{e}}_1 = 2\tau(\dot{e} - \dot{\hat{e}}_1) + (e - \hat{e}_1)$$

$$\dot{\hat{e}}_2 = \frac{2}{\tau}(\dot{e} - \hat{e}_2) + \frac{1}{\tau^2}(e - \hat{e}_1)$$

$$\dot{\hat{e}}_2 = \frac{2}{\tau}\tilde{e}_2 + \frac{1}{\tau^2}\tilde{e}_1 \tag{3.35}$$

$$\dot{\tilde{e}}_2 = -\frac{1}{\tau^2}\tilde{e}_1 - \frac{2}{\tau}\tilde{e}_2 + \ddot{e} \tag{3.36}$$

The estimation error equations can be expressed in the state variable form as,

$$\dot{\tilde{e}}_1 = \hat{e}_2 \tag{3.37}$$

$$\dot{\tilde{e}}_2 = -\frac{1}{\tau^2}\tilde{e}_1 - \frac{2}{\tau}\tilde{e}_2 + \ddot{e} \tag{3.38}$$

$$\dot{\tilde{e}} = A_o \tilde{e} + E\ddot{e} \tag{3.39}$$

where

$$\tilde{e} = \begin{bmatrix} \tilde{e}_1 \\ \tilde{e}_2 \end{bmatrix}, \quad A_o = \begin{bmatrix} 0 & 1 \\ -\frac{1}{\tau^2} & -\frac{2}{\tau} \end{bmatrix}, \quad E = \begin{bmatrix} 0 \\ 1 \end{bmatrix} \tag{3.40}$$

Therefore, with a second order filter,

$$\hat{e}_1 = (b^T g)^{-1} \left(\frac{2}{\tau}\sigma + \frac{2\tau k + 1}{\tau^2} \int_0^t \sigma + \frac{k}{\tau^2} \int_0^t \int_0^t \sigma\right) \tag{3.41}$$

3.5 Design of Observer

The uncertain plant in (3.1) is rewritten as,

$$\left.\begin{array}{rcl} \dot{x}(t) & = & f(x,t) + g(x,t)u + \Delta f(x,t) + \Delta g(x,t)u + d(x,t) \\ y(t) & = & Cx(t) \end{array}\right\} \tag{3.42}$$

where x is the plant state vector, y is the plant output and u is the input.

The plant in (3.42) is modified as,

$$\left.\begin{array}{rcl} \dot{x}(t) & = & Ax(t) + Bu(t) + Be(x,u,t) \\ y(t) & = & Cx(t) \end{array}\right\} \tag{3.43}$$

where A and B are user chosen matrix, with all eigenvalues of A having negative real parts. The term $e(x,u,t)$ is lumped uncertainty and is given as,

$$e(x,u,t) = f(x,t) + g(x,t)u + \Delta f(x,t) + \Delta g(x,t)u + d(x,t) - Ax - Bu \tag{3.44}$$

The lumped uncertainty $e(x,u,t)$ comprises of system nonlinearities, uncertainties and external disturbances.

An observer for (3.43) can be developed as,

$$\left.\begin{array}{rcl} \dot{\hat{x}}(t) & = & A\hat{x}(t) + Bu(t) + B\hat{e}(\hat{x},u,t) + J(y(t) - \hat{y}(t)) \\ \hat{y}(t) & = & C\hat{x}(t) \end{array}\right\} \tag{3.45}$$

where $\hat{x}$ is the observer state vector, $\hat{y}$ is the observer output, $\hat{e}(\hat{x},u,t)$ is an estimate of the lumped disturbance e and J is the observer gain matrix to be designed.

The observer error dynamics can be derived by using (3.43) and (3.45) as,

$$\dot{\tilde{x}}(t) = (A - JC)\tilde{x}(t) + B\tilde{e}(x,u,t) \tag{3.46}$$

where $\tilde{x} = x - \hat{x}$ is the state estimation error

Remark 3.4 *It is seen from* (3.46) *that, the state estimation error* $\tilde{x} \to 0$*, if the uncertainty estimation error* $\tilde{e} \to 0$ *asymptotically or at least remains ultimately bounded. As such uncertainty estimation is crucial in asymptotically stabilizing the observer, thus robustifying the control.*

Using (3.43),

$$e(x,u,t) = B^{+}(\dot{x}(t) - Ax(t) - Bu(t)) \tag{3.47}$$

where $B^{+} = (B^T B)^{-1} B^T$ is the pseudo-inverse of B.

The lumped uncertainty is estimated by passing through a low-pass filter of appropriate bandwidth. As the plant states are not available, the uncertainty is also estimated with observed states.

$$\hat{e}(\hat{x},u,t) = G_f(s)\, B^{+}(\dot{\hat{x}}(t) - A\hat{x}(t) - Bu(t)) \tag{3.48}$$

For a first order filter of the form,

$$G_f(s) = \frac{1}{1+\tau s} \tag{3.49}$$

where τ is a small positive constant.

Using (3.49) and (3.45) in (3.48),

$$\tau\dot{\hat{e}}(\hat{x},u,t) + \hat{e}(\hat{x},u,t) = B^{+}JC(x(t) - \hat{x}(t)) + \hat{e}(\hat{x},u,t) \tag{3.50}$$

Therefore,

$$\hat{e} = \frac{B^{+}JC}{\tau}(x - \hat{x}) = \frac{B^{+}J}{\tau}(y - \hat{y}) \tag{3.51}$$

3.5.1 Observer-Controller Structure

The proposed observer gives the estimates of plant states x and lumped uncertainty e. The control developed in section 3.3.2 is synthesized by replacing x with $\hat{x}$.

The sliding surface in (3.9) can be rewritten as,

$$\hat{\sigma} = B^T\hat{x} + \hat{z}, \qquad \hat{z}(0) = -b^T\hat{x}(0) \tag{3.52}$$

$$\dot{\hat{z}} = -B^T A_m \hat{x} - B^T b_m u_m \tag{3.53}$$

The control can then be written as,

$$u_{eq} = -L_1\hat{x} + M_1 u_m - (B^T B)^{-1} k\hat{\sigma} \tag{3.54}$$

$$u_n = -\hat{e} \tag{3.55}$$

with L_1 and M_1 are similar as in Assumption 3.3 and $\hat{e}$ computed from (3.51)

3.6 Stability

The error dynamics are rewritten using (3.46) and (3.51) as,

$$\begin{aligned} \dot{\tilde{x}}(t) &= (A - JC)\tilde{x}(t) + B\tilde{e}(x,u,t) && (3.56) \\ \dot{\tilde{e}}(t) &= -\frac{B^{+}JC}{\tau}\tilde{x}(t) + \dot{e}(t) && (3.57) \end{aligned}$$

Using (3.56) and (3.57)

$$\begin{bmatrix} \dot{\tilde{x}} \\ \dot{\tilde{e}} \end{bmatrix} = \begin{bmatrix} (A - JC) & B \\ -\frac{B^{+}JC}{\tau} & 0 \end{bmatrix} \begin{bmatrix} \tilde{x} \\ \tilde{e} \end{bmatrix} + \begin{bmatrix} 0 \\ 1 \end{bmatrix} \dot{e} \tag{3.58}$$

A compact form of (3.58) can be written as,

$$\dot{w} = A_k\, w + T\dot{e} \tag{3.59}$$

Assuming the plant is observable, it is possible to select the observer gains in such a way that the eigen values of A_k can be placed arbitrarily. If the observer gains are selected such that all eigen values of A_k have negative real parts, one can always find a positive definite matrix P such that,

$$PA_k + A_k^T P = -Q \tag{3.60}$$

for a given positive definite matrix Q. Let λ be the smallest eigen value of Q.

Defining a Lyapunov function as,

$$V(w) = w^T P\, w \tag{3.61}$$

Taking derivative of $V(w)$ along (3.59)

$$\begin{aligned} \dot{V}(w) &= w^T P\dot{w} + \dot{w}^T P w && (3.62) \\ &= w^T(PA_k + A_K^T P)w + 2w^T PT\dot{e} && (3.63) \\ &= -w^T Q w + 2w^T PT\dot{e} && (3.64) \\ &\leq -\lambda\|w\|^2 + 2\|w\|\,\|PT\|\,\mu && (3.65) \\ &\leq -\|w\|\,(\|w\|\lambda - 2\|PT\|\mu) && (3.66) \end{aligned}$$

Thus, $\|w\|$ is ultimately bounded by,

$$\|w\| \leq \frac{2\,\|PT\|\,\mu}{\lambda} \tag{3.67}$$

This implies,

$$\|\tilde{x}\| \leq \lambda_1 = \frac{2\,\|PT\|\,\mu}{\lambda} \tag{3.68}$$

$$\|\tilde{e}\| \leq \lambda_2 = \frac{2\,\|PT\|\,\mu}{\lambda} \tag{3.69}$$

Using (3.45), (3.52), (3.53), (3.54), (3.55), the dynamics of $\hat{\sigma}$ can be written as,

$$\dot{\hat{\sigma}} = -k\hat{\sigma} + B^T JC\tilde{x} \tag{3.70}$$

Therefore,

$$\begin{aligned} \hat{\sigma}\dot{\hat{\sigma}} &= -k\hat{\sigma}^2 + B^T JC\hat{\sigma}\tilde{x} && (3.71)\\ &\leq -k|\hat{\sigma}|^2 + |B^T JC|\,|\hat{\sigma}|\,\|\tilde{x}\| && (3.72)\\ &\leq -|\hat{\sigma}|\left(k\,|\hat{\sigma}| - |B^T JC|\,\lambda_1\right) && (3.73) \end{aligned}$$

Thus, the sliding variable ($\hat{\sigma}$) is ultimately bounded by,

$$|\hat{\sigma}| \leq \lambda_3 = \frac{|B^T JC|\,\lambda_1}{k} \tag{3.74}$$

It is seen from (3.68), (3.69) and (3.74) that, $\|\tilde{x}\|$, $\|\tilde{e}\|$ and $|\hat{\sigma}|$ are ultimately bounded. The bounds can be lowered by appropriate choice of control parameters k, J and τ.

The model following error can be written using,

$$\dot{x} = Ax + Bu + Be \tag{3.75}$$

$$\dot{x_m} = A_m x_m + b_m u_m \tag{3.76}$$

Therefore,

$$\dot{\tilde{x}}_m = Ax + Bu + Be - A_m x_m - b_m u_m \tag{3.77}$$

With the control designed in (3.54) and (3.55),

$$\dot{\tilde{x}}_m = A\tilde{x}_m + (A - A_m)\tilde{x} + B\tilde{e} - k\hat{\sigma} \tag{3.78}$$

As $\|\tilde{x}\|$, $\|\tilde{e}\|$ and $|\hat{\sigma}|$ are ultimately bounded, $\dot{\tilde{x}}_m$ is also bounded. If the bounds go to 0, the asymptotic stability of model following error is assured.

The practical stability is thus proved in the sense of *Corless and Leitmann* (1981)

3.7 Numerical Example

The effectiveness of the proposed strategy is illustrated with the numerical example as in (*Chang and Lee*, 1994). The plant dynamics are as in (3.1) with,

$$f(x,t) = \begin{bmatrix} 0 & 1 \\ \dfrac{2x_2 \sin x_1}{\frac{2}{3} + \cos x_1} & \dfrac{\cos x_1}{\frac{2}{3} + \cos x_1} \end{bmatrix} \begin{bmatrix} x_1 \\ x_2 \end{bmatrix} \tag{3.79}$$

$$\Delta f(x,t) = \begin{bmatrix} 0 & 0 \\ 0.2 \sin x_2 & 0.1 \cos x_2 \end{bmatrix} \begin{bmatrix} x_1 \\ x_2 \end{bmatrix} \tag{3.80}$$

$$g(x,t) = \begin{bmatrix} 0 \\ \dfrac{1}{\frac{2}{3} + \cos x_1} \end{bmatrix}, \quad \Delta g(x,t) = \begin{bmatrix} 0 \\ 0.1 \sin x_2 \end{bmatrix} \tag{3.81}$$

The structure of the model to be followed is as in (3.7) with,

$$A_m = \begin{bmatrix} 0 & 1 \\ -\omega_n^2 & -2\zeta\omega_n \end{bmatrix}, \quad b_m = \begin{bmatrix} 0 \\ -\omega_n^2 \end{bmatrix} \tag{3.82}$$

The initial conditions for the plant and model are,

$$x(0) = [1 \quad 0]^T \qquad x_m(0) = [0 \quad 1]^T \tag{3.83}$$

The disturbance is,

$$d(x,t) = \begin{bmatrix} 0 \\ x_1^2 \sin(t) + x_2 \cos(t) + 1 \end{bmatrix} \tag{3.84}$$

The results are verified for model-following control with uncertainty estimated by UDE. The model parameters are $\zeta = 1$ and $\omega_n = 6$ in (3.82). The plant and model have an initial condition mismatch (3.83). The control gain is $k = 2$ and filter time constant is $\tau = 1\,ms$. The reference input is a square wave of amplitude 1 and frequency 0.9 rad/sec.

3.7.1 Case 1 : Model Following

The efficacy of observer to estimate the states and uncertainty in Fig. 3.1. A first order UDE (3.29) with filter time constant of $\tau = 1\,ms$ is considered.

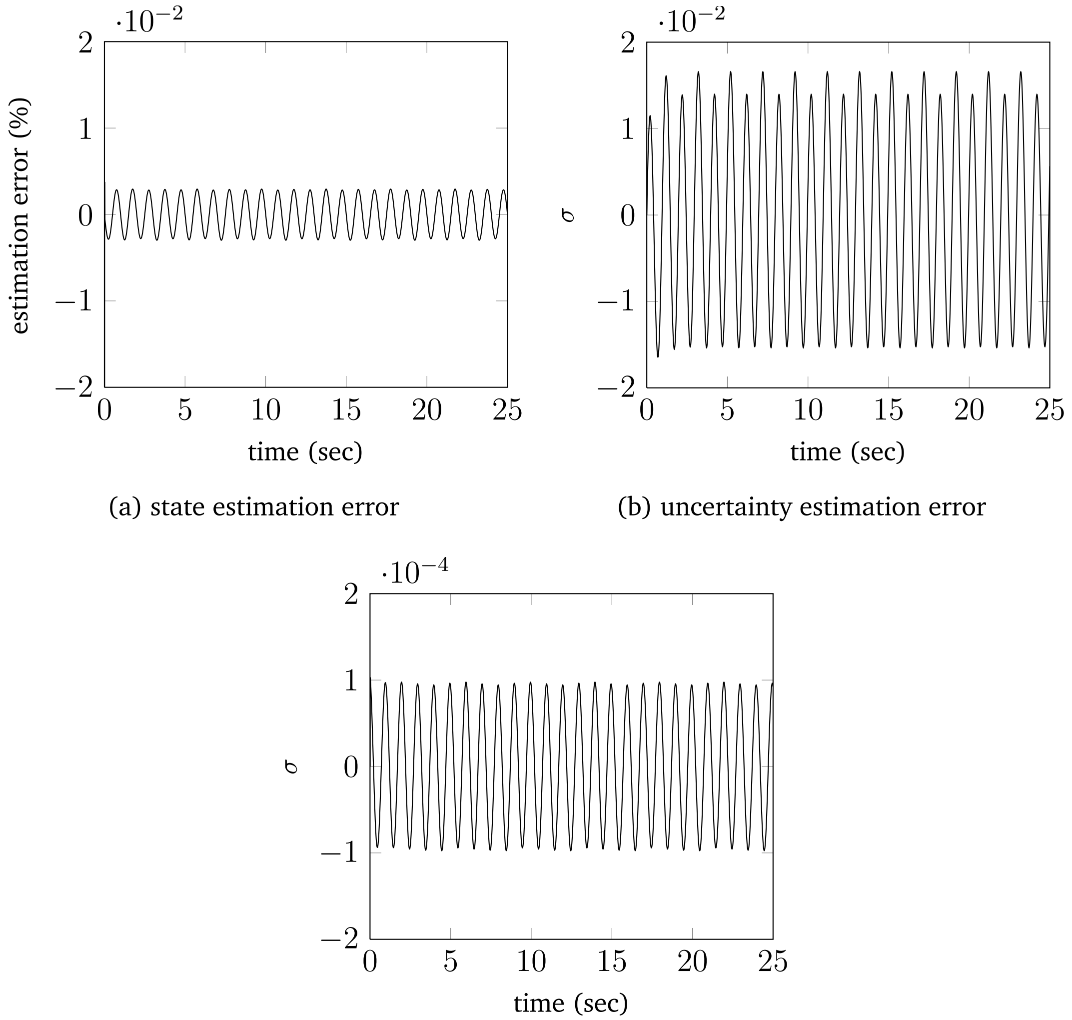

(a) state estimation error

(b) uncertainty estimation error

(c) sliding variable

Figure 3.1: Estimation of states and uncertainty with first order UDE

The state estimation error ($\tilde{x}$) and uncertainty estimation error ($\tilde{e}$) is bounded as seen in Fig. 3.1a and 3.1b. This clearly illustrates the capability of UDE to estimate the uncertainties and disturbances. The sliding variable (σ) is also bounded as seen in Fig. 3.1c. The Fig. 3.1 demonstrates the robust performance of observer designed using UDE.

The model following performance with uncertainty estimated by a first order UDE (3.29) is considered here and the results are showed in Fig. 3.2.

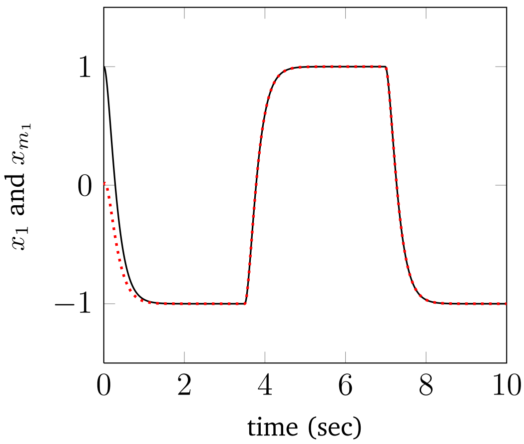

(a) plant (-) and model (...) state x_1

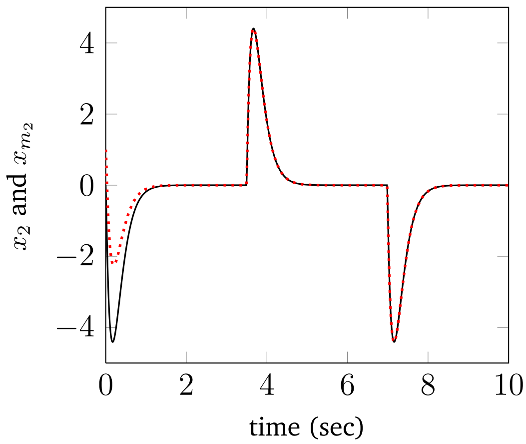

(b) plant (-) and model (...) state x_2

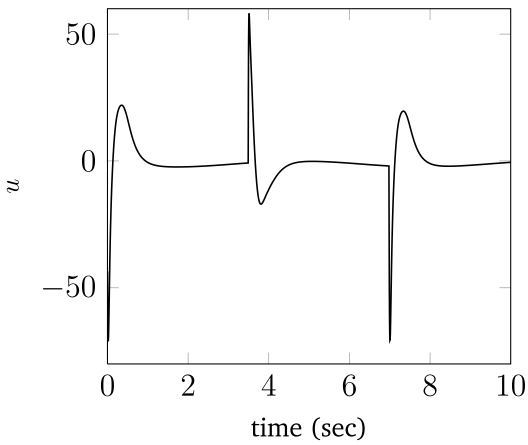

(c) control

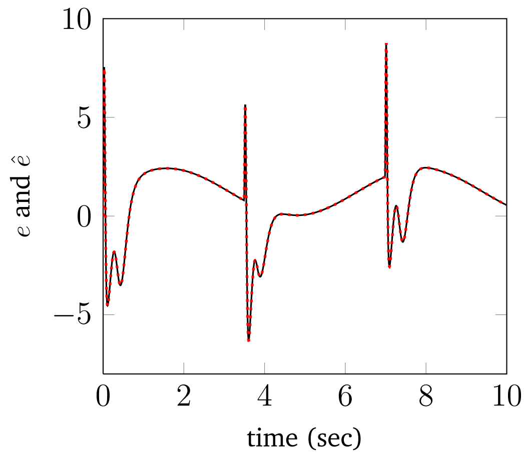

(d) uncertainty e (–) and $\hat{e}$ (...)

Figure 3.2: Model following with uncertainty estimation

The response of the plant states (x), in Fig. 3.2a and 3.2b shows that the plant follows the model very closely even with uncertainty in plant as well as input vector, as also state dependent nonlinear disturbance. The sliding variable (σ) and estimation error ($\tilde{e}$) is bounded. The implication of this boundedness can be seen in control (u) being within limits as seen in Fig. 3.2c. The tracking of lumped certainty is evident in Fig. 3.2d.

3.7.2 Case 2 : Robustness

The uncertainty in $f(x,t)$ is same as in Case 1 whereas the uncertainty in $g(x,t)$ is increased to $g(x,t) = [0 \quad 0.6\sin x_2]^T$. The results are shown in Fig. 3.3.

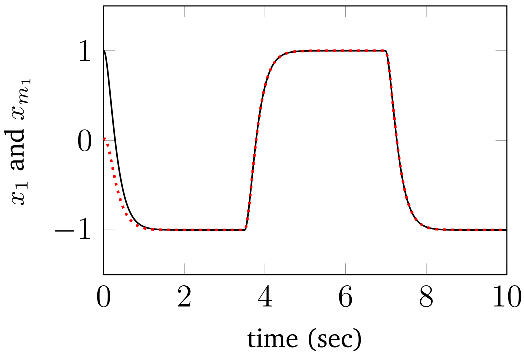

(a) plant (-) and model (...) state x_1

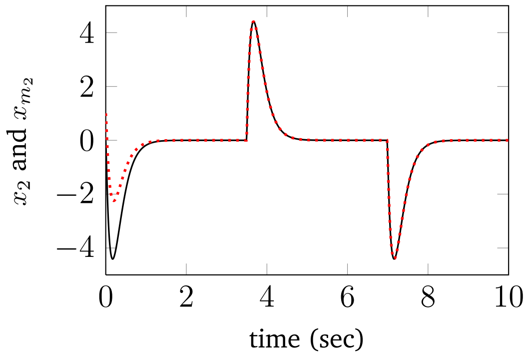

(b) plant (-) and model (...) state x_2

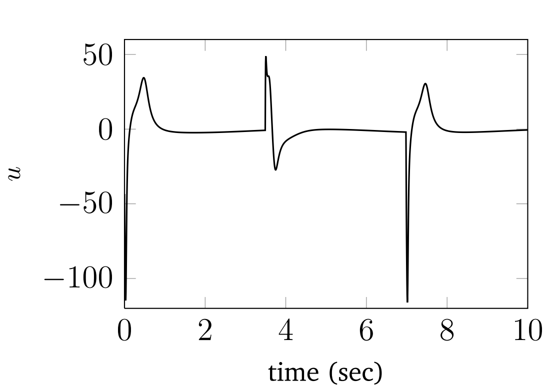

(c) control

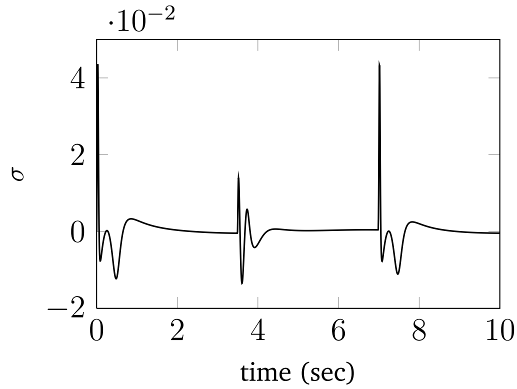

(d) sliding variable

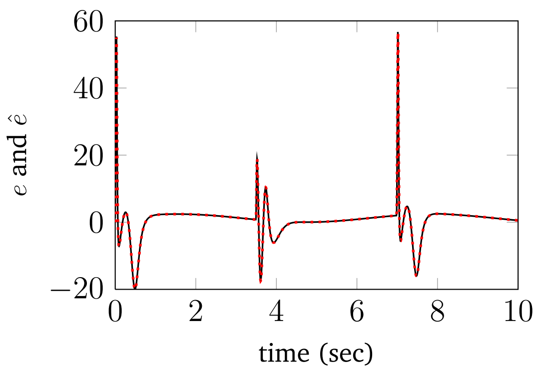

(e) uncertainty e (–) and $\hat{e}$ (...)

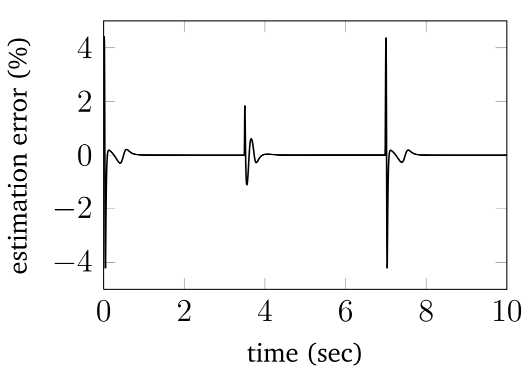

(f) estimation error

Figure 3.3: Robustness for increased uncertainty in $g(x,t)$

The estimation of uncertainty is good, resulting in good tracking accuracy.

The performance of first order UDE (3.29) is also tested for a fast disturbance. The disturbance considered is $d(x,t) = x_1^2 \sin(10t) + x_2 \cos(10t) + 1$ and the results are shown in Fig. 3.4. The UDE is able to estimate even fast disturbance, enabling good tracking accuracy.

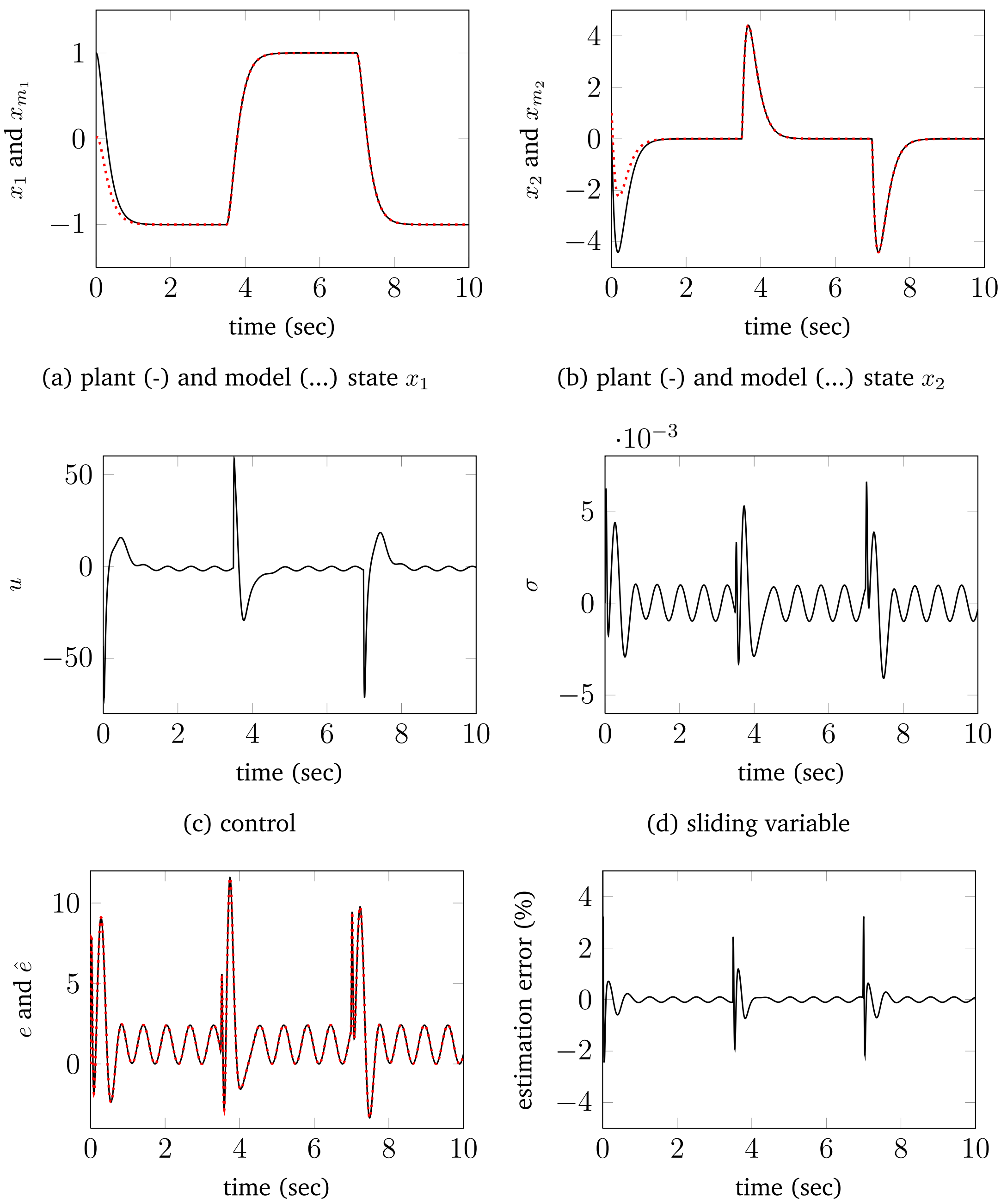

(a) plant (-) and model (...) state x_1

(b) plant (-) and model (...) state x_2

(c) control

(d) sliding variable

(e) uncertainty e (–) and $\hat{e}$ (...)

(f) estimation error

Figure 3.4: Robustness for fast disturbance

The results are in confirmance to the theory and UDE can indeed compensate fast varying disturbances and large input vector uncertainties. This implies a good model following and the same is evident from Fig. 3.3a, 3.3b and Fig. 3.4a, 3.4b. The sliding variable (σ) and estimation error ($\tilde{e}$) is also bounded as expected.

3.7.3 Case 3 : Improvement with higher order filter

The improvement in accuracy of estimation using a second order UDE (3.41) is presented here. The reduction of σ and $\tilde{e}$ in comparison to Case 1 is shown in Fig. 3.5. It can be seen that the bounds are reduced by a factor of more than 10.

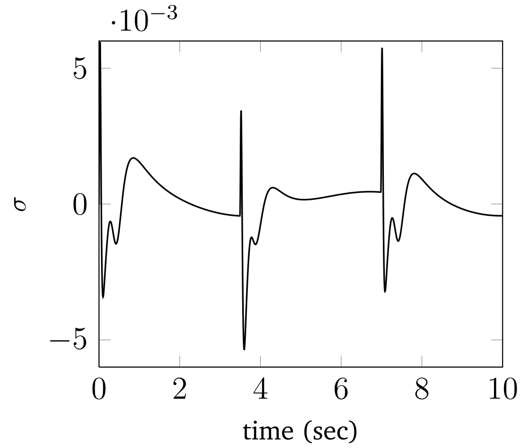

(a) σ with 1^{st} order filter

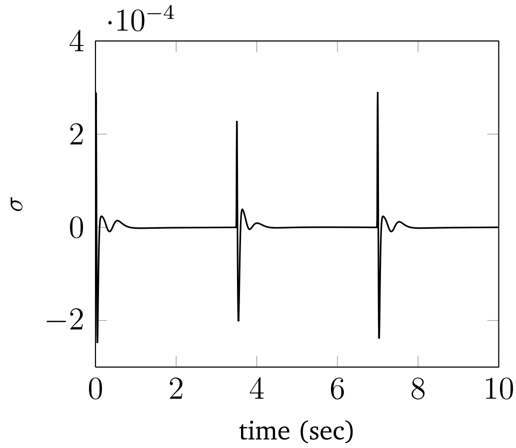

(b) σ with 2^{nd} order filter

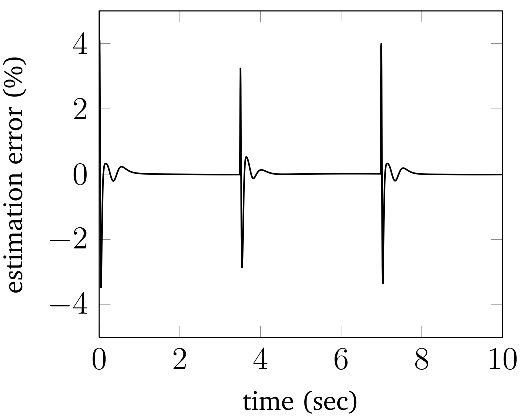

(c) $\tilde{e}$ with 1^{st} order filter

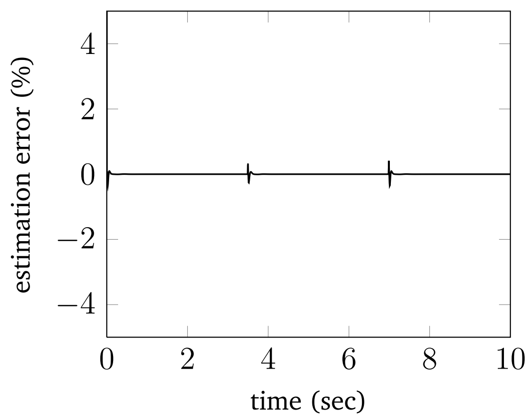

(d) $\tilde{e}$ with 2^{nd} order filter

Figure 3.5: Comparison between first order and second order UDE

3.8 Application : Inverted Pendulum System

The inverted pendulum system is widely used in literature to check the validity of control strategies, owing to its challenging dynamic structure. A nonlinear control based on sliding plane (*Jia and Wang*, 2008), QFT (*Rajapakse et al.*, 2007), adaptive-H_∞ control (*Koofigar et al.*, 2009) are some of the nonlinear designs reported in literature. A SMC combined with self-tuning fuzzy inference scheme (*Chaouch et al.*, 2011) provides good tracking performance. However, the control input is very high initially; it is effectively addressed in the proposed design by choice of a suitable sliding surface and auxiliary variable.

3.8.1 Dynamic Model

The dynamics of the inverted pendulum can be written as in (*Slotine and Li*, 1991; *Jia and Wang*, 2008).

$$\left.\begin{array}{rcl} \dot{x_1} & = & x_2 \\ \dot{x_2} & = & \dfrac{g\sin(x_1) - \frac{mlx_2^2\cos(x_1)\sin x_1}{(m_c+m)}}{l\left[\frac{4}{3} - \frac{m\cos^2(x_1)}{(m_c+m)}\right]} + \dfrac{\frac{\cos(x_1)}{(m_c+m)}}{l\left[\frac{4}{3} - \frac{m\cos^2(x_1)}{(m_c+m)}\right]}u(t) + d(t) \\ y & = & x_1 \end{array}\right\} \tag{3.85}$$

where $[x_1 \quad x_2]^T$ are the state variables – position and velocity of the pole in radians and radians/sec, $u(t)$ is the control input in V, $d(t)$ is the external disturbance and y is the output. The model parameters are: m_c is the mass of cart, m is the mass of pole and l is half length of the pole.

The system state equations in (3.85) can be represented generically as,

$$\dot{x} = f(x,t) + g(x,t)u + d(x,t) \tag{3.86}$$

where, $x \,\epsilon\, \mathbb{R}^2$ is the state vector and $u \,\epsilon\, \mathbb{R}^1$ is the control input
$f(x,t)$ is known nonlinear system vector
$g(x,t)$ is known nonlinear input vector
$d(x,t)$ is unmeasurable disturbances

It is evident from (3.85) and (3.86) that,

$$\begin{aligned} f(x) &= \begin{bmatrix} x(2) \\ \dfrac{g\sin(x_1) - mlx_2^2\cos(x_1)\sin x_1/(m_c+m)}{l\left[\frac{4}{3} - m\cos^2(x_1)/(m_c+m)\right]} \end{bmatrix} \\ g(x) &= \begin{bmatrix} 0 \\ \dfrac{\cos(x_1)/(m_c+m)}{l\left[\frac{4}{3} - m\cos^2(x_1)/(m_c+m)\right]} \end{bmatrix} \\ d(t) &= \begin{bmatrix} 0 \\ 20\sin(2\pi t) \end{bmatrix} \end{aligned}$$

The nonlinear system and input vector may have uncertainties; $\Delta f(x,t)$, $\Delta g(x,t)$. As is evident, the uncertainties $\Delta f, \Delta g$ and disturbance $d(x,t)$ satisfy matching conditions. Thus, the system (3.86) can now be rewritten as in (3.5),

$$\dot{x} = f(x,t) + g(x,t)u + g(x,t)\cdot e(x,u,t) \tag{3.87}$$

where $e(x,u,t)$ is the lumped uncertainty as in (3.3) comprising uncertainty in plant and input vector as well as unknown disturbance.

3.8.2 Results

The nonlinear sliding mode control design is applied to an inverted pendulum stabilization problem. The stabilization problem is to design a controller to keep the pendulum in its unstable equilibrium point in the presence of disturbances.

A trajectory tracking control with uncertainty estimated by a first order UDE (3.29) is considered here and the simulation results are shown in Fig. 3.6. The reference is $r(t) = 0.2\sin\left(\pi\, t + \dfrac{\pi}{2}\right)$. The nominal values of model parameters are: $m_c = 1\,kg$, $m = 0.1\,kg$, $l = 0.5\,m$. An uncertainty of 50% is added in m to check the robustness of control.

The results are verified for 2 different cases; with and without disturbance. The disturbance considered is time-varying. The improvement in accuracy with a second order filter is also verified and confirmed.

Case 1: Without disturbance

The control performance for tracking a sinusoidal reference is illustrated in Fig. 3.6 with no disturbance added for this case.

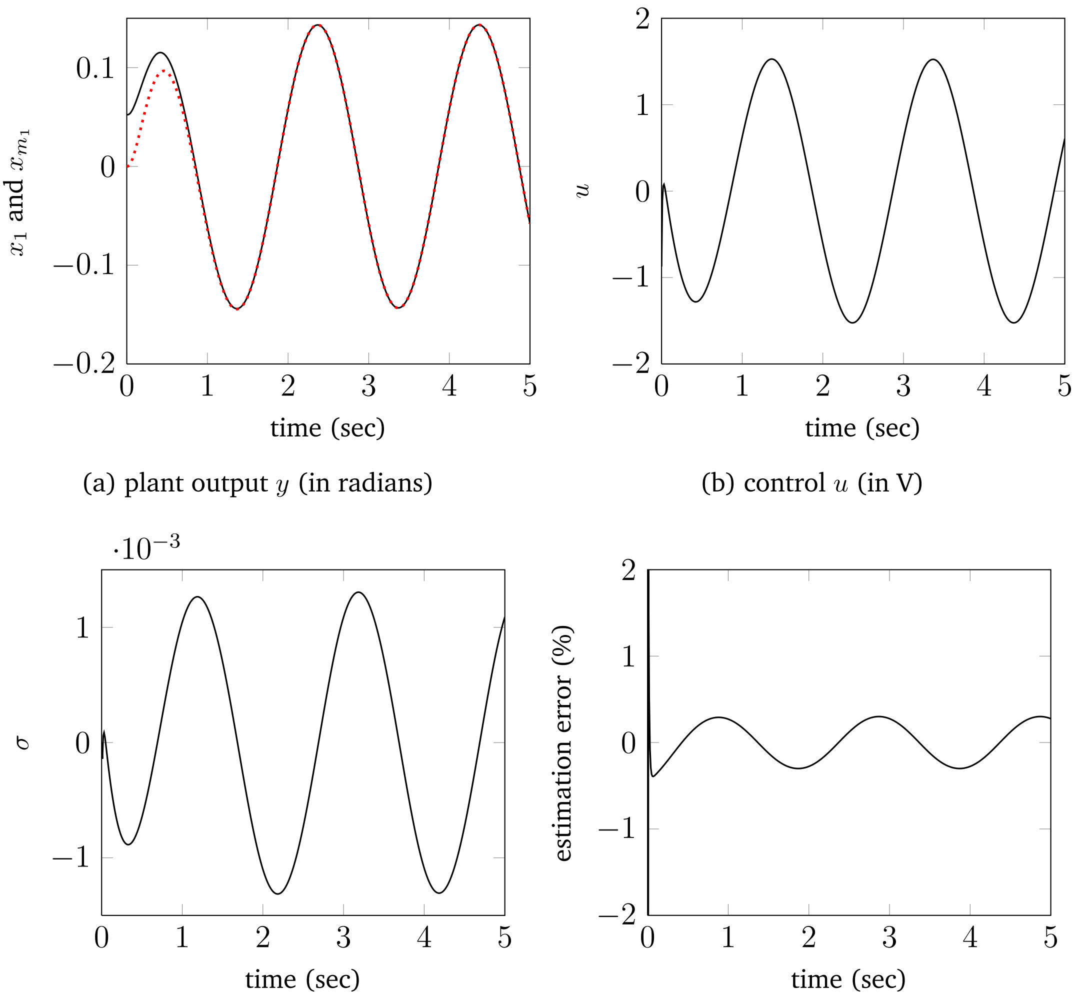

(a) plant output y (in radians)

(b) control u (in V)

(c) sliding variable

(d) estimation error $\tilde{e}$ (in %)

Figure 3.6: Inverted Pendulum without disturbance

It is observed from Fig. 3.6a that the tracking accuracy is good inspite of uncertainties. The control is smooth and within practical limits, and the same is evident in Fig. 3.6b. The sliding variable (σ) and estimation error ($\tilde{e}$) is bounded; as seen in Fig. 3.6c and Fig. 3.6d. It may be noted that the estimated states are used in the control design.

Case 2: With disturbance

A time varying disturbance is added to the plant and trajectory tracking control performance is shown in Fig. 3.7. The disturbance considered is $d(t) = 20\sin(2\pi t)$, with all other parameters same as case 1.

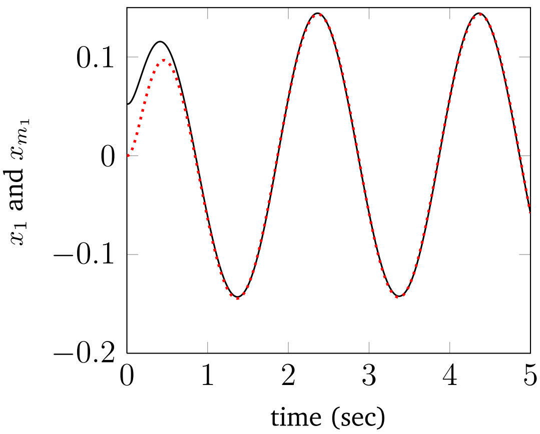

(a) plant output y (in radians)

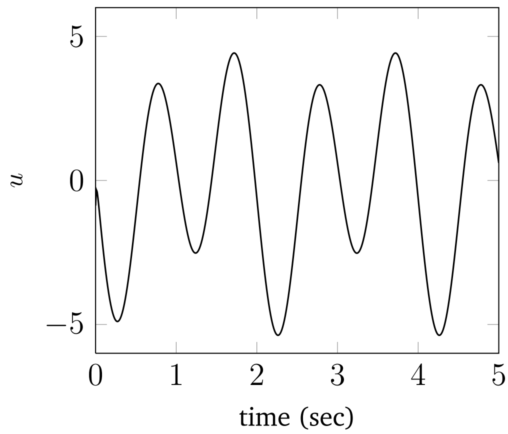

(b) control u (in V)

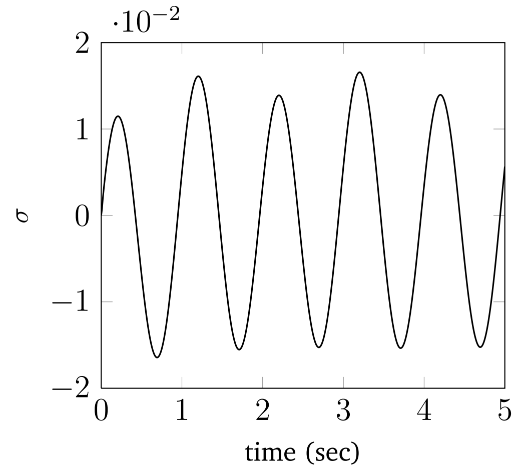

(c) sliding variable

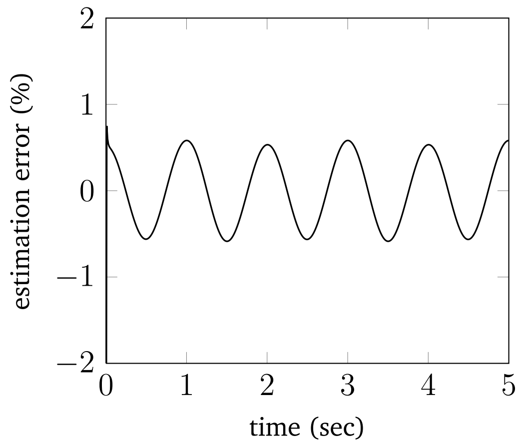

(d) estimation error $\tilde{e}$ (in %)

Figure 3.7: Inverted Pendulum with disturbance

The UDE is able to compensate this time varying disturbance and the control ensures a good tracking performance and disturbance rejection as seen in Fig. 3.7a. The plot of $\tilde{e}$ which is the difference between e and $\hat{e}$ is also sinusoidal but bounded. The choice of sliding surface ensures that magnitude of control, is within limits.

Case 3: Improvement in accuracy

The bounds can be lowered using a smaller value of τ. The accuracy of estimation can be further improved using a second order filter and comparative results are shown in Fig. 3.8

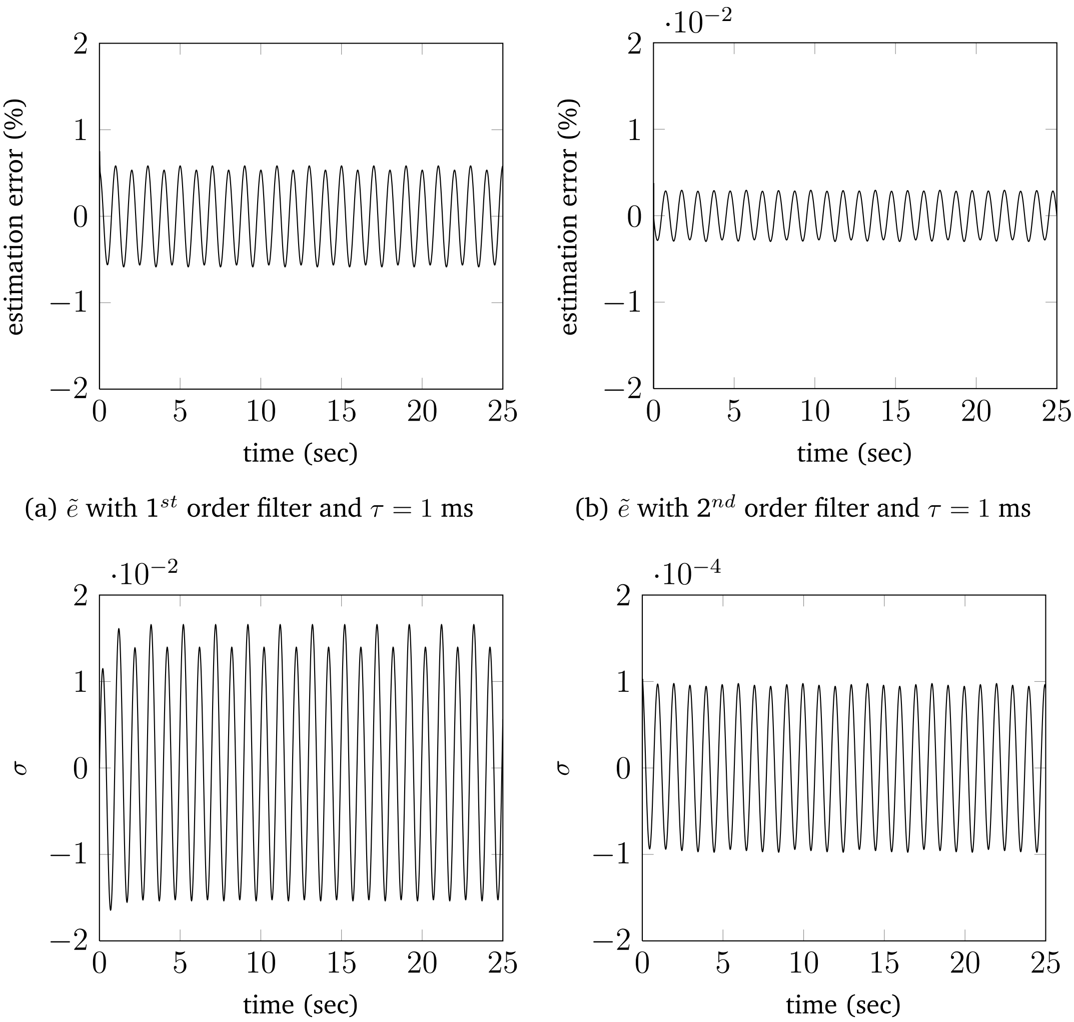

(a) $\tilde{e}$ with 1^{st} order filter and $\tau = 1$ ms

(b) $\tilde{e}$ with 2^{nd} order filter and $\tau = 1$ ms

(c) σ with 1^{st} order filter and $\tau = 1$ ms

(d) σ with 2^{nd} order filter and $\tau = 1$ ms

Figure 3.8: Increased robustness with 2^{nd} order filter

The results in Fig. 3.8a and Fig. 3.8b prove that, bound on estimation error ($\tilde{e}$) is indeed lowered by using a second order filter. The bounds on sliding variable (σ) is also reduced as can be seen from Fig. 3.8c and Fig. 3.8d. The decrease in bounds is significant and is dependent on time-constant (τ) and filter order.

3.9 Summary

A robust SMC strategy using UDE is extended to uncertain nonlinear system with, nonlinearity in plant as well as input vector and subjected to time varying disturbance. The proposed control enforces sliding, without using discontinuous control and without requiring knowledge of uncertainties or their bounds. The UDE is able to compensate significant uncertainties as well as fast disturbances. An approach for improving the accuracy of estimation, to cover a large class of disturbances is also presented. The control law is made implementable by estimating states, to give a robust controller-observer structure.

It is proved that the ultimate boundedness of state estimation error, uncertainty estimation error and sliding variable is guaranteed; and the bounds can be lowered by appropriate choice of design parameters. The theoretically expected results are verified by simulation in MATLAB-SIMULINK environment. The efficacy of the design is also confirmed on an application to inverted pendulum system.

Chapter 4

SMC for Mismatched Uncertain System using EID Method

The chapter explains design of SMC law for mismatched uncertain system, with state-dependent uncertainties. The issue of mismatched uncertainties is addressed by estimating EID with a low-pass filter. The design is validated for slip regulation in an anti lock braking system problem.

The chapter starts with an introduction in section 4.1 followed by problem formulation in section 4.2. Section 4.3 describes the estimation of EID using low-pass filter. A control based on SMC is explained in Section 4.4 and the proposed control in section 4.5. Section 4.6 gives the proof of boundedness using Lyapunov analysis. The performance is illustrated by an application to anti lock braking system in section 4.7. The chapter concludes with a summary in section 4.8.

4.1 Introduction

The conventional SMC design can guarantee invariance to only matched uncertainties (*Drazenovic*, 1969). This poses severe limitations on the applicability of SMC, as there many applications where; uncertainties and disturbances act in channels in which, a control input is not present.

A variety of control strategies like adaptive control (*Wen and Cheng*, 2008), LMI-based control (*Choi*, 2007), fuzzy (*Tao et al.*, 2003; *Zhang et al.*, 2010), integral sliding mode control (*Liang et al.*, 2012) have been proposed in literature to address the problem of mismatched uncertainties. The integrator back-stepping (IB) (*Kanellakopoulos et al.*, 1991; *Krstic et al.*, 1995) is a widely used method for control of mismatched systems. This method has been extended to multiple surface sliding control (*Won and Hedrick*, 1996) and adaptive multiple-surface sliding control (*Huang and Chen*, 2004). A novel sliding surface that includes the estimate of unmatched disturbances obtained using DO is proposed in (*Yang et al.*, 2013). This method is augmented with an extended-DO in (*Ginoya et al.*, 2014).

The Equivalent Input Disturbance (EID) approach is a promising technique for control of uncertain systems; both matched and mismatched. An EID is a disturbance on the control input channel that produces the same effect on the controlled output as actual disturbances do. An EID always exists for a controllable and observable plant with no zeros on imaginary axis (*She et al.*, 2008). This technique is concerned with the estimation of equivalent input disturbance instead of actual disturbance. The fundamental premise is that; the disturbance may be acting on any channel, but it is the control signal that is used for disturbance rejection. The EID is always different from the actual disturbance imposed on plant.

The EID system is just a system, reconstructed based on the output of plant, so that the state of EID system and the actual state of original plant are usually different (*She et al.*, 2008). The EID approach has been validated for disturbance rejection performance in linear systems (*She et al.*, 2008). This method has been extended for MIMO (*She and Xin*, 2007), under-actuated (*She et al.*, 2012) and non-minimum phase (*Liu et al.*, 2013) systems.

In this work, SMC is combined with EID and extended to a nonlinear system with mismatched uncertainties and disturbances. The system formulation considered here covers a large class of applications, and admits a large class of uncertainties. The robustness is assured through estimate of EID mechanized through a low-pass filter, and the performance is improved by using a higher-order filter. The EID helps SMC mitigate the effect of mismatched disturbances. The composite control is applied to a representative problem of anti-lock braking system.

4.2 Problem Formulation

Consider an uncertain nonlinear system given by,

$$\left.\begin{aligned} \dot{x}(t) &= Ax(t) + f(x,t) + Bu(t) + g(x,t)u(t) + B_d d(x,t) \\ y(t) &= Cx(t) \end{aligned}\right\} \tag{4.1}$$

where
$x(t) \in \mathbb{R}^n$ is the state vector
$u(t) \in \mathbb{R}^m$ is the control input
$y(t) \in \mathbb{R}^1$ is the output of plant
$f(x,t)$ is the uncertain nonlinear plant vector
$g(x,t)$ is the uncertain nonlinear input vector
$d(x,t) \in \mathbb{R}^n$ is external unmeasurable disturbance
A, B and C are the plant, input and output matrices representing nominal plant

It is evident from (4.1) that the disturbance may be imposed on a channel other than that of the control input, and the number of disturbances and associated input channels may be larger than one.

The uncertain nonlinear plant $f(x,t)$ and input vector $g(x,t)\,u$ can be considered as state and input dependent disturbance and is lumped with external unmeasurable disturbances ($B_d\,d$). The plant in (4.1) can be thus modified as,

$$\left.\begin{aligned} \dot{x}(t) &= Ax(t) + Bu(t) + \{f(x,t) + g(x,t)u + B_d d(x,t)\} \\ y(t) &= Cx(t) \end{aligned}\right\} \tag{4.2}$$

As the existence of EID is guaranteed for both matched and mismatched disturbances (*She et al.*, 2008), there always exists a signal d_e on control input channel that produces the same effect on output as ($f(x,t) + g(x,t)\,u + B_d\,d(x,t)$) does. The plant is now given by,

$$\left.\begin{aligned} \dot{x}(t) &= Ax(t) + Bu(t) + Bd_e(x,u,t) \\ y(t) &= Cx(t) \end{aligned}\right\} \tag{4.3}$$

where $d_e = f(x,t) + g(x,t)\,u + B_d\,d(x,t)$

Assumption 4.1 *This assumption is necessary to guarantee the existence of EID*

1. *The pair (A, B) is controllable*
2. *The pair (A, C) is observable*
3. *The triplet (A, C, B) has no invariant zeros, i.e. for all $\lambda \epsilon C$*

$$Rank \begin{bmatrix} \lambda I - A & -B \\ C & 0 \end{bmatrix} = n + 1$$

Assumption 4.2 *The EID $d_e(x, t)$ is continuous and satisfies,*

$$\left| \frac{d^{(j)} d_e(x, u, t)}{dt^{(j)}} \right| \leq \mu \qquad \textit{for } j = 0, 1, 2, \ldots, r \tag{4.4}$$

where μ is a small positive number.

Remark 4.1 *The Assumption 4.2 implies that the uncertainty $d_e(x, u, t)$ and its derivatives up to some finite order (r) be bounded but the bound is not required to be known. The assumption includes a fairly large class of uncertainties and disturbances that can be estimated by EID.*

The objective is to design a control (u) such that, the output (y) of uncertain plant (4.1) follows the desired trajectory. The control is expected to ensure robust tracking in presence of uncertainties and disturbances of varying kind.

The EID approach usually uses a state-feedback with integral as a nominal control with estimates of EID for improved disturbance rejection. The EID is normally estimated with a first-order low-pass filter.

The limitations of integral action are to be mitigated by designing a sliding-mode law for nominal plant. The synthesis of control law is envisaged using the states of observer. The issue of chatter is addressed by using a linear and saturation gain. The observed states are also required for estimating EID, which is then combined with SMC to yield a robust control law. The performance improvement by using a higher-order filter to estimate EID and its derivatives is to be validated.

4.3 Estimation of EID

A servo control system with an EID estimator is shown in Fig. 4.1.

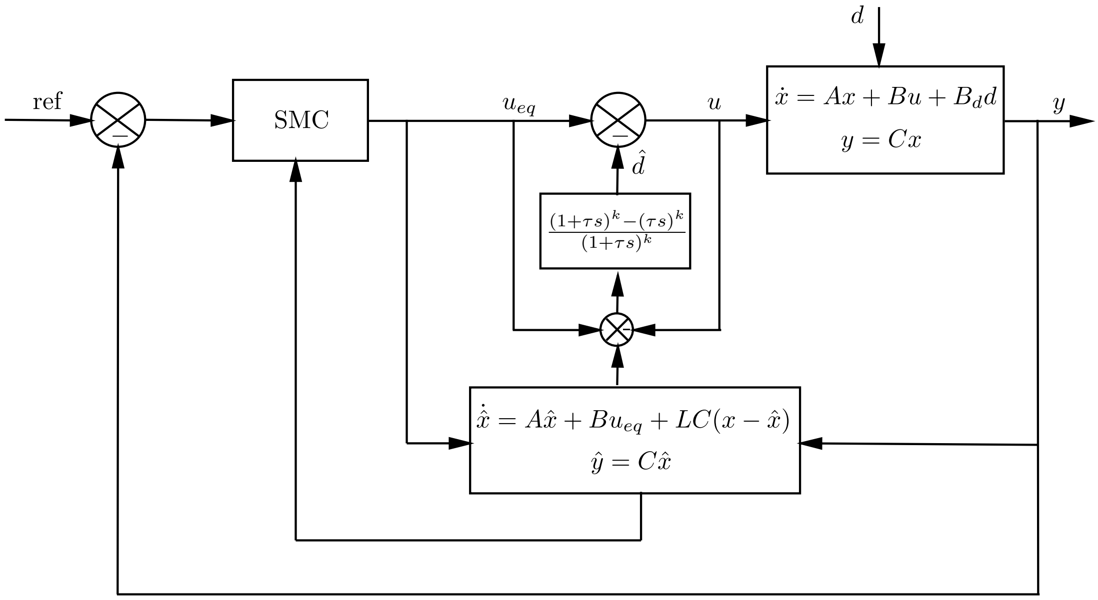

Figure 4.1: Configuration of system with SMC and EID

Using (4.3)

$$d_e = B^{+}(\dot{x} - Ax - Bu) \tag{4.5}$$

Remark 4.2 *The equation* (4.5) *requires all the states, however the channel on which EID is imposed may be different from that of actual disturbance. The available states of the plant (in the presence of disturbance) may be different from those of the plant with an EID. As such a full-order observer is imperative to estimate EID. It is important to guarantee that* $y(t) - \hat{y}(t)$ *converge to zero.*

The observer is given as,

$$\left.\begin{array}{rcl} \dot{\hat{x}} & = & A\hat{x} + Bu_{eq} + LC\,(x - \hat{x}) \\ \hat{y} & = & C\hat{x} \end{array}\right\} \tag{4.6}$$

where, L is the observer gain and u_{eq} is the nominal control.

The state estimation error can be written as,

$$\left.\begin{aligned} \tilde{x} &= x - \hat{x} \\ \dot{\tilde{x}} &= \dot{x} - \dot{\hat{x}} \end{aligned}\right\} \tag{4.7}$$

The observer error dynamics can be determined by using (4.3) and (4.6) in (4.7)

$$\left.\begin{aligned} \dot{\tilde{x}} &= A(x - \hat{x}) + B(u - u_{eq}) + Bd_e - LC\,(x - \hat{x}) \\ &= (A - LC)\tilde{x} - B\hat{d} + Bd_e \\ &= (A - LC)\tilde{x} + B\tilde{d} \end{aligned}\right\} \tag{4.8}$$

where $\tilde{d} = d_e - \hat{d}$

The EID (d_e) in (4.5) can now be estimated with the observed states as,

$$\left.\begin{aligned} d^* &= B^+(\dot{\hat{x}} - A\hat{x} - Bu) \\ &= B^+(A\hat{x} + Bu_{eq} + LC\,\tilde{x} - A\hat{x} - Bu) \\ &= B^+LC\,\tilde{x} + u_{eq} - u \\ &= B^+LC\,\tilde{x} + \hat{d} \end{aligned}\right\} \tag{4.9}$$

The estimate ($\hat{d}$) is obtained by passing (d^*) through a low-pass filter $G_f(s)$

$$\hat{d} = G_f(s)\,d^* \tag{4.10}$$

where, τ is a small positive constant.

For a first order filter, (4.10) becomes,

$$\hat{d} = \frac{d^*}{1 + \tau s} \tag{4.11}$$

Therefore,

$$\left.\begin{aligned} \hat{d} + \tau\dot{\hat{d}} &= d^* \\ \hat{d} + \tau\dot{\hat{d}} &= B^+LC\,\tilde{x} + \hat{d} \\ \dot{\hat{d}} &= \frac{B^+LC}{\tau}\,\tilde{x} \end{aligned}\right\} \tag{4.12}$$

Thus, the estimate of EID is given by,

$$\hat{d} = \frac{B^+LC}{\tau}\int \tilde{x} \tag{4.13}$$

The estimation error dynamics can be determined as,

$$\dot{d}_e - \dot{\hat{d}} = -\frac{B^+LC}{\tau}\,\tilde{x} + \dot{d}_e \tag{4.14}$$

Therefore,

$$\dot{\tilde{d}} = -\frac{B^+LC}{\tau}\,\tilde{x} + \dot{d}_e \tag{4.15}$$

Using (4.8) and (4.15)

$$\begin{bmatrix} \dot{\tilde{x}} \\ \dot{\tilde{d}} \end{bmatrix} = \begin{bmatrix} (A-LC) & B \\ -\dfrac{B^+LC}{\tau} & 0 \end{bmatrix} \begin{bmatrix} \tilde{x} \\ \tilde{d} \end{bmatrix} + \begin{bmatrix} 0 \\ 1 \end{bmatrix} \dot{d}_e \tag{4.16}$$

The error dynamics in (4.16) can be further simplified as,

$$\begin{bmatrix} \dot{\tilde{x}} \\ \dot{\tilde{d}} \end{bmatrix} = \left(\begin{bmatrix} A & B \\ 0_{1\times 2} & 0 \end{bmatrix} - \begin{bmatrix} L \\ \dfrac{B^+L}{\tau} \end{bmatrix} \begin{bmatrix} C & 0 \end{bmatrix} \right) \begin{bmatrix} \tilde{x} \\ \tilde{d} \end{bmatrix} + \begin{bmatrix} 0_{2\times 1} \\ 1 \end{bmatrix} \dot{d}_e \tag{4.17}$$

A compact form of (4.17) can be written as,

$$\dot{\tilde{e}} = (H - K\,G)\,\tilde{e} + E\,\dot{d}_e \tag{4.18}$$

where,

$$\tilde{e} = \begin{bmatrix} \tilde{x} \\ \tilde{d} \end{bmatrix} \qquad H = \begin{bmatrix} A & B \\ 0_{1\times 2} & 0 \end{bmatrix} \qquad K = \begin{bmatrix} L \\ \dfrac{B^+L}{\tau} \end{bmatrix}$$

$$G = \begin{bmatrix} C & 0 \end{bmatrix} \qquad E = \begin{bmatrix} 0 & 0 & 1 \end{bmatrix}^T$$

Remark 4.3 *It is evident from* (4.18) *that, the error dynamics is driven by* $\dot{d}_e$. *Thus the error dynamics is asymptotically stable if* $\dot{d}_e \approx 0$. *It is obvious that for bounded* $\dot{d}_e$, *bounded input-bounded output stability is assured. However, asymptotic stability for the error dynamics can always be assured if some higher derivative of the uncertainty is equal to zero.*

4.3.1 Improvement in Estimation – 2^{nd} order filter

The EID (d_e) and its derivative ($\dot{d}_e$) can be estimated using a second order filter of the form,

$$G_f(s) = \frac{1+2\tau s}{\tau^2 s^2 + 2\tau s + 1} \tag{4.19}$$

where τ is a small positive constant.

Therefore using (4.9), (4.10) and (4.19)

$$\hat{d}_1 = \frac{1+2\tau s}{\tau^2 s^2 + 2\tau s + 1}\left[B^+ LC\,\tilde{x} + \hat{d}_1\right] \tag{4.20}$$

Therefore,

$$\left.\begin{aligned}
\tau^2\ddot{\hat{d}}_1 + 2\tau\dot{\hat{d}}_1 + \hat{d}_1 &= B^+LC\tilde{x} + 2\tau B^+LC\dot{\tilde{x}} + \hat{d}_1 + 2\tau\dot{\hat{d}}_1 \\
\tau^2\ddot{\hat{d}}_1 &= B^+LC\tilde{x} + 2\tau B^+LC\dot{\tilde{x}} \\
\ddot{\hat{d}}_1 &= \frac{1}{\tau^2}B^+LC\,\tilde{x} + \frac{2}{\tau}B^+LC\,\dot{\tilde{x}} \\
\ddot{\hat{d}}_1 &= \dot{\hat{d}}_2 + \frac{2}{\tau}B^+LC\,\dot{\tilde{x}}
\end{aligned}\right\} \tag{4.21}$$

Therefore,

$$\left.\begin{aligned}
\dot{\hat{d}}_1 &= \frac{2}{\tau}B^+LC\,\tilde{x} + \hat{d}_2 \\
\dot{\hat{d}}_2 &= \frac{1}{\tau^2}B^+LC\,\tilde{x}
\end{aligned}\right\} \tag{4.22}$$

The estimation error is written as,

$$\left.\begin{aligned}
\dot{\tilde{d}}_1 &= -\frac{2}{\tau}B^+LC\,\tilde{x} + \tilde{d}_2 \\
\dot{\tilde{d}}_2 &= -\frac{1}{\tau^2}B^+LC\,\tilde{x} + \ddot{d}_e
\end{aligned}\right\} \tag{4.23}$$

The error dynamics can be written using (4.8) and (4.23) as,

$$\begin{bmatrix} \dot{\tilde{x}} \\ \dot{\tilde{d}}_1 \\ \dot{\tilde{d}}_2 \end{bmatrix} = \left(\begin{bmatrix} A & B \\ 0_{2\times 2} & 0_{2\times 1} \end{bmatrix} - \begin{bmatrix} L \\ \frac{2}{\tau}B^+L \\ \frac{1}{\tau^2}B^+L \end{bmatrix} \begin{bmatrix} C & 0_{1\times 2} \end{bmatrix} \right) \begin{bmatrix} \tilde{x} \\ \tilde{d}_1 \\ \tilde{d}_2 \end{bmatrix} + \begin{bmatrix} 0 \\ 0_{1\times 1} \\ 1 \end{bmatrix} \ddot{d}_e \tag{4.24}$$

A compact form of (4.24) can be written as,

$$\dot{\tilde{e}} = (H - K\,G)\,\tilde{e} + E\,\ddot{d}_e \tag{4.25}$$

where,

$$\tilde{e} = \begin{bmatrix} \tilde{x} \\ \tilde{d}_1 \\ \tilde{d}_2 \end{bmatrix} \qquad H = \begin{bmatrix} A & B \\ 0_{2\times 2} & 0_{2\times 1} \end{bmatrix} \qquad K = \begin{bmatrix} L \\ \frac{2}{\tau} B^+ L \\ \frac{1}{\tau^2} B^+ L \end{bmatrix}$$

$$G = \begin{bmatrix} C & 0_{1\times 2} \end{bmatrix} \qquad E = \begin{bmatrix} 0 & 0 & 0 & 1 \end{bmatrix}^T$$

Remark 4.4 *It is evident from* (4.25) *that, the error dynamics is driven by $\ddot{d}_e$. Thus the error dynamics is asymptotically stable if $\ddot{d}_e \approx 0$. The estimation accuracy is thus improved as both d_e and $\dot{d}_e$ are estimated.*

4.3.2 Generalization – k^{th} order filter

In general, if k^{th} derivative of the disturbance, ${d_e}^{(k)}$ is zero; the asymptotic stability for error dynamics is guaranteed, if one chooses the filter as,

$$G_f(s) = \frac{(1+\tau s)^k - (\tau s)^k}{(1+\tau s)^k} \tag{4.26}$$

The equations for estimate of EID and its derivatives can be written as,

$$\left.\begin{aligned} \dot{\hat{d}}_1 &= \frac{k}{\tau} B^+ LC\,\tilde{x} + \hat{d}_2 \\ \dot{\hat{d}}_2 &= \frac{k}{\tau^2} B^+ LC\,\tilde{x} + \hat{d}_3 \\ &\vdots \\ \dot{\hat{d}}_{k-1} &= \frac{k}{\tau^{k-1}} B^+ LC\,\tilde{x} + \hat{d}_k \\ \dot{\hat{d}}_k &= \frac{1}{\tau^k} B^+ LC\,\tilde{x} \end{aligned}\right\} \tag{4.27}$$

where d_1 is the estimate of EID d_e and d_i, $i = 2, 3, \ldots\ldots, k$ are the estimates of derivatives of EID ${d_e}^{(j)}$ $j = 1, 2, \ldots\ldots, (k-1)$.

Defining the estimate of EID and its derivatives as $d_1 = d_e, d_2 = \dot{d}_e, \ldots, d_k = {d_e}^{(k-1)}$ and defining the estimation errors as, $\tilde{d}_i = d_i - \hat{d}_i$ for $i = 1, 2, \ldots, k$

The dynamics of estimation error is written as,

$$\left.\begin{array}{lll} \dot{\tilde{d}}_1 & = & -\frac{k}{\tau} B^+ LC\,\tilde{x} + \tilde{d}_2 \\ \dot{\tilde{d}}_2 & = & -\frac{k}{\tau^2} B^+ LC\,\tilde{x} + \tilde{d}_3 \\ \vdots & & \\ \dot{\tilde{d}}_{k-1} & = & -\frac{k}{\tau^{k-1}} B^+ LC\,\tilde{x} + \tilde{d}_k \\ \dot{\tilde{d}}_k & = & -\frac{1}{\tau^k} B^+ LC\,\tilde{x} + {d_e}^{(k)} \end{array}\right\} \tag{4.28}$$

The error dynamics can now be written using (4.8) and (4.28) as,

$$\begin{bmatrix} \dot{\tilde{x}} \\ \dot{\tilde{d}}_1 \\ \dot{\tilde{d}}_2 \\ \vdots \\ \dot{\tilde{d}}_{k-1} \\ \dot{\tilde{d}}_k \end{bmatrix} = \left(\begin{bmatrix} A & B \\ 0_{k\times 2} & 0_{k\times 1} \end{bmatrix} - \begin{bmatrix} L \\ \frac{k}{\tau} B^+ L \\ \frac{k}{\tau^2} B^+ L \\ \vdots \\ \frac{k}{\tau^{k-1}} B^+ L \\ \frac{1}{\tau^k} B^+ L \end{bmatrix} \begin{bmatrix} C & 0_{1\times k} \end{bmatrix} \right) \begin{bmatrix} \tilde{x} \\ \tilde{d}_1 \\ \tilde{d}_2 \\ \vdots \\ \tilde{d}_{k-1} \\ \tilde{d}_k \end{bmatrix} + \begin{bmatrix} 0 \\ 0_{(k-1)\times 1} \\ 1 \end{bmatrix} {d_e}^{(k)} \tag{4.29}$$

A compact form of (4.29) can be written as,

$$\dot{\tilde{e}} = (H - K\,G)\,\tilde{e} + E\,{d_e}^{(k)} \tag{4.30}$$

where,

$$\tilde{e} = \begin{bmatrix} \dot{\tilde{x}} \\ \dot{\tilde{d}}_1 \\ \dot{\tilde{d}}_2 \\ \vdots \\ \dot{\tilde{d}}_{k-1} \\ \dot{\tilde{d}}_k \end{bmatrix} \quad H = \begin{bmatrix} A & B \\ 0_{k\times 2} & 0_{k\times 1} \end{bmatrix} \quad K = \begin{bmatrix} L \\ \frac{k}{\tau} B^+ L \\ \frac{k}{\tau^2} B^+ L \\ \vdots \\ \frac{k}{\tau^{k-1}} B^+ L \\ \frac{1}{\tau^k} B^+ L \end{bmatrix}$$

$$G = \begin{bmatrix} C & 0_{1\times k} \end{bmatrix} \quad E = \begin{bmatrix} 0 & 0 & 0_{(k-1)\times 1} & 1 \end{bmatrix}^T$$

4.4 Design of Control

The EID can be combined with any control design to improve the performance of system. A SMC combined with EID is proposed here to address the issue of matched and/or mismatched uncertainty. The objective is to control the output (y) in the presence of parametric uncertainties and external disturbances.

The control (u) in (4.3) can be written as,

$$u = u_{eq} + u_n \tag{4.31}$$

where u_{eq} is the nominal control designed using sliding-mode and $u_n = -\hat{d}$ is the control for uncertain part with $\hat{d}$ as the estimate of d_e

4.4.1 Sliding Surface

The sliding surface is defined as,

$$\sigma = y - y_d \tag{4.32}$$

where y_d is the desired trajectory of output.

Using (4.3) in (4.32),

$$\sigma = Cx - y_d \tag{4.33}$$

The estimation of EID is based on observed states, as such the control (u_{eq}) is also designed using estimated states ($\hat{x}$). Therefore, the sliding surface is written as,

$$\hat{\sigma} = C\hat{x} - y_d \tag{4.34}$$

The sliding surface (4.34) is modified as,

$$\hat{\sigma}^* = \hat{\sigma} - \hat{\sigma}(0)\, e^{-\alpha t} \tag{4.35}$$

where α is a user chosen positive constant.

Remark 4.5 *The sliding surface of* (4.35) *eliminates reaching phase and also aids in mitigating chatter (Deshpande and Phadke, 2012). The modified sliding variable $\hat{\sigma}^*$ is zero at $t = 0$, thus precluding the initial control from taking large values. Additionally, $\hat{\sigma}^* \to \hat{\sigma}$ as $t \to \infty$.*

4.4.2 Sliding Mode Control

A control is designed such that, the sliding condition is satisfied and plant follows the desired trajectory.

Differentiating (4.35) and using (4.34) and (4.6),

$$\dot{\hat{\sigma}}^* = CA\hat{x} + CBu_{\text{eq}} + CLC\tilde{x} + \alpha\hat{\sigma}(0)e^{-\alpha t} - \dot{y}_d \tag{4.36}$$

The control that ensures sliding can be written as,

$$u_{eq} = -(CB)^{-1}\left\{CA\hat{x} + \alpha\hat{\sigma}(0)e^{-\alpha t} - \dot{y}_d + k_l\hat{\sigma}^* + k_s\,\text{sat}(\hat{\sigma}^*)\right\} \tag{4.37}$$

where $k_l > 0$ is the linear gain and $k_s > 0$ is the switching gain to be designed and,

$$\text{sat}\,(\hat{\sigma}^*) = \begin{cases} \text{sgn}\,(\hat{\sigma}^*) & \text{if } |\hat{\sigma}^*| > \epsilon,\ \epsilon > 0 \\ \hat{\sigma}^*/\epsilon & \text{if } |\hat{\sigma}^*| \leq \epsilon \end{cases}$$

With the control in (4.37), the dynamics of sliding surface can be written as,

$$\dot{\hat{\sigma}}^* = -k_l\hat{\sigma}^* - k_s\,\text{sat}(\hat{\sigma}^*) + CLC\tilde{x} \tag{4.38}$$

Remark 4.6 *It is seen from* (4.38) *that, as $\tilde{x} \to 0$, sliding condition is satisfied and $\hat{\sigma}^*$ will asymptotically approach 0, if $k_l > 0$ and $k_s > 0$.*

4.5 Proposed Control

The proposed SMC law combined with EID can be written as,

$$\left.\begin{aligned} u_{eq} &= -(CB)^{-1}\left\{CA\hat{x} + \alpha\hat{\sigma}(0)e^{-\alpha t} - \dot{y}_d + k_l\hat{\sigma}^* + k_s\,\text{sat}(\hat{\sigma}^*)\right\} \\ u_n &= -\hat{d} \\ \hat{d} &= \frac{B^+LC}{\tau}\int \tilde{x} \end{aligned}\right\} \tag{4.39}$$

It may be noted that the EID in (4.39) is estimated with a first-order filter.

Remark 4.7 *The control proposed here* (4.39) *is different from the one developed in (She et al., 2008). The nominal control i.e. state-feedback with integral is replaced with a sliding-mode here. The estimation of EID is generalized to a k^{th} order filter to include a large class of uncertainties and disturbances.*

4.6 Stability

The error dynamics are rewritten using (4.16) as,

$$\begin{bmatrix} \dot{\tilde{x}} \\ \dot{\tilde{d}} \end{bmatrix} = \begin{bmatrix} (A - LC) & B \\ -\dfrac{B^{+}LC}{\tau} & 0 \end{bmatrix} \begin{bmatrix} \tilde{x} \\ \tilde{d} \end{bmatrix} + \begin{bmatrix} 0 \\ 1 \end{bmatrix} \dot{d}_e \tag{4.40}$$

A compact form of (4.40) can be written as,

$$\dot{\tilde{e}} = D\,\tilde{e} + E\,\dot{d}_e \qquad \text{where } \tilde{e} = [\ \tilde{x} \quad \tilde{d}\ ]^T \tag{4.41}$$

It is evident from (4.41) that eigen values of D can be placed arbitrarily. If the observer gain L is selected such that all eigen values of D have negative real parts, one can always find a positive definite matrix P such that,

$$PD + D^T P = -Q \tag{4.42}$$

for a given positive definite matrix Q. Let λ_e be the smallest eigen value of Q.

Defining a Lyapunov function as,

$$V(\tilde{e}) = \tilde{e}^T P\,\tilde{e} \tag{4.43}$$

Taking derivative of $V(\tilde{e})$ along (4.41)

$$\begin{aligned} \dot{V}(\tilde{e}) &= \tilde{e}^T P\dot{\tilde{e}} + \dot{\tilde{e}}^T P\tilde{e} && (4.44) \\ &= \tilde{e}^T(PD + D^T P)\tilde{e} + 2\tilde{e}^T PE\dot{d}_e && (4.45) \\ &= -\tilde{e}^T Q\tilde{e} + 2\tilde{e}^T PE\dot{d}_e && (4.46) \\ &\le -\lambda_e\|\tilde{e}\|^2 + 2\|\tilde{e}\|\,\|PE\|\,\mu && (4.47) \\ &\le -\|\tilde{e}\|\,(\|\tilde{e}\|\lambda_e - 2\|PE\|\mu) && (4.48) \end{aligned}$$

It is seen from (4.48) that, $\|\tilde{e}\|$ is ultimately bounded and remains in a ball of radius $\frac{2\,\|PE\|\,\mu}{\lambda_e}$, which guarantees that,

$$\|\tilde{x}\| \le \lambda_1 = \frac{2\,\|PE\|\,\mu}{\lambda_e} \tag{4.49}$$

$$\|\tilde{d}\| \le \lambda_2 = \frac{2\,\|PE\|\,\mu}{\lambda_e} \tag{4.50}$$

The dynamics of $\hat{\sigma}^*$ can be written using (4.38) as,

$$\dot{\hat{\sigma}}^* = -k_l\hat{\sigma}^* - k_s \operatorname{sat}(\hat{\sigma}^*) + CLC\tilde{x} \tag{4.51}$$

Therefore,

$$\begin{aligned} \hat{\sigma}^*\dot{\hat{\sigma}}^* &= -k_l{\hat{\sigma}^*}^2 - k_s\hat{\sigma}^* \operatorname{sat}(\hat{\sigma}^*) + \hat{\sigma}^* CLC\tilde{x} && (4.52)\\ &\leq -k_l|\hat{\sigma}^*|^2 - k_s|\hat{\sigma}^*| \operatorname{sat}(\hat{\sigma}^*) + |CLC|\,|\hat{\sigma}^*|\,\|\tilde{x}\| && (4.53)\\ &\leq -k_l|\hat{\sigma}^*|^2 - k_s|\hat{\sigma}^*| \operatorname{sat}(\hat{\sigma}^*) + |CLC|\,|\hat{\sigma}^*|\,\lambda_1 && (4.54)\end{aligned}$$

Define,

$$\zeta = |CLC|\,\lambda_1 \tag{4.55}$$

Therefore,

$$\hat{\sigma}^*\dot{\hat{\sigma}}^* = -k_l|\hat{\sigma}^*|^2 - k_s|\hat{\sigma}^*| \operatorname{sat}(\hat{\sigma}^*) + |\hat{\sigma}^*|\,\zeta \tag{4.56}$$

if $|\hat{\sigma}^*| > \epsilon$

$$\hat{\sigma}^*\dot{\hat{\sigma}}^* = -|\hat{\sigma}^*|\,(k_l\,|\hat{\sigma}^*| + k_s - \zeta) \tag{4.57}$$

Therefore,

$$|\hat{\sigma}^*| \leq \frac{\zeta - k_s}{k_l} \tag{4.58}$$

if $|\hat{\sigma}^*| \leq \epsilon$

$$\hat{\sigma}^*\dot{\hat{\sigma}}^* = -|\hat{\sigma}^*|\left(k_l\,|\hat{\sigma}^*| + \frac{k_s}{\epsilon}|\hat{\sigma}^*| - \zeta\right) \tag{4.59}$$

Therefore,

$$|\hat{\sigma}^*| \leq \frac{\zeta}{k_l + \frac{k_s}{\epsilon}} \tag{4.60}$$

Thus, the sliding variable ($\hat{\sigma}^*$) is ultimately bounded by,

$$|\hat{\sigma}^*| \leq \lambda_3 = \max\left(\frac{\zeta - k_s}{k_l}, \frac{\zeta}{k_l + \frac{k_s}{\epsilon}}\right) \tag{4.61}$$

In view of (4.61), it is evident that $\|\tilde{y} = y - y_d\|$ shall be bounded.

It is seen from (4.49), (4.50) and (4.61) that, $\|\tilde{x}\|$, $\|\tilde{d}\|$ and $|\hat{\sigma}^*|$ are ultimately bounded. The bounds can be lowered by appropriate choice of control parameters k_l, k_s and L.

The practical stability is thus proved in the sense of *Corless and Leitmann* (1981)

4.7 Application : Anti Lock Braking System

The Antilock Braking System (ABS) is an integral component of safety in modern cars. The prime objective of ABS is to prevent locking of wheels and reduce the stopping distance. The dynamics of ABS is complex due to the presence of nonlinearities and uncertainties. The tire-road friction coefficient is a crucial information required for design of control (*Pacejka*, 2005; *Kiencke and Nielsen*, 2005). The uncertainties in vehicle mass and changes in road gradient are also challenges in efficient ABS control.

The problem of slip regulation in ABS control is addressed using diverse control strategies as PID control (*Song et al.*, 2007), feedback linearization (*Poursamad*, 2009), fuzzy control (*Lin and Hsu*, 2003), observer based adaptive fuzzy-neural (*Wang et al.*, 2009), model based control (*Shi et al.*, 2010) and optimal control (*Mirzaei et al.*, 2006) and SMC (*Kayacan et al.*, 2009; *Wu and Shih*, 2001).

4.7.1 Dynamic Model

The dynamic model of ABS is derived from free body diagram of quarter car model shown in Figure 4.2. The setup of quarter car model used is Inteco (*Inteco*, 2013).

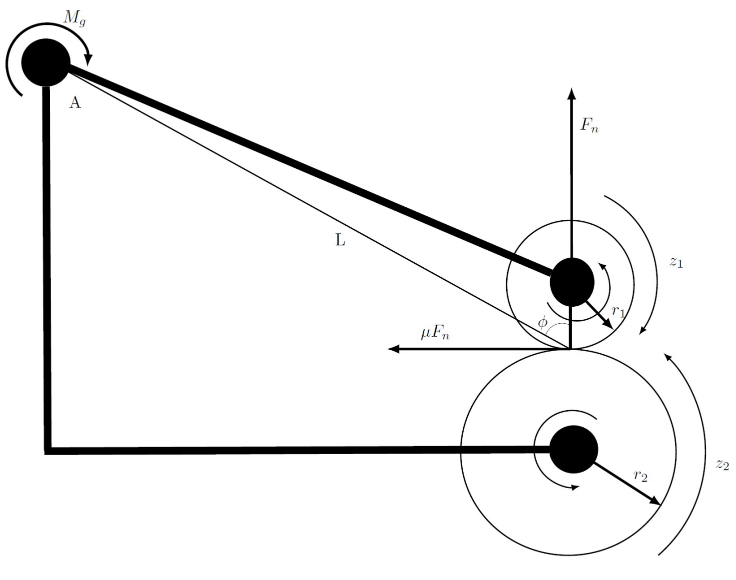

Figure 4.2: Free body diagram of ABS setup

The description of ABS parameters is given in Table 4.1.

Table 4.1: Parameters of ABS

Parameter	Description	Value	Unit
r_1	radius of upper wheel	9.95e-2	m
r_2	radius of lower wheel	9.90e-2	m
J_1	moment of inertia of upper wheel	7.53e-3	kgm^2
J_2	moment of inertia of lower wheel	2.56e-2	kgm^2
q_1	viscous friction coeff. of upper wheel	1.18e-4	kgm^2/s
q_2	viscous friction coeff. of lower wheel	2.14e-4	kgm^2/s
M_{10}	static friction of upper wheel	3.2e-3	Nm
M_{20}	static friction of lower wheel	9.25e-2	Nm
M_g	gravitational and shock absorber torques acting on the balance lever	19.62	Nm
L	distance between the contact point of wheels and the rotational axis of the balance lever	0.370	m
ϕ	Angle between the normal in the contact point and line L	65.61	$degrees$

There are three torques acting on the upper wheel; the braking torque (T_b), the friction torque in upper wheel bearing and the friction torque among wheels. The equation for upper wheel dynamics can be written as,

$$J_1\dot{z}_1 = F_n r_1 S\mu(\lambda) - q_1 z_1 - s_1 M_{10} - s_1 T_b \tag{4.62}$$

There are two torques acting on the lower wheel; the friction torque in lower bearing and the friction torque among wheels. The equation for lower wheel dynamics can be written as,

$$J_2\dot{z}_2 = -F_n r_2 S\mu(\lambda) - q_2 z_2 - s_2 M_{20} \tag{4.63}$$

The normal force (F_n) is sum of the torques at point A and it is calculated as,

$$F_n = \frac{M_g + s_1 T_b + s_1 M_{10} + q_1 z_1}{L\left(\sin(\phi) - S\mu(\lambda)\cos(\phi)\right)} \tag{4.64}$$

The auxiliary variables are defined as, $S = sgn(r_2 z_2 - r_1 z_1)$ and $s_1 = sgn(z_1)$, with sgn as the *signum* function.

z_1 is the angular velocity of the upper wheel and z_2 is the angular velocity of the lower wheel.

Define $S(\lambda)$ as,

$$S(\lambda) = \frac{S\mu(\lambda)}{L\left(\sin(\phi) - S\mu(\lambda)\cos(\phi)\right)} \tag{4.65}$$

Using (4.64) and (4.65) in (4.62) and (4.63)

$$\dot{z}_1 = S(\lambda)\left(c_{11} z_1 + c_{12}\right) + c_{13} z_1 + c_{14} + s_1 T_b \left(c_{15} S(\lambda) + c_{16}\right) \tag{4.66}$$

$$\dot{z}_2 = S(\lambda)\left(c_{21} z_1 + c_{22}\right) + c_{23} z_2 + c_{24} + S(\lambda) c_{25} s_1 T_b \tag{4.67}$$

The constants in (4.66) and (4.67) are described in Table 4.2.

Table 4.2: Nominal values of constant

Name	Description	Value	Name	Description	Value
c_{11}	$\frac{r_1 q_1}{J_1}$	0.0015	c_{21}	$-\frac{r_2 q_1}{J_2}$	0.000464
c_{12}	$\frac{(s_1 M_{10} + M_g) r_1}{J_1}$	2.5933e2	c_{22}	$\frac{(s_1 M_{10} + M_g) r_2}{J_2}$	75.8696
c_{13}	$\frac{-q_1}{J_1}$	0.0159	c_{23}	$\frac{-q_2}{J_2}$	0.00878
c_{14}	$\frac{-s_1 M_{10}}{J_1}$	0.3985	c_{24}	$\frac{-s_2 M_{20}}{J_2}$	3.6323
c_{15}	$\frac{r_1}{J_1}$	13.2171	c_{25}	$-\frac{r_2}{J_2}$	3.8667
c_{16}	$\frac{-1}{J_1}$	132.8356			

The road adhesion friction coefficient is a nonlinear function of slip, given as,

$$\mu(\lambda) = \frac{w_4\lambda^p}{a+\lambda^p} + w_3\lambda^3 + w_2\lambda^2 + w_1\lambda \tag{4.68}$$

where λ is the wheel slip. The other constants are, $a = 2.5 \times 10^{-4}$, $p = 2.099$, $w_1 = -0.042$, $w_2 = 0.29 \times 10^{-9}$, $w_3 = 0.035$ and $w_4 = 0.406$.

The wheel slip is defined as,

$$\lambda = \frac{r_2 z_2 - r_1 z_1}{r_2 z_2} \tag{4.69}$$

Differentiating (4.69) and using (4.66) and (4.67), the dynamics of the wheel slip can be written as,

$$\dot{\lambda} = f(\lambda, z_2) + g(\lambda, z_2)T_b \tag{4.70}$$

where the nonlinear function $f(\lambda, z_2)$ and $g(\lambda, z_2)$ are given as,

$$\begin{aligned} f(\lambda, z_2) &= -\left(S(\lambda)c_{11} + c_{13}\right)(1-\lambda) - \left(\frac{r_1}{r_2 z_2}\right)\left(S(\lambda)c_{12} + c_{14}\right) \\ &+ \frac{(1-\lambda)}{z_2}\left(\left(S(\lambda)(1-\lambda)\frac{r_2}{r_1}c_{21} + c_{23}\right)z_2\right) \\ &+ \frac{(1-\lambda)}{z_2}\left(S(\lambda)c_{22} + c_{24}\right) \end{aligned} \tag{4.71}$$

$$g(\lambda, z_2) = -\frac{r_1}{r_2 z_2}s_1\left(S(\lambda)c_{15} - c_{16} + (1-\lambda)\frac{r_2}{r_1}S(\lambda)c_{25}\right) \tag{4.72}$$

The braking torque is generated by an actuator; the dynamics are represented as,

$$\dot{T}_b = c_{31}\left(b(u) - T_b\right) \tag{4.73}$$

where,

$$b(u) = \begin{cases} b_1 u + b_2, & u \geq u_0 \\ 0, & u < u_0 \end{cases} \tag{4.74}$$

with, $c_{31} = 20.37$, $b_1 = 15.264$, $b_2 = -6.21$ and $u_0 = 0.415$ are constants.

The objective of control is to achieve the desired slip in presence of matched and mismatched disturbances and parametric uncertainties. The plant dynamics can be written using (4.70) and (4.73) as,

$$\dot{\lambda} = f(\lambda, z_2) + g(\lambda, z_2)T_b \tag{4.75}$$

$$\dot{T}_b = -c_{31}T_b + c_{31}b_1 u + c_{31}b_2 \tag{4.76}$$

4.7.2 Control Design

The dynamics in (4.75) and (4.76) can be rewritten as,

$$\begin{aligned} \dot{\lambda} &= T_b + d_1 \qquad (4.77) \\ \dot{T}_b &= bu + d_2 \qquad (4.78) \end{aligned}$$

where $b = c_{31}b_1$ is a constant and d_1, d_2 are mismatched and matched uncertainty respectively, with

$$\begin{aligned} d_1 &= f(\lambda, z_2) + g(\lambda, z_2)T_b - T_b \qquad (4.79) \\ d_2 &= c_{31}b_2 - c_{31}T_b \qquad (4.80) \end{aligned}$$

The system in (4.77) and (4.78) can be written in a compact form as,

$$\dot{x} = Ax + Bu + B_d d \qquad (4.81)$$

where,

$$x = \begin{bmatrix} \lambda \\ T_b \end{bmatrix} \qquad A = \begin{bmatrix} 0 & 1 \\ 0 & 0 \end{bmatrix} \qquad B = \begin{bmatrix} 0 \\ b \end{bmatrix} \qquad B_d = \begin{bmatrix} 1 & 0 \\ 0 & 1 \end{bmatrix} \qquad d = \begin{bmatrix} d_1 \\ d_2 \end{bmatrix}$$

An observer is designed as,

$$\left.\begin{aligned} \dot{\hat{x}} &= A\hat{x} + Bu_{eq} + LC(x - \hat{x}) \\ \hat{y} &= C\hat{x} \end{aligned}\right\} \qquad (4.82)$$

where, L is the observer gain and u_{eq} is the nominal control.

The sliding surface is selected as,

$$\begin{aligned} \sigma &= C(\hat{x} - [\lambda_d \ , 0]^T) \qquad C = [1 \ \ 0] \qquad (4.83) \\ \sigma^* &= \sigma - \sigma(0)e^{-\alpha t} \qquad \alpha > 1 \qquad (4.84) \end{aligned}$$

The control is designed to enforce sliding along (4.84)

The proposed SMC law combined with EID estimate can be written as,

$$\left.\begin{aligned} u &= -(CB)^{-1}\left\{CA\hat{x} + \alpha\hat{\sigma}(0)e^{-\alpha t} - \dot{\lambda}_d + k_l\hat{\sigma}^* + k_s \operatorname{sat}(\hat{\sigma}^*)\right\} - \hat{d} \\ \hat{d} &= \frac{B^+LC}{\tau}\int \tilde{x} \end{aligned}\right\} \qquad (4.85)$$

4.7.3 Results

The slip (λ) is controlled using SMC supplemented with estimate of EID. The control strategy is tested for different cases without changing the controller parameters The following cases are considered;

- Case 1: uncertain plant with nominal parameters
- Case 2: uncertainty in mass (m)
- Case 3: Uncertainty in road gradient (θ)
- Case 4: different friction models

The observer poles are located at $[-20 \quad -30 \quad -50]$ and controller gains are set at $k_l = 10$ and $k_s = 2$. The value of τ is derived from the observer poles. The reference slip is $\lambda_d = 0.2$. The initial value of z_1 and z_2 is set to 1700 rpm.

Case 1: Nominal plant

The control performance for nominal plant with parameters as in Table 4.1 is shown in Fig. 4.3. The state-dependent non-linearities are estimated by EID. The slip ratio (λ) and control effort (u) is depicted in Fig. 4.3a and 4.3b.

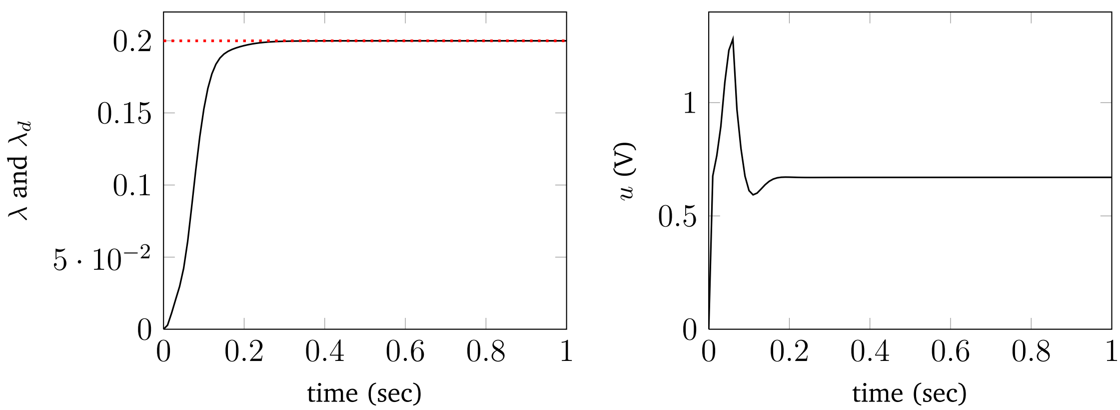

(a) slip ratio (b) control

Figure 4.3: Slip regulation for nominal plant with uncertainty

The plot of other variables for case 1 is shown in Fig. 4.4. The braking torque (T_b) is shown in Fig. 4.4a and the corresponding car velocity and wheel velocity is shown in Fig. 4.4b. The sliding variable (σ) is shown in Fig. 4.4d.

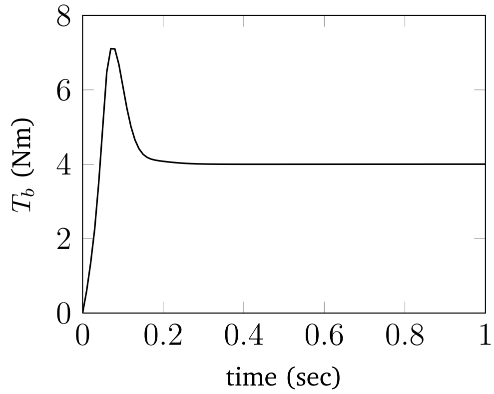

(a) braking torque

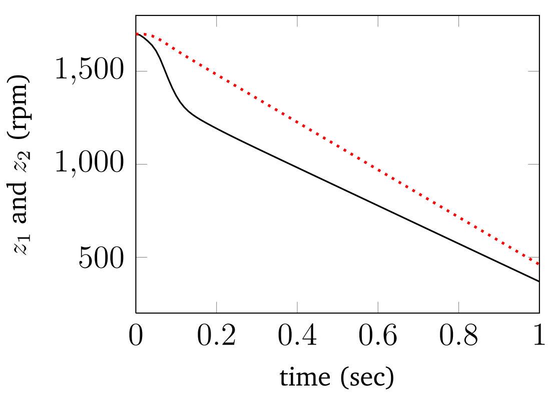

(b) angular velocity ($z_1(-)$ and z_2 (...))

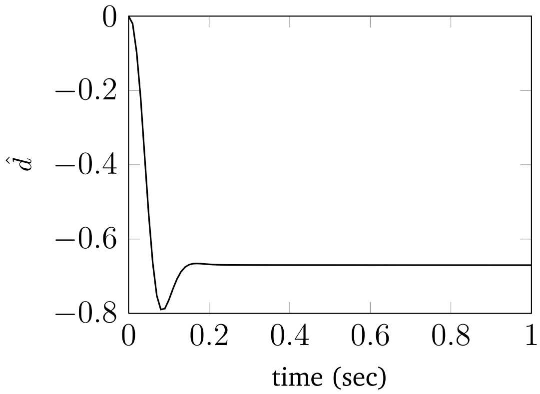

(c) estimate of EID

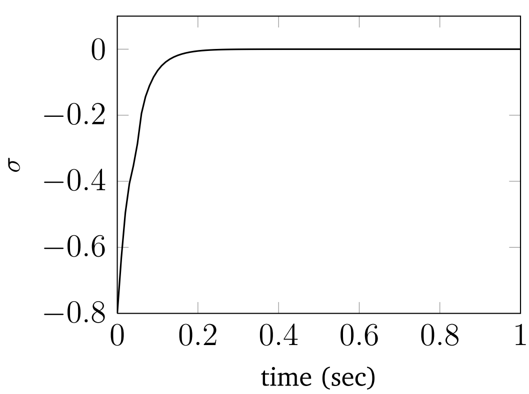

(d) sliding variable

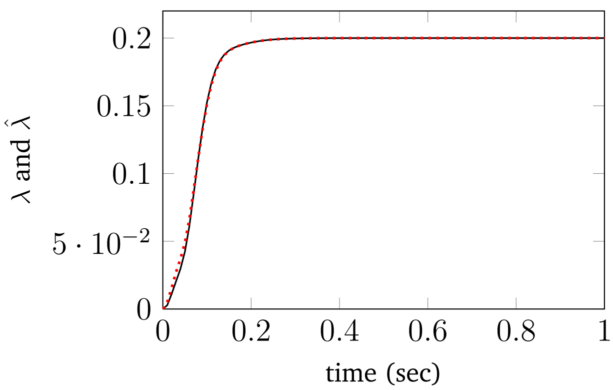

(e) λ (solid) and $\hat{\lambda}$ (dashed)

Figure 4.4: Control performance for nominal plant with uncertainty

Case 2 :Uncertainty in mass (m)

The nominal plant is modified by changing vehicle mass (m) in the defined range over its nominal value. The vehicle mass is changed in the range of $\pm 40\%$. The Figure 4.5a shows the behavior of slip (λ) and Figure 4.5b shows the corresponding control effort with nominal (solid), +30% (dashed) and −30% (dashed-dot).

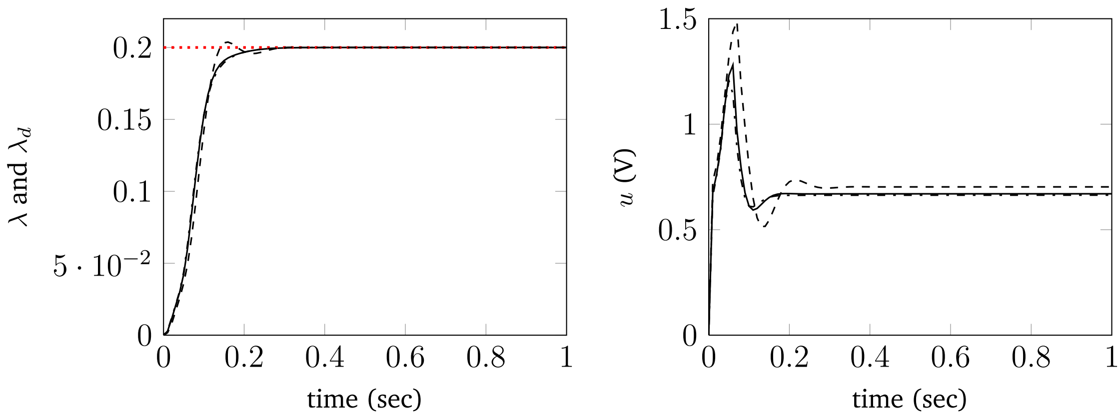

(a) slip ratio

(b) control

Figure 4.5: Control performance with uncertainty in mass

The Table 4.3 depicts the estimation and control performance for robust tracking of slip for different mass uncertainties.

Table 4.3: Performance analysis for mass uncertainty

Uncertainty in mass (%)	$\tilde{\lambda}$ $(\lambda - \lambda_{ref})$	u	σ	$\tilde{y}$ $(y - \hat{y})$
+20	0.0455	0.7296	0.1115	0.0016
–20	0.0440	0.6924	0.1094	0.0013
+30	0.0459	0.7394	0.1121	0.0017
–30	0.0436	0.6834	0.1091	0.0013
+40	0.0462	0.7493	0.1127	0.0017
–40	0.0433	0.6745	0.1088	0.0012

Case 3 : Uncertainty in road gradient (θ)

The slip regulation is tested for different road inclination angle (θ). The relative performance for different angles is shown in Table 4.4.

Table 4.4: Performance analysis for road inclination angle

Road inclination angle (deg.)	$\tilde{\lambda}$ $(\lambda - \lambda_{ref})$	u	σ	$\tilde{y}$ $(y - \hat{y})$
+10	0.0446	0.7064	0.1103	0.0015
+20	0.0445	0.6940	0.1101	0.0014
+30	0.0442	0.6735	0.1097	0.0014
+40	0.0439	0.6462	0.1092	0.0014
+50	0.0434	0.6122	0.1086	0.0013

Case 4 : Different friction models (μ)

The control performance is assessed for variation in $\mu(\lambda)$. The values of coefficients are changed by $\pm 25\%$ to test the effectiveness of estimation. The results are shown in Fig. 4.6 with nominal (solid), +25% (dashed) and -25% (dashed-dot) .

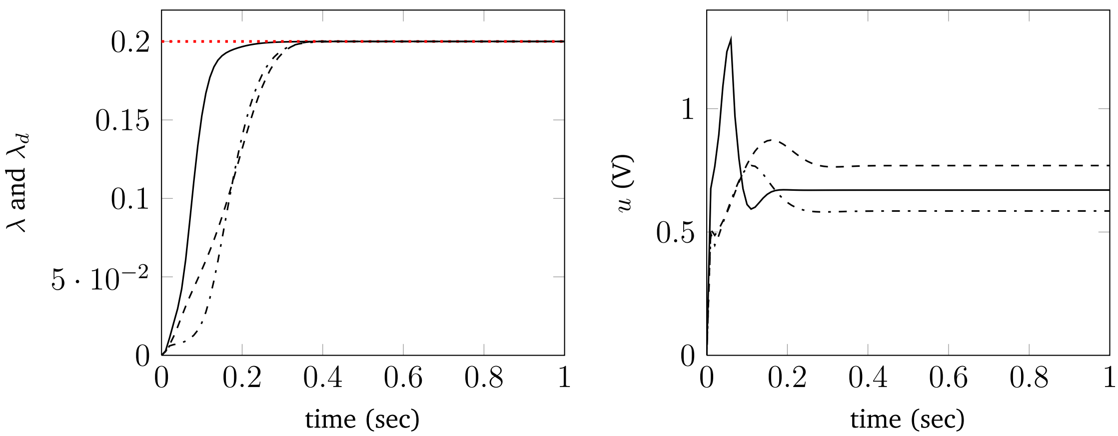

(a) slip ratio (b) control

Figure 4.6: Control performance with variation in $\mu(\lambda)$

The robustness is further validated by testing the designed control for different friction models. The 3 friction models used are,

1. Inteco formula

$$\mu(\lambda) = \frac{w_4 \lambda^p}{a + \lambda^p} + w_3\lambda^3 + w_2\lambda^2 + w_1\lambda \tag{4.86}$$

   where $a = 2.5 \times 10^{-4}$, $p = 2.099$, $w_1 = -0.042$, $w_2 = 0.29 \times 10^{-9}$, $w_3 = 0.035$ and $w_4 = 0.406$

2. Magic formula

$$\mu = D_m \sin\left\{C_m \tan^{-1}(B_m\lambda - E_m \tan^{-1}(B_m\lambda))\right\} \tag{4.87}$$

   where $D_m = 0.5$, $C_m = 1.65$, $B_m = 10.38$ and $E_m = 0.65663$

3. Burckhardt formula

$$\mu = c_1\left(1 - e^{-c_2\lambda}\right) - c_3\lambda \tag{4.88}$$

   where $c_1 = 0.4004$, $c_2 = 33.7080$, $c_3 = 0.1204$

The results are shown in Fig. 4.7.

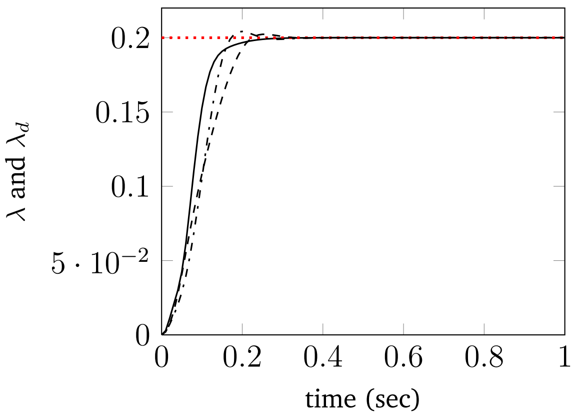

(a) slip ratio

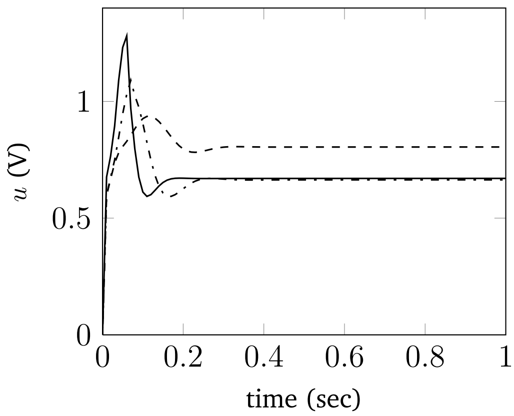

(b) control

Figure 4.7: Control performance for different friction models

The control performance is robust for all friction models, as is evident in Fig. 4.7 for Inteco (solid), Magic formula (dashed) and Burckhardt formula (dashed-dot).

4.8 Summary

A SMC is combined with EID and extended to a nonlinear system with mismatched uncertainties. The use of SMC for nominal control mitigates the need of integral action used in conventional EID based control. The designed control enforces sliding with no chatter. The SMC law is supplemented with estimate of EID to ensure robustness. The EID aids SMC in mitigating the effects of mismatched disturbances. The control performance is further improved by using a higher-order filter to estimate EID and its derivatives. A generalization to $k^{\mathbf{th}}$-order filter is presented.

It is proved that the ultimate boundedness of state estimation error, uncertainty estimation error and sliding variable is guaranteed; and the bounds can be lowered by appropriate choice of design parameters. The efficacy of composite control is tested for slip regulation in anti lock braking system. The design is validated for varied disturbances and parametric uncertainties. The actuator dynamics is also included in the model. The results demonstrate robustness of the proposed scheme for uncertainties in vehicle mass, road gradient and friction, for regulating the vehicle slip and provide short stopping distance.

Chapter 5

SMC for Uncertain Nonlinear System using EID and DO

The chapter explains design of a SMC algorithm for a nonlinear system, with matched and/or mismatched uncertainties. The control law is robustified by employing a DO for estimating EID. The design is validated for trajectory tracking in an active steering control problem.

The chapter begins with an introduction in section 5.1 followed by problem formulation in section 5.2. Section 5.3 describes the estimation of EID using DO. The SMC for nominal plant is designed in Section 5.4 and the composite control is elucidated in section 5.5. Section 5.6 gives the stability analysis using Lyapunov criterion. The control is validated on an application to active steering control in section 5.7. The chapter concludes with a summary in section 5.8.

5.1 Introduction

An Equivalent Input Disturbance (EID) is a disturbance on the control input channel that produces the same effect on controlled output as actual disturbances do. An EID always exists for a controllable and observable plant with no zeros on the imaginary axis (*She et al.*, 2008).

The EID system is reconstructed based on the output of plant, so that the state of EID system and actual state of original plant are usually different (*She et al.*, 2008). The EID approach has mostly been validated for disturbance rejection performance in linear systems (*She et al.*, 2008). The EID method has been extended for control of MIMO (*She and Xin*, 2007) and under-actuated (*She et al.*, 2012), systems. EID has been designed for applications in power systems (*Hu et al.*, 2013), automotive control systems (*She et al.*, 2007), mechatronics (*She et al.*, 2011) and motion control (*She et al.*, 2014). The EID is combined with GESO for missile auto-pilot design (*Li et al.*, 2014).

Disturbance observer (DO) is a technique that uses an auxiliary dynamical system to estimate the uncertainties and disturbances (*Chen et al.*, 2000; *Chen*, 2003). The disturbance estimates are then used in the control law to compensate the effect of uncertainty. The DO has been applied for control of matched systems (*Lu*, 2009), mismatched nonlinear systems (*Yang et al.*, 2011a), mismatched MIMO systems (*Yang et al.*, 2012b). The SMC using a novel sliding surface and extended DO (*Ginoya et al.*, 2014) is an interesting solution.

Active steering control (ASC) is a vital aspect in vehicle stability. The yaw moment control is promising for enhancing vehicle handling and safety under severe driving maneuvers. A control using feedforward and feedback H_∞ for improvement in vehicle handling is presented in (*Mammar and Koenig*, 2002). A nested PID control for lane-keeping (*Marino et al.*, 2011) and LQR (*Yang et al.*, 2009) are some basic designs available. Several other techniques like fuzzy logic (*Boada et al.*, 2005), adaptive control (*Yamaguchi and Murakami*, 2009; *Ding and Taheri*, 2010), model reference controller (*Fukao et al.*, 2004), gain scheduling (*Zhang et al.*, 2014), model predictive control (*Falcone et al.*, 2008), are reported. A vehicle lateral dynamics control can be seen in (*Zhang and Wang*, 2015)

In this work, EID is estimated using a DO and combined with SMC to yield a robust strategy for nonlinear systems with matched and/or mismatched uncertainties and disturbances. The system formulation considered here covers a large class of practical applications. The use of extended DO enables the improvement in estimation accuracy of EID. The composite control is applied to a representative problem of active steering (*Rajamani*, 2011) in automotive control.

5.2 Problem Formulation

An uncertain nonlinear plant with an EID can be written as in (4.3) as,

$$\left.\begin{aligned} \dot{x}(t) &= Ax(t) + Bu(t) + Bd_e(x,u,t) \\ y(t) &= Cx(t) \end{aligned}\right\} \tag{5.1}$$

where d_e is the equivalent input disturbance, which has same effect on output (y), that uncertainties and disturbances in either or all channels would have.

The EID (d_e) is guaranteed under Assumption 4.1.

Assumption 5.1 *The EID $d_e(x,t)$ is continuous and satisfies,*

$$\left|\frac{d^{(j)}d_e(x,u,t)}{dt^{(j)}}\right| \leq \mu \qquad \textit{for } j = 0,1,2,\ldots,r \tag{5.2}$$

where μ is a small positive number.

Remark 5.1 *The Assumption 5.1 implies that the uncertainty $d_e(x,u,t)$ and its derivatives up to some finite order (r) be bounded but the bound is not required to be known. The assumption includes a fairly large class of uncertainties and disturbances that can be estimated by EID.*

The objective is to design a control (u) such that, the output (y) of uncertain plant follows the desired trajectory. The control is expected to ensure robust tracking in presence of uncertainties and disturbances of varying kind.

The EID approach usually uses a state-feedback with integral as a nominal control with estimates of EID for improved disturbance rejection. The EID is normally estimated with a first-order low-pass filter.

The limitations of integral action are to be mitigated by designing a sliding-mode law for nominal plant. The EID is to be estimated using the states of observer and DO, which is then combined with SMC to yield a robust control law. The performance improvement by using a higher-order DO to estimate EID and its derivatives is to be validated.

5.3 Estimation of EID

A servo control system with an EID estimator is shown in Fig. 5.1.

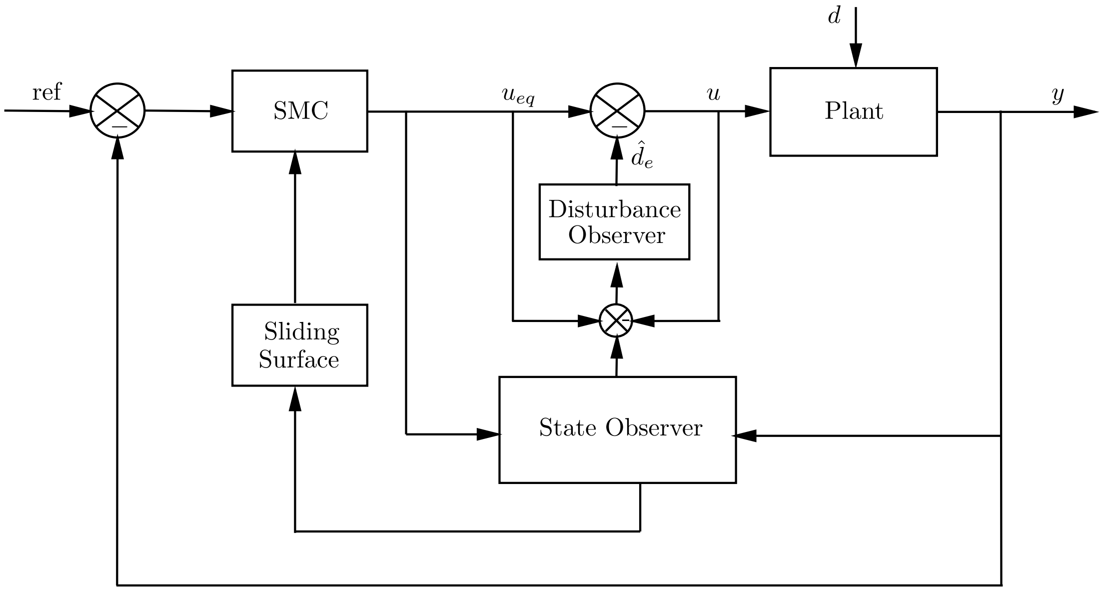

Figure 5.1: Configuration of system with SMC and EID plus DO

The control (u) can be written as,

$$u = u_{eq} - \hat{d}_e \tag{5.3}$$

where u_{eq} is the nominal control designed using sliding-mode and $\hat{d}_e$ is the estimate of d_e that takes care of uncertain part.

Using (5.1)

$$d_e = B^{+}(\dot{x} - Ax - Bu) \tag{5.4}$$

Remark 5.2 *The equation* (5.4) *requires all the states, however the channel on which EID is imposed may be different from that of actual disturbance. The available states of the plant (in the presence of disturbance) may be different from those of the plant with an EID. As such a full-order observer is imperative to estimate EID. It is important to guarantee that* $y(t) - \hat{y}(t)$ *converge to zero.*

The observer is given as,

$$\left.\begin{aligned} \dot{\hat{x}} &= A\hat{x} + Bu_{eq} + L\left(y - \hat{y}\right) \\ \hat{y} &= C\hat{x} \end{aligned}\right\} \tag{5.5}$$

where, L is the observer gain and u_{eq} is the nominal control.

The state estimation error can be written as,

$$\left.\begin{aligned} \tilde{x} &= x - \hat{x} \\ \dot{\tilde{x}} &= \dot{x} - \dot{\hat{x}} \end{aligned}\right\} \tag{5.6}$$

The observer error dynamics are written by using (5.1), (5.3) and (5.5) in (5.6)

$$\left.\begin{aligned} \dot{\tilde{x}} &= A(x - \hat{x}) + B(u - u_{eq}) + Bd_e - LC\left(x - \hat{x}\right) \\ &= (A - LC)\tilde{x} - B\hat{d}_e + Bd_e \\ &= (A - LC)\tilde{x} + B\tilde{d}_e \end{aligned}\right\} \tag{5.7}$$

where $\tilde{d}_e = d_e - \hat{d}_e$

The EID (d_e) in (5.4) can now be estimated with the observed states, with a disturbance observer of the form,

$$\hat{d}_e = p + J\hat{x} \tag{5.8}$$

$$\dot{p} = -J(A\hat{x} + Bu + B\hat{d}_e) \tag{5.9}$$

where p is an auxiliary variable vector, J is a constant gain matrix to be designed.

Differentiating (5.8) and using (5.9), (5.5),

$$\left.\begin{aligned} \dot{\hat{d}}_e &= \dot{p} + J\dot{\hat{x}} \\ &= JLC(x - \hat{x}) \\ &= JLC\tilde{x} \end{aligned}\right\} \tag{5.10}$$

The error dynamics can be written by subtracting both sides of (5.10) from $\dot{d}_e$ as,

$$\left.\begin{aligned} \dot{d}_e - \dot{\hat{d}}_e &= -JLC\tilde{x} + \dot{d}_e \\ \dot{\tilde{d}}_e &= -JLC\tilde{x} + \dot{d}_e \end{aligned}\right\} \tag{5.11}$$

Using (5.7) and (5.11)

$$\begin{bmatrix} \dot{\tilde{x}} \\ \dot{\tilde{d}}_e \end{bmatrix} = \begin{bmatrix} (A-LC) & B \\ -JLC & 0 \end{bmatrix} \begin{bmatrix} \tilde{x} \\ \tilde{d}_e \end{bmatrix} + \begin{bmatrix} 0 \\ 1 \end{bmatrix} \dot{d}_e \tag{5.12}$$

The error dynamics in (5.12) can be further simplified as,

$$\begin{bmatrix} \dot{\tilde{x}} \\ \dot{\tilde{d}}_e \end{bmatrix} = \left(\begin{bmatrix} A & B \\ 0_{1\times 2} & 0 \end{bmatrix} - \begin{bmatrix} L \\ JL \end{bmatrix} \begin{bmatrix} C & 0 \end{bmatrix} \right) \begin{bmatrix} \tilde{x} \\ \tilde{d}_e \end{bmatrix} + \begin{bmatrix} 0_{2\times 1} \\ 1 \end{bmatrix} \dot{d}_e \tag{5.13}$$

A compact form of (5.13) can be written as,

$$\dot{\tilde{e}} = (H - K\,G)\,\tilde{e} + E\,\dot{d}_e \qquad \text{with,} \tag{5.14}$$

$$\tilde{e} = \begin{bmatrix} \tilde{x} \\ \tilde{d}_e \end{bmatrix} \qquad H = \begin{bmatrix} A & B \\ 0_{1\times 2} & 0 \end{bmatrix} \qquad K = \begin{bmatrix} L \\ JL \end{bmatrix}$$

$$G = \begin{bmatrix} C & 0 \end{bmatrix} \qquad E = \begin{bmatrix} 0 & 0 & 1 \end{bmatrix}^T$$

Remark 5.3 *It is evident from* (5.14) *that, the error dynamics is driven by* $\dot{d}_e$*. Thus the error dynamics is asymptotically stable if* $\dot{d}_e \approx 0$*. It is obvious that for bounded* $\dot{d}_e$*, BIBO stability is assured. However, asymptotic stability for the error dynamics can always be assured if some higher derivative of the uncertainty is equal to zero.*

5.3.1 Improvement in Estimation – 2^{nd} order DO

The EID (d_e) and its derivative ($\dot{d}_e$) can be estimated using a second order DO as,

$$\hat{d}_e = p_1 + J_1\hat{x} \tag{5.15}$$

$$\dot{p}_1 = -J_1(A\hat{x} + Bu + B\hat{d}_e) + \hat{\dot{d}}_e \tag{5.16}$$

$$\hat{\dot{d}}_e = p_2 + J_2\hat{x} \tag{5.17}$$

$$\dot{p}_2 = -J_2(A\hat{x} + Bu + B\hat{d}_e) \tag{5.18}$$

where p_1, p_2 are auxiliary variable vectors, and J_1, J_2 are constant gain matrices.

Differentiating (5.15) and (5.17), and using (5.16) and (5.18) with (5.5),

$$\dot{\hat{d}}_e = J_1 LC\tilde{x} + \hat{\dot{d}}_e \tag{5.19}$$

$$\dot{\hat{\dot{d}}}_e = J_2 LC\tilde{x} \tag{5.20}$$

The error dynamics can be written as,

$$\left.\begin{aligned} \dot{\tilde{d}}_e &= -J_1 LC\tilde{x} + \tilde{\dot{d}}_e \\ \dot{\tilde{\dot{d}}}_e &= -J_2 LC\tilde{x} + \ddot{d}_e \end{aligned}\right\} \tag{5.21}$$

The error dynamics can be written using (5.7) and (5.21) as,

$$\begin{bmatrix} \dot{\tilde{x}} \\ \dot{\tilde{d}}_e \\ \dot{\tilde{\dot{d}}}_e \end{bmatrix} = \left(\begin{bmatrix} A & B \\ 0_{2\times2} & 0_{2\times1} \end{bmatrix} - \begin{bmatrix} L \\ -J_1 LC \\ -J_2 LC \end{bmatrix} \begin{bmatrix} C & 0_{1\times2} \end{bmatrix} \right) \begin{bmatrix} \tilde{x} \\ \tilde{d}_e \\ \tilde{\dot{d}}_e \end{bmatrix} + \begin{bmatrix} 0 \\ 0_{1\times1} \\ 1 \end{bmatrix} \ddot{d}_e \tag{5.22}$$

A compact form of (5.22) can be written as,

$$\dot{\tilde{e}} = (H - K\,G)\,\tilde{e} + E\,\ddot{d}_e \tag{5.23}$$

where,

$$\tilde{e} = \begin{bmatrix} \tilde{x} \\ \tilde{d}_e \\ \tilde{\dot{d}}_e \end{bmatrix} \qquad H = \begin{bmatrix} A & B \\ 0_{2\times2} & 0_{2\times1} \end{bmatrix} \qquad K = \begin{bmatrix} L \\ -J_1 LC \\ -J_2 LC \end{bmatrix}$$

$$G = \begin{bmatrix} C & 0_{1\times2} \end{bmatrix} \qquad E = \begin{bmatrix} 0 & 0 & 0 & 1 \end{bmatrix}^T$$

Remark 5.4 *It is evident from* (5.23) *that, the error dynamics is driven by $\ddot{d}_e$. Thus the error dynamics is asymptotically stable if $\ddot{d}_e \approx 0$. The estimation accuracy is thus improved as both d_e and $\dot{d}_e$ are estimated.*

5.3.2 Generalization – n^{th} order DO

In general, if n^{th} derivative of the disturbance, ${d_e}^{(n)}$ is zero; the estimation can be extended to a n^{th} order DO for estimating d_e and its $n-1$ derivatives.

The equations for estimate of EID and its derivatives can be written as,

$$\left.\begin{array}{lcl} \dot{\hat{d}}_e & = & J_1 LC\,\tilde{x} + \hat{\dot{d}}_e \\ \dot{\hat{\dot{d}}}_e & = & J_2 LC\;\tilde{x} + \hat{\ddot{d}}_e \\ \vdots & & \\ \dot{\widehat{d_e^{(n-1)}}} & = & J_{n-1} LC\,\tilde{x} + \widehat{d_e^{(n)}} \\ \dot{\widehat{d_e^{(n)}}} & = & J_n LC\,\tilde{x} \end{array}\right\} \tag{5.24}$$

where $\hat{d}_e$ is the estimate of EID d_e and $\hat{d}_e^{(i)}$, $i = 2, 3, \ldots\ldots, n$ are the estimates of derivatives of EID ${d_e}^{(j)}$ $j = 1, 2, \ldots\ldots, (n-1)$.

The dynamics of estimation error is written as,

$$\left.\begin{array}{lcl} \dot{\tilde{d}}_e & = & -J_1 LC\,\tilde{x} + \tilde{\dot{d}}_e \\ \dot{\tilde{\dot{d}}}_e & = & -J_2 LC\,\tilde{x} + \tilde{\ddot{d}}_e \\ \vdots & & \\ \dot{\widetilde{d_e^{(n-1)}}} & = & -J_{n-1} LC\,\tilde{x} + \widetilde{d_e^{(n)}} \\ \dot{\widetilde{d_e^{(n)}}} & = & -J_n LC\,\tilde{x} + {d_e}^{(n)} \end{array}\right\} \tag{5.25}$$

The error dynamics can now be written using (5.7) and (5.25) as,

$$\begin{bmatrix} \dot{\tilde{x}} \\ \dot{\tilde{d}}_e \\ \dot{\tilde{\dot{d}}}_e \\ \vdots \\ \dot{\widetilde{d_e^{(n-1)}}} \\ \dot{\widetilde{d_e^{(n)}}} \end{bmatrix} = \left(\begin{bmatrix} A & B \\ 0_{k\times 2} & 0_{k\times 1} \end{bmatrix} - \begin{bmatrix} L \\ J_1 L \\ J_2 L \\ \vdots \\ J_{n-1} L \\ J_n L \end{bmatrix} \begin{bmatrix} C & 0_{1\times k} \end{bmatrix} \right) \begin{bmatrix} \tilde{x} \\ \tilde{d}_e \\ \tilde{\dot{d}}_e \\ \vdots \\ \widetilde{d_e^{(n-1)}} \\ \widetilde{d_e^{(n)}} \end{bmatrix} + \begin{bmatrix} 0 \\ 0_{(n-1)\times 1} \\ 1 \end{bmatrix} {d_e}^{(n)} \tag{5.26}$$

A compact form of (5.26) can be written as,

$$\dot{\tilde{e}} = (H - K\,G)\,\tilde{e} + E\,d_e^{(n)} \tag{5.27}$$

5.4 Design of Control

The EID can be combined with any control design to improve the performance of system. A SMC combined with EID is proposed here to address the issue of matched and/or mismatched uncertainty. The objective is to control output (y) in the presence of parametric uncertainties.

The control u in (5.1) can be written as,

$$u = u_{eq} + u_n \tag{5.28}$$

where u_{eq} is the nominal control designed using sliding-mode and $u_n = -\hat{d}$ is the control for the uncertain part with $\hat{d}$ as the estimate of d_e

5.4.1 Sliding Surface

The sliding surface is defined as,

$$\sigma = y - y_d \tag{5.29}$$

where y_d is the desired trajectory of output.

Using (5.1) in (5.29),

$$\sigma = Cx - y_d \tag{5.30}$$

The estimation of EID is based on observed states, as such the control (u_{eq}) is also designed using estimated states ($\hat{x}$). Therefore, the sliding surface is rewritten as,

$$\sigma = C\hat{x} - y_d \tag{5.31}$$

The sliding surface (5.31) is modified as,

$$\sigma^* = \sigma - \sigma(0)\, e^{-\alpha t} \tag{5.32}$$

where α is a user chosen positive constant.

Remark 5.5 *The sliding surface of* (5.32) *eliminates reaching phase and also aids in mitigating chatter (Deshpande and Phadke, 2012). The modified sliding variable σ^* is zero at $t = 0$, thus precluding the initial control from taking large values. Additionally, $\sigma^* \to \sigma$ as $t \to \infty$.*

5.4.2 Sliding Mode Control

A control is designed such that, the sliding condition is satisfied and plant follows the desired trajectory.

Differentiating (5.32) and using (5.31) and (5.5),

$$\dot{\sigma}^* = CA\hat{x} + CBu_{\text{eq}} + CLC\tilde{x} + \alpha\sigma(0)e^{-\alpha t} - \dot{y}_d \tag{5.33}$$

The control that ensures sliding can be written as,

$$u_{eq} = -(CB)^{-1}\left\{CA\hat{x} + \alpha\sigma(0)e^{-\alpha t} - \dot{y}_d + k_l\sigma^* + k_s\,\text{sat}(\sigma^*)\right\} \tag{5.34}$$

where $k_l > 0$ is the linear gain and $k_s > 0$ is the switching gain to be designed and,

$$\text{sat}\,(\sigma^*) = \begin{cases} \text{sgn}\,(\sigma^*) & \text{if } |\sigma^*| > \epsilon,\ \epsilon > 0 \\ \sigma^*/\epsilon & \text{if } |\sigma^*| \leq \epsilon \end{cases}$$

With the control in (5.34), the dynamics of sliding surface can be written as,

$$\dot{\sigma}^* = -k_l\sigma^* - k_s\,\text{sat}(\sigma^*) + CLC\tilde{x} \tag{5.35}$$

Remark 5.6 *It is seen from* (5.35) *that, as $\tilde{x} \to 0$, sliding condition is satisfied and σ^* will asymptotically approach 0, if $k_l > 0$ and $k_s > 0$.*

5.5 Proposed Control

The proposed SMC law combined with EID can be written as,

$$\left.\begin{aligned} u_{eq} &= -(CB)^{-1}\{CA\hat{x} + \alpha\sigma(0)e^{-\alpha t} - \dot{y}_d + k_l\sigma^* + k_s\,\text{sat}(\sigma^*)\} \\ u_n &= -\hat{d}_e \\ \hat{d}_e &= p + J\hat{x} \\ \dot{p} &= -J(A\hat{x} + Bu + B\hat{d}_e) + \dot{\hat{d}}_e \end{aligned}\right\} \tag{5.36}$$

It may be noted that the EID in (5.36) is estimated with a first-order DO. The same can be extended to any order DO for improving the robustness.

5.6 Stability

The error dynamics are rewritten using (5.12) as,

$$\begin{bmatrix} \dot{\tilde{x}} \\ \dot{\tilde{d}}_e \end{bmatrix} = \begin{bmatrix} (A-LC) & B \\ -J_1 LC & 0 \end{bmatrix} \begin{bmatrix} \tilde{x} \\ \tilde{d}_e \end{bmatrix} + \begin{bmatrix} 0 \\ 1 \end{bmatrix} \dot{d}_e \tag{5.37}$$

A compact form of (5.37) can be written as,

$$\dot{\tilde{e}} = M\,\tilde{e} + N\,\dot{d}_e \qquad \text{where } \tilde{e} = [\ \tilde{x} \ \ \tilde{d}\ ]^T \tag{5.38}$$

It is evident from (5.38) that eigen values of M can be placed arbitrarily by selecting observer gain L. If the eigen values of M have negative real parts, one can always find a positive definite matrix P such that,

$$PM + M^T P = -Q \tag{5.39}$$

for a given positive definite matrix Q. Let λ_q be the smallest eigen value of Q.

Mefining a Lyapunov function as,

$$V(\tilde{e}) = \tilde{e}^T P\,\tilde{e} \tag{5.40}$$

Taking derivative of $V(\tilde{e})$ along (5.38)

$$\begin{aligned} \dot{V}(\tilde{e}) &= \tilde{e}^T P\dot{\tilde{e}} + \dot{\tilde{e}}^T P\tilde{e} & (5.41)\\ &= \tilde{e}^T(PM + M^T P)\tilde{e} + 2\tilde{e}^T PN\dot{d}_e & (5.42)\\ &= -\tilde{e}^T Q\tilde{e} + 2\tilde{e}^T PN\dot{d}_e & (5.43)\\ &\leq -\lambda_q\|\tilde{e}\|^2 + 2\|\tilde{e}\|\,\|PN\|\,\mu & (5.44)\\ &\leq -\|\tilde{e}\|\,(\|\tilde{e}\|\lambda_q - 2\|PN\|\mu) & (5.45) \end{aligned}$$

It is seen from (5.45) that, $\|\tilde{e}\|$ is ultimately bounded and remains in a ball of radius $\frac{2\,\|PN\|\,\mu}{\lambda_q}$, which guarantees that,

$$\|\tilde{x}\| \leq \lambda_1 = \frac{2\,\|PN\|\,\mu}{\lambda_q} \tag{5.46}$$

$$\|\tilde{d}\| \leq \lambda_2 = \frac{2\,\|PN\|\,\mu}{\lambda_q} \tag{5.47}$$

The dynamics of σ^* can be written using (5.35) as,

$$\dot{\sigma}^* = -k_l\sigma^* - k_s\,\mathrm{sat}(\sigma^*) + CLC\tilde{x} \tag{5.48}$$

Therefore,

$$\begin{aligned} \sigma^*\dot{\sigma}^* &= -k_l{\sigma^*}^2 - k_s\sigma^*\,\mathrm{sat}(\sigma^*) + \sigma^* CLC\tilde{x} & (5.49)\\ &\leq -k_l|\hat{\sigma}^*|^2 - k_s|\sigma^*|\,\mathrm{sat}(\sigma^*) + |CLC|\,|\hat{\sigma}^*|\,\|\tilde{x}\| & (5.50)\\ &\leq -k_l|\hat{\sigma}^*|^2 - k_s|\sigma^*|\,\mathrm{sat}(\sigma^*) + |CLC|\,|\hat{\sigma}^*|\,\lambda_1 & (5.51) \end{aligned}$$

Define,

$$\zeta = |CLC|\,\lambda_1 \tag{5.52}$$

Therefore,

$$\sigma^*\dot{\sigma}^* = -k_l|\hat{\sigma}^*|^2 - k_s|\sigma^*|\,\mathrm{sat}(\sigma^*) + |\hat{\sigma}^*|\,\zeta \tag{5.53}$$

if $|\sigma^*| > \epsilon$

$$\sigma^*\dot{\sigma}^* = -|\hat{\sigma}^*|\,(k_l\,|\hat{\sigma}^*| + k_s - \zeta) \tag{5.54}$$

Therefore,

$$|\sigma^*| \leq \frac{\zeta - k_s}{k_l} \tag{5.55}$$

if $|\sigma^*| \leq \epsilon$

$$\sigma^*\dot{\sigma}^* = -|\hat{\sigma}^*|\left(k_l\,|\hat{\sigma}^*| + \frac{k_s}{\epsilon}|\hat{\sigma}^*| - \zeta\right) \tag{5.56}$$

Therefore,

$$|\sigma^*| \leq \frac{\zeta}{k_l + \frac{k_s}{\epsilon}} \tag{5.57}$$

Thus, the sliding variable ($\hat{\sigma}^*$) is ultimately bounded by,

$$|\hat{\sigma}^*| \leq \lambda_3 = \max\left(\frac{\zeta - k_s}{k_l}, \frac{\zeta}{k_l + \frac{k_s}{\epsilon}}\right) \tag{5.58}$$

In view of (5.58), it is evident that $\|\tilde{y} = y - y_d\|$ shall be bounded.

It is seen from (5.46), (5.47) and (5.58) that, $\|\tilde{x}\|$, $\|\tilde{d}\|$ and $|\hat{\sigma}^*|$ are ultimately bounded. The bounds can be lowered by appropriate choice of control parameters k_l, k_s and L.

The practical stability is thus proved in the sense of *Corless and Leitmann* (1981)

5.7 Application : Active Steering Control

Active steering control is a strategy of electronically modifying steering angle to the wheels (*Rajamani*, 2011). It works on the principle that, the input given to front wheel is sum of driver input and controlled motor input (*Klier et al.*, 2004). The yaw moment control is regarded as one of the most promising means of chassis control, considerably enhancing vehicle handling and safety under severe driving maneuvers. A nested PID control (*Marino et al.*, 2011), LQR (*Yang et al.*, 2009), kalman filter (*Baffet et al.*, 2009; *Nam et al.*, 2013), adaptive control (*Yamaguchi and Murakami*, 2009) are some of the designs reported in literature.

5.7.1 Dynamic Model

A single track bicycle model is shown in Fig. 5.2.

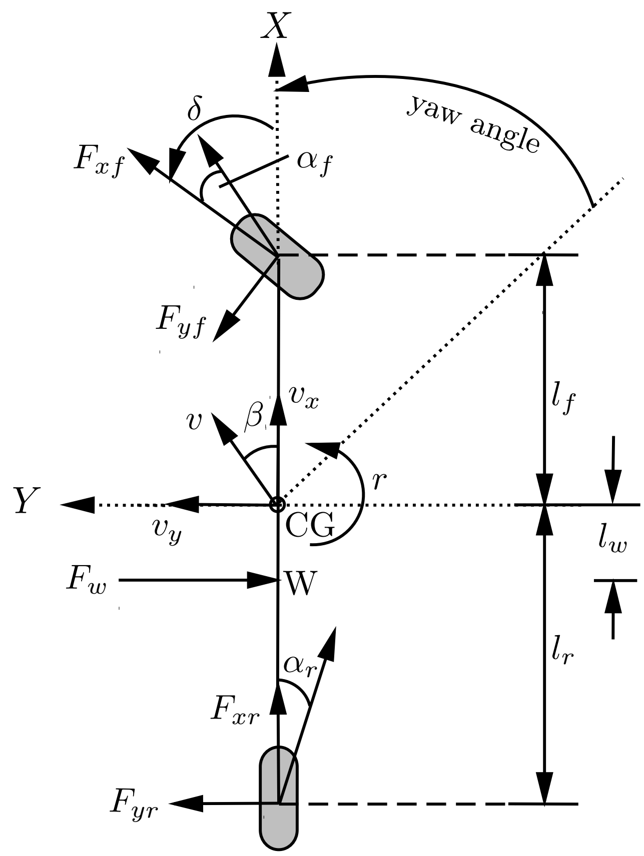

Figure 5.2: Single track bicycle model

A single track bicycle model is derived with the following assumptions,

1. The height of vehicle's center of gravity (CG) is at the level of road surface, hence vehicle does not experience rolling motion during cornering.
2. The longitudinal velocity of the vehicle is assumed to be constant.

At the vehicle's CG, the following equations can be written as,

1. Using Newton's 2nd law (in vehicle lateral direction),

$$m(\dot{v_y} + v_x\,\dot{\psi}) = F_{yf}\cos\delta + F_{yr} - F_w \tag{5.59}$$

2. Conservation of angular momentum about the Z-axis (through vehicle's center of gravity),

$$J\ddot{\psi} = F_{yf}l_f\cos\delta - F_{yr}l_r + l_wF_w \tag{5.60}$$

where
δ is the front wheel steer angle

F_{yf} and F_{yr} are the lateral forces in the front and rear tire respectively

l_f and l_r are the distances from vehicle's center of mass to front and rear axis

m is the vehicle mass

v_x and v_y are longitudinal velocity and lateral velocity respectively

β and $\dot{\psi}$ are the vehicle side-slip angle and yaw rate respectively

J is the moment of inertia of the vehicle about Z-axis

F_w is the resultant wind disturbance acting at l_w from the CG of vehicle

Using small angle assumption, lateral forces of both the axes can be expressed as,

$$F_{yf} = -\mu\,C_f\,\alpha_f, \qquad F_{yr} = -\mu\,C_r\,\alpha_f \tag{5.61}$$

where C_f, C_r are the front and rear tire cornering stiffness, α_f, α_r are the slip angles of the front and rear tire respectively and μ describes the road surface condition i.e. $\mu = 1$ for dry road, $\mu = 0.5$ for wet road, and $\mu = 0.2$ for icy road surface.

The tire slip angle (α) is defined as the angle between; direction the tire is pointing and the direction of its movement.

Using simple geometrical relations and considering small angle assumptions,

$$\alpha_f = \delta - \beta + \frac{l_f}{v_x}\dot{\psi} \tag{5.62}$$

$$\alpha_r = -\beta + \frac{l_r}{v_x}\dot{\psi} \tag{5.63}$$

The side-slip angle (β) at CG is defined as angle between vehicle longitudinal axis and local direction of travel, and is given as,

$$\beta = \arctan\left(\frac{v_y}{v_x}\right) \tag{5.64}$$

For small angles, β can be approximated as,

$$\beta \approx \frac{v_y}{v_x} \tag{5.65}$$

The lateral acceleration (a_y) at the vehicle CG is given as,

$$a_y = v_x(\dot{\beta} + \dot{\psi}) \tag{5.66}$$

Rewriting (5.59) and (5.60),

$$m(\dot{v_y} + v_x\,\dot{\psi}) = F_{yf} + F_{yr} + F_{yf}\cos\delta - F_{yf} - F_w \tag{5.67}$$

$$J\ddot{\psi} = F_{yf}l_f - F_{yr}l_r + F_{yf}l_f\cos\delta - F_{yf}l_f + l_wF_w \tag{5.68}$$

The nonlinear terms in (5.67),(5.68) along with uncertainties in lateral forces due to cornering stiffness (being dependent on friction coefficient and vehicle mass variations) are taken into disturbance without modifying the system equations as,

$$m(\dot{v_y} + v_x\,\dot{\psi}) = F_{yf} + F_{yr} + d_1 \tag{5.69}$$

$$J\ddot{\psi} = F_{yf}l_f - F_{yr}l_r + d_2 \tag{5.70}$$

Rearranging the terms of (5.69) and (5.70) using (5.65) gives,

$$\dot{\beta} = \frac{F_{yf} + F_{yr}}{mv_x} + d_1 \quad \text{and} \quad \ddot{\psi} = \frac{F_{yf}l_f - F_{yr}l_r}{J} + d_2 \tag{5.71}$$

where,

$$d_1 = \frac{F_{yf}\cos\delta - F_{yf} - F_w}{mv_x} + \frac{\Delta F_{yf}\cos\delta + \Delta F_{yr}}{\Delta mv_x} - \dot{\psi} \tag{5.72}$$

$$d_2 = \frac{F_{yf}l_f\cos\delta - F_{yf}l_f + l_wF_w}{J} + \frac{\Delta F_{yf}l_f\cos\delta - \Delta F_{yr}l_r}{J} \tag{5.73}$$

Writing the system matrices in state space form using (5.61), (5.66) in (5.71),

$$\dot{x} = Ax + Bu + B_d d \tag{5.74}$$

$$y = Cx + Du \tag{5.75}$$

where, $x = [\,\beta \quad \dot{\psi}\,]^T, \quad u = \delta, \quad y = [\,a_y \quad \dot{\psi}\,]^T, \quad d = [\,d_1 \quad d_2\,]^T$

$$A = \begin{bmatrix} \dfrac{-C_f - C_r}{mv_x} & \dfrac{-l_fC_f + l_rC_r}{mv_x^2} - 1 \\[2ex] \dfrac{-l_fC_f + l_rC_r}{J} & \dfrac{-l_f^2C_f - l_r^2C_r}{Jv_x} \end{bmatrix}, \quad B = \begin{bmatrix} \dfrac{C_f}{mv_x} \\[2ex] \dfrac{l_fC_f}{J} \end{bmatrix} \tag{5.76}$$

$$C = \begin{bmatrix} \dfrac{-C_f - C_r}{m} & \dfrac{-l_fC_f + l_fC_r}{mv_x} \\[2ex] 0 & 1 \end{bmatrix}, \quad D = \begin{bmatrix} \dfrac{C_f}{m} \\[1ex] 0 \end{bmatrix}, \; B_d = \begin{bmatrix} 1 & 0 \\ 0 & 1 \end{bmatrix}$$

5.7.2 Reference Model

The desired steering response is given by a reference model. The model has zero vehicle sideslip angle β at the center of gravity and the desired yaw rate described by the front wheel steering angle and the longitudinal velocity of the vehicle.

The steady state gain of sideslip angle and yaw rate is given as,

$$\begin{aligned} \beta_d &= 0 \\ \dot{\psi}_d &= \frac{v_x}{l + K_u v_x^2}\delta_f \end{aligned} \tag{5.77}$$

where $l = l_f + l_r$ is the total wheel-base length of the vehicle and,

$$K_u = \frac{m(l_rC_r - l_fC_f)}{lC_fC_r} \tag{5.78}$$

is the vehicle stability parameter describing steering characteristics of the vehicle.

5.7.3 Results

The yaw-rate ($\dot{\psi}$) is controlled using sliding mode control supplemented with estimation of EID. The parameters of model used are,

Table 5.1: Specifications of vehicle

Parameters	Value	Unit
Vehicle mass (m)	1430	kg
Yaw moment inertia (J)	2430	kg m^2
Distance from CG to front axle (l_f)	1.1	m
Distance from CG to rear axle (l_r)	1.4	m
Front cornering stiffness (C_f)	40000	N/rad
Rear cornering stiffness (C_r)	42503	N/rad
Front tire relaxation length (a_f)	0.75	m
Rear tire relaxation length (a_r)	0.75	m

The design is tested for 2-different maneuvers; viz. Double Lane Change (DLC) and Single Lane Change (SLC). The stabilization problem is to maintain the yaw-rate for different cases. The following cases for each maneuver are considered, without changing the controller parameters,

- Case 1: uncertainty in road adhesion coefficient (μ)
- Case 2: uncertainty in mass and inertia (m and J)
- Case 3: variable longitudinal velocity v_x with wind disturbance F_w
- Case 4: effect of second-order filter

The observer poles are located at $[-10 \quad -20 \quad -30]$ and controller gains are set at $k_l = 20$ and $k_s = 2$. The value of τ is derived from the observer poles.

A trajectory tracking control with EID estimated by a filter is considered here and results are shown in Fig. 5.3 to Fig. 5.7.

Case 1: Uncertainty in road adhesion coefficient (μ)

The vehicle is considered to be moving with a constant longitudinal velocity (v_x) of 40 m/sec with uncertainty in the road adhesion coefficient. The control is tested for 3 different road adhesion coefficients: $\mu = 0.3, \mu = 0.5$ and $\mu = 0.8$. The results for $\mu = 0.3$ are shown in Fig. 5.3

The yaw-rate ($\dot{\psi}$) for SLC and DLC maneuver is shown in Fig. 5.3a and Fig. 5.3b, with their corresponding control in Fig. 5.3c and Fig. 5.3d respectively.

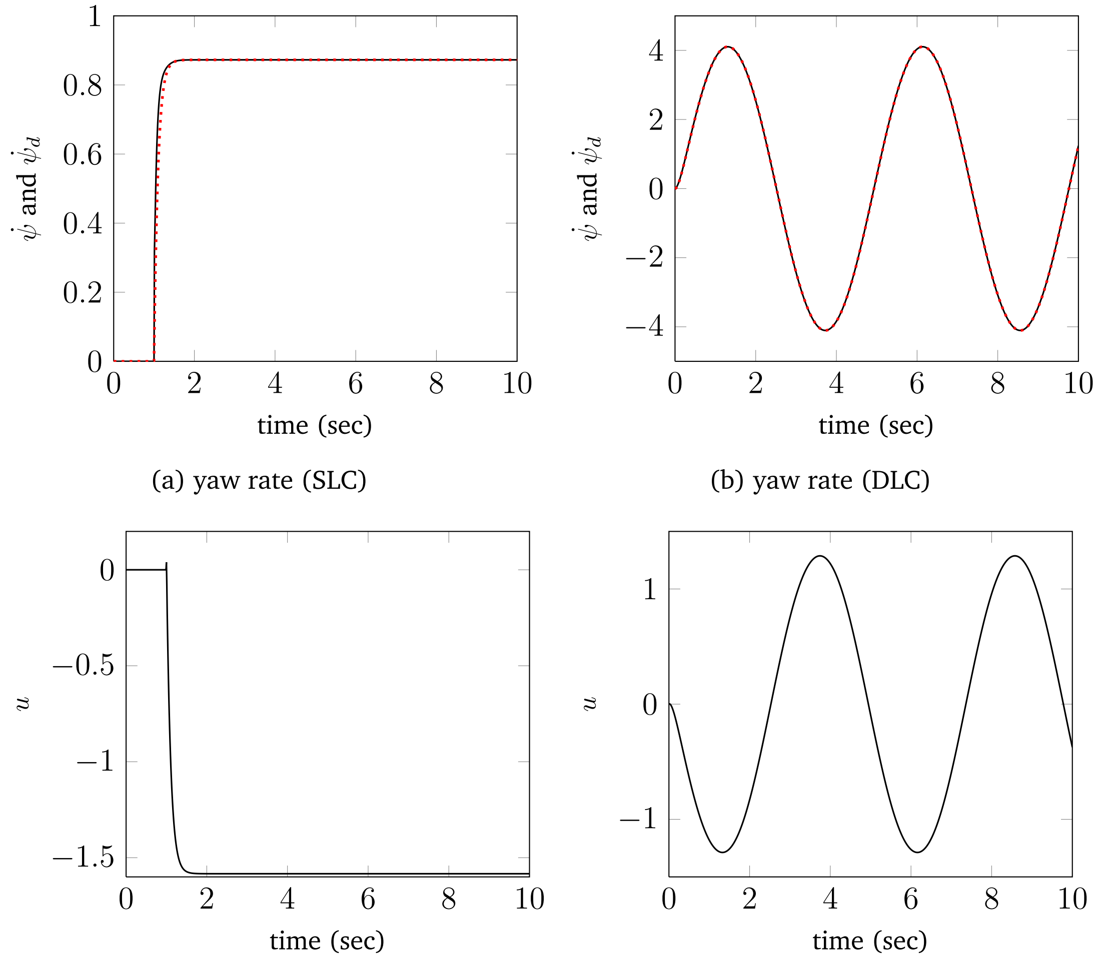

(a) yaw rate (SLC)

(b) yaw rate (DLC)

(c) control (SLC)

(d) control (DLC)

Figure 5.3: Control performance with uncertainty in road adhesion coefficient

The output follows desired trajectory [actual (-) and reference (...)] for both the maneuvers and control inputs vary to keep the output at desired values.

The tracking and estimation error for DLC maneuver with $\mu = 0.3$ is shown in Fig. 5.4. The tracking error in output is shown in Fig. 5.4a where the error is to the scale of 0.01. This is a result of efficient estimation of EID as shown in Fig. 5.4c. The EID estimate is dependent on the efficiency of observer. The tracking performance of observer is shown in Fig. 5.4b where the error is to order of 0.001. The results are similar for SLC maneuver as well.

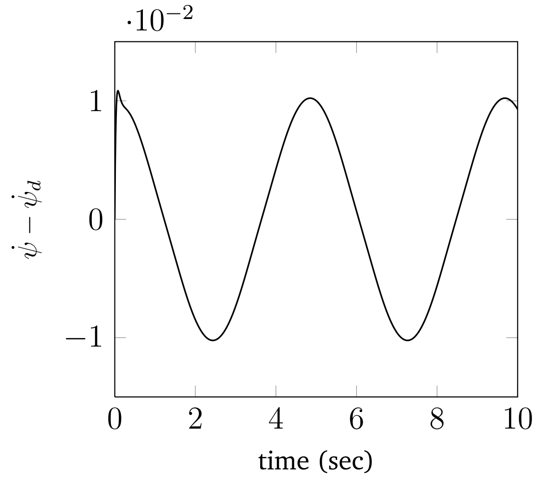

(a) output tracking error

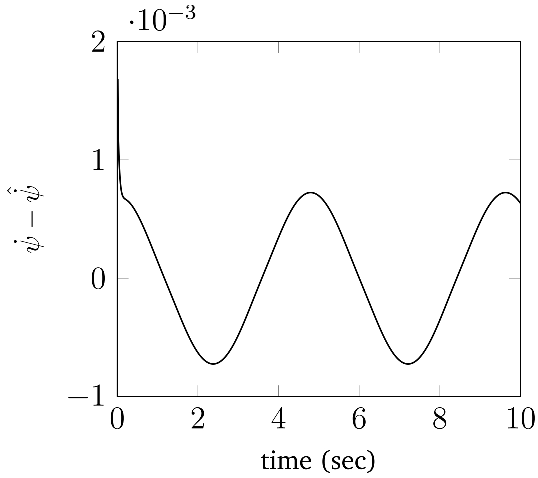

(b) output estimation error

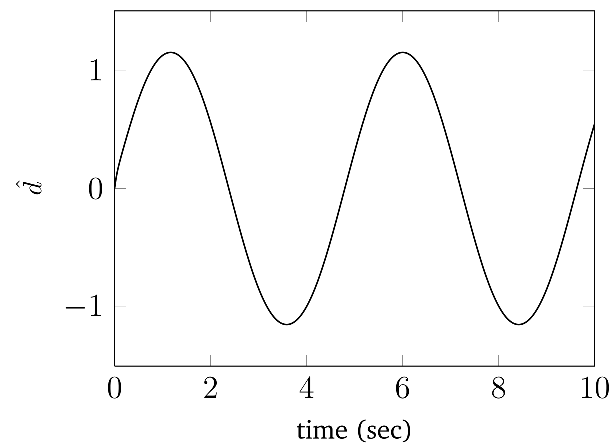

(c) estimate of EID

Figure 5.4: Tracking and estimation accuracy

The performance under different road adhesion coefficients is almost same because of accurate estimation of EID. A summary of results is placed in Table 5.2 and Table 5.3 for DLC and SLC respectively.

Case 2: Uncertainty in vehicle mass (m) and moment of inertia (J)

The mass (m) and inertia (J) are assumed to be uncertain, lying in the range of $\pm 25\%$ over their nominal values. The road adhesion coefficients is $\mu = 0.5$ and longitudinal velocity is $v_x = 40$ m/sec. The results for $+25\%$ are shown in Fig. 5.5.

The yaw-rate ($\dot{\psi}$) for SLC and DLC maneuver is shown in Fig. 5.5a and Fig. 5.5b, with their corresponding control in Fig. 5.5c and Fig. 5.5d respectively.

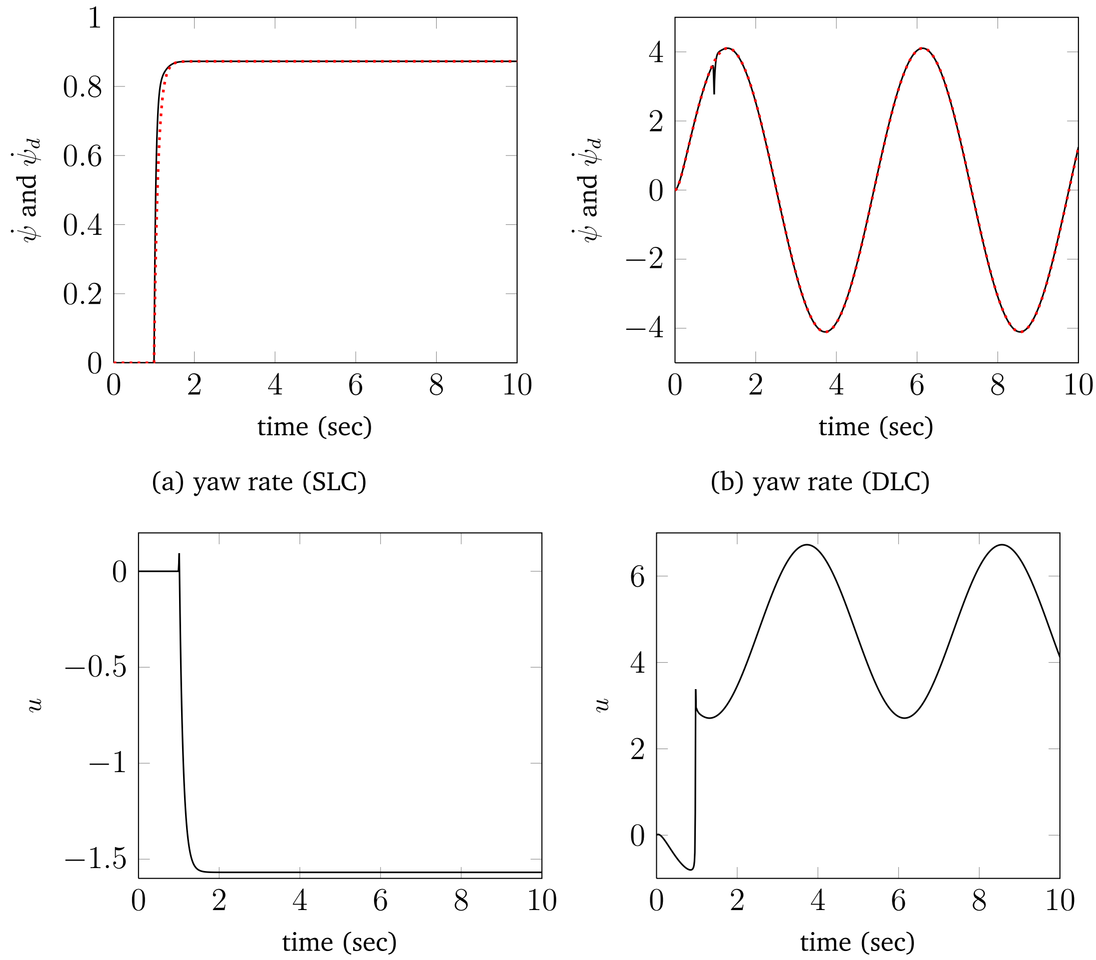

(a) yaw rate (SLC) (b) yaw rate (DLC)

(c) control (SLC) (d) control (DLC)

Figure 5.5: Control performance with uncertainty in mass and inertia

The output follows desired trajectory [actual (-) and reference (...)] for both the maneuvers and control inputs vary to keep the output at desired values.

Case 3: Varying longitudinal velocity (vx)

The longitudinal velocity is considered varying, as a 40m/sec sinusoid with a bias of 50m/sec. The parametric uncertainties are same as case 2. A wind disturbance of magnitude 5N is applied in from 2 to 7 sec. The results are shown in Fig. 5.6.

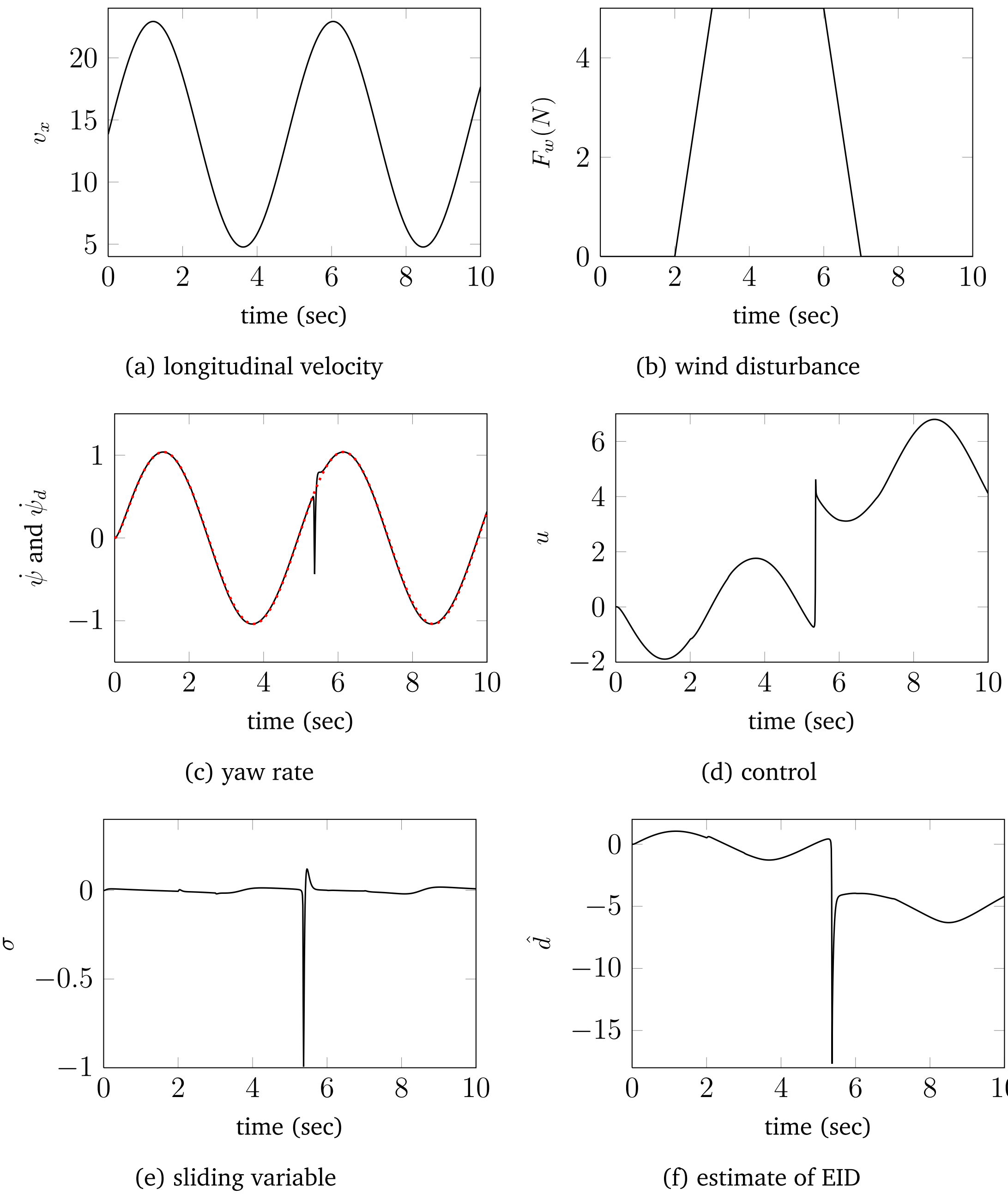

(a) longitudinal velocity

(b) wind disturbance

(c) yaw rate

(d) control

(e) sliding variable

(f) estimate of EID

Figure 5.6: Control performance with varying longitudinal velocity

Case 4: Improvement with extended DO

The tracking performance is improved with the use of a second order filter. The same is illustrated for a DLC maneuver in Fig. 5.7. A comparison is made between EID estimated using first-order and second-order filter for uncertainties and disturbances as in Case 3. The results obtained with second-order filter are superimposed on results obtained using first-order filter for case 3. The output tracking error for SLC maneuver in Fig. 5.7a shows a marginal improvement but the tracking for DLC maneuver in Fig. 5.7b shows a markedly improved tracking performance.

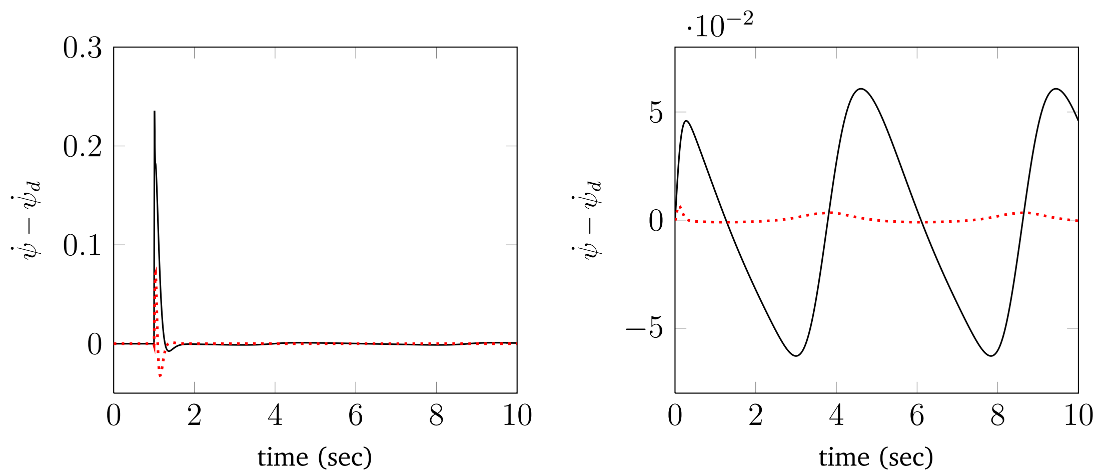

(a) output tracking error (SLC) (b) output tracking error (DLC)

Figure 5.7: Comparative performance with first order (-) and second order (...) filter

It is worth noting here that the performance is improved without changing the pole locations of observer or gains of controller. The bound on tracking error is lowered on account of improved estimation of EID by a second order filter.

Summary of Performance

The results for all the cases (Case 1 to Case 4) are summarized in Table 5.2 and Table 5.3 for DLC and SLC maneuver respectively. The results prove that; the proposed control can successfully track the desired yaw-rate, inspite of uncertainties, variations and disturbances for any maneuver.

It is evident from both the tables that, the proposed control design is able to track yaw-rate for all cases. The estimation of output is crucial for estimation of EID and the same is evident in the tables. The control (u) is also within limits.

Table 5.2: Summary of performance : DLC maneuver

	Uncertainty	β-$\beta_d \times 10^{-3}$	$\dot{\psi}$-$\dot{\psi}_d \times 10^{-3}$	$y - \hat{y} \times 10^{-3}$	u_{RMS}
Case 1	$\mu = 0.3$	111	9.28	0.63	0.3748
	$\mu = 0.5$	116	9.37	0.66	0.3821
	$\mu = 0.8$	119	9.68	0.67	0.3892
Case 2	Δm, $\Delta J = +20\%$	73.9	15.02	1.03	4.1237
	Δm, $\Delta J = -20\%$	74.6	12.78	0.84	2.2343
Case 3	varying v_x	49.5	23.74	0.56	4.1172
Case 4	2^{nd} order filter	12.89	3.26	0.52	0.1638

Table 5.3: Summary of performance : SLC maneuver

	Uncertainty	β-$\beta_d \times 10^{-3}$	$\dot{\psi}$-$\dot{\psi}_d \times 10^{-3}$	$y - \hat{y} \times 10^{-3}$	u_{RMS}
Case 1	$\mu = 0.3$	77.03	7.38	0.23	1.584
	$\mu = 0.5$	81.6	7.87	0.29	1.585
	$\mu = 0.8$	83.4	8.45	0.37	1.586
Case 2	Δm, $\Delta J = +20\%$	37.12	8.76	0.87	1.569
	Δm, $\Delta J = -20\%$	39.43	7.37	0.74	1.573
Case 3	varying v_x	46.95	19.7	0.27	2.7342
Case 4	2^{nd} order filter	6.58	1.7	0.31	1.6218

5.8 Summary

A SMC is combined with EID and extended to a nonlinear system with matched as well as mismatched uncertainties and disturbances. The use of SMC for nominal control mitigates the need of integral action used in conventional EID based control. The designed control enforces sliding with no chatter. The SMC law is supplemented with estimate of EID to ensure robustness. The control performance is further improved by using a higher-order filter to estimate EID and its derivatives. A generalization to $k^{\mathbf{th}}$-order filter is presented.

It is proved that the ultimate boundedness of state estimation error, uncertainty estimation error and sliding variable is guaranteed; and the bounds can be lowered by appropriate choice of design parameters. The efficacy of composite control is tested for tracking of yaw-rate in an active steering control problem. The design is validated for maneuverability with varying types of uncertainties and disturbances. However the roll motion of vehicle and load variations affecting the longitudinal forces on tire and need to be considered for better vehicle stability.

Chapter 6

Discrete SMC Algorithm using UDE

The chapter details design and validation of a delta-operator based discrete SMC algorithm for uncertain systems. The control law is synthesized by estimating states and uncertainties using UDE. The design is tested for motion control problem.

The motivation and idea is introduced in section 6.1. Section 6.2 describes the problem formulation with necessary assumptions. The design of unifying sliding condition is illustrated in 6.3. Section 6.4 includes the model-following control along with uncertainty estimation. The design of observer is explained next in section 6.5. Section 6.6 elaborates the Lyapunov stability analysis. The performance is illustrated by an application to motion control in section 6.7. The chapter concludes with a summary in Section 6.8.

6.1 Introduction

The pervasive use of digital controllers has necessitated a need to generalize the concept of sliding mode to discrete-time control systems (*Misawa*, 1997a,b). The digital implementation requires a certain sampling interval, which causes not only chattering along the sliding surface but also possible instability with a large gain. The discrete systems may become unstable with a large sampling period. The performance of discrete controllers at moderate sampling periods is of importance.

In discrete-time, the control input is computed at discrete instants of time and avoid instantaneous switching. The system can thus undergo only quasi-sliding motion i.e. the state of the system can approach the switching surface but cannot generally stay on it (*Utkin*, 1977; *Sarpturk et al.*, 1987). The magnitude of quasi-sliding depends on the extent of uncertainty and sampling period (*Furuta*, 1990). A large number of control laws for discrete time sliding mode (*Bartoszewicz*, 1998; *Milosavljevic*, 1985; *Chan*, 1999; *Gao et al.*, 1995; *Yu and Yu*, 2000; *Ramirez*, 1991) have been proposed in the literature.

The delta-operator (*Middleton and Goodwin*, 1986) can be used for synthesizing a discrete-time-controller (*Jabbari*, 1991; *Collins*, 1999; *Veselic et al.*, 2008). The delta-operator approach offers attractive features like superior finite world length coefficient representation and convergence to its continuous counterpart as the sampling period decreases to zero. The issue of matching conditions in discretized systems is addressed in (*Tesfaye and Tomizuka*, 1995) and unification of sliding condition in (*Ginoya et al.*, 2015b).

The traditional SMC also requires all system states to be available. The increased number of sensors for state measurement makes overall system complex and expensive. Observer design for systems with uncertainties, disturbances and noise, is a major problem. A sliding mode observer is designed in (*Slotine et al.*, 1987) that uses additional switching terms to counter the effects of uncertainties. The problem of state observation in presence of uncertainties of known bounds is dealt in (*Walcott and Zak*, 1988). An improvement is proposed in (*Chen and Saif*, 2006). A combined state and perturbation observer for discrete-time systems is available in (*Kwon and Chung*, 2003).

In this work, continuous-time SMC combined with UDE is extended to a discrete-time case. The UDE used in combination with SMC makes it possible to use a smooth control without having to employ a smoothing approximation. A notable feature of the proposed control is that it affords control over the magnitude of the quasi-sliding for a given sampling period. A unifying sliding condition is used and control is designed for model-following. The design is robustified by designing a observer that estimates states, uncertainty and disturbance. The control design is validated on a benchmark motion control problem.

6.2 Problem Formulation

Consider a continuous-time linear plant described by,

$$\dot{x}(t) = A_c x(t) + B_c u(t) + F_c d(t) \tag{6.1}$$

where $A_c = A_{nc} + \Delta A_c, \quad B_c = B_{nc} + \Delta B_c.$, with '$nc$' as the nominal part of uncertain continuous time system, $x(t)$ is state vector, $u(t)$ is control input, $d(t)$ is unknown disturbance and ΔA_c and ΔB_c are uncertainties.

Assumption 6.1 *A_c and B_c is stabilizable and the uncertainties ΔA_c and ΔB_c satisfy matching conditions given by,*

$$\Delta A_c = B_{nc}\Delta_a \quad \Delta B_c = B_{nc}\Delta_b \quad F_c = B_{nc}\Delta_f \tag{6.2}$$

The plant in (6.1) is discretized using δ operator (*Middleton and Goodwin*, 1990) and the modified form given by *Tesfaye and Tomizuka* (1995).

The plant in (6.1) can now be written as,

$$\delta x_k = A x_k + B u_k + B(b u_k + E_k) \tag{6.3}$$

where

$$E_k = \Delta A x_k + w_k$$

$$w_k = (1 + \Delta_a B_{nc} T/2)\Delta_f d_k$$

and the system parameters are given by:

$$A = \frac{e^{A_{nc}T} - I}{T}, \quad B = \frac{1}{T}\int_0^T \frac{e^{A_{nc}\tau} - I}{T} B_{nc} d\tau \tag{6.4}$$

$$b = \Delta_a B_{nc}(1 + \Delta_b)(T/2) + \Delta_b \tag{6.5}$$

$$\Delta A = \Delta_a[I + (A_{nc} + B_{nc}\Delta_a)T/2] \tag{6.6}$$

This system can be written as

$$\delta x_k = A x_k + B u_k + B e_k \tag{6.7}$$

where e_k is the lumped uncertainty.

Remark 6.1 *Shift operator and z-transform which forms the basis of most discrete time analysis are inappropriate with fast sampling, have no continuous counterpart (Middleton and Goodwin, 1990). Better correspondence is obtained between continuous and discrete time, if the shift operator is replaced with a different operator, more like derivative.*

$$\delta = \frac{q-1}{T}$$

where T is a sampling period

$$\delta x_k = \frac{x_{k+1} - x_k}{T} \tag{6.8}$$

Remark 6.2 *Generally q leads to simpler expressions and emphasizes the sequential nature of sampled signals. On the other hand δ leads to models that are more alike models in d/dt. Using the operator δ, any polynomial in q of degree n will be exactly equivalent to some polynomial in δ of degree n.*

Assumption 6.2 *The disturbance vector d_k is such that its derivatives up to $r-th$ order are bounded. More specifically*

$$\|\delta^{(r)} e_k\| \leq \mu \quad \textit{for} \quad r \geq 0 \tag{6.9}$$

where μ is a positive constant and $\delta^{(r)} e_k$ stands for the $r-th$ derivative of e_k.

Remark 6.3 *This assumption admits a fairly large class of uncertainties. It may be noted that the constant μ is not required to be known.*

The objective is to design a discrete control (u_k) such that, the uncertain plant follows the desired model inspite of uncertainties and disturbances (e_k). The control is expected to ensure robust performance for varying cases.

The control is to be designed initially, by assuming that the plant states (x) are available. However, the issue of non-availability of states is also expected to be addressed. An observer to estimate states in presence of parametric uncertainties and disturbances is required; and UDE is to be utilized for estimation of states and disturbances. The estimated states and disturbances are to be employed to synthesize a robust discrete observer-controller structure.

6.3 Sliding Condition

Let s_k be the value of the continuous sliding variable σ at the k^{th} sampling instant and $\Delta s_k = s_{k+1} - s_k$. For sliding to occur,

$$s_{k+1}^2 < s_k^2 \tag{6.10}$$

$$s_{k+1}^2 - s_k^2 < 0 \tag{6.11}$$

Rearranging (6.11),

$$(s_{k+1} - s_k)(s_{k+1} - s_k + 2s_k) < 0 \tag{6.12}$$

The equation (6.12) can be written as,

$$\Delta s_k(\Delta s_k + 2s_k) < 0 \tag{6.13}$$

$$\Delta s_k^2 < -2s_k\Delta s_k \tag{6.14}$$

The necessary and sufficient condition for (6.14) to hold is derived.

For sliding to occur, if $s_k > 0$, then $\Delta s_k < 0$. Using this in (6.14)

$$\left.\begin{aligned} &-2s_k < \Delta s_k \\ &-2s_k < \Delta s_k < 0 \end{aligned}\right\} \tag{6.15}$$

Similarly if $s_k < 0$, then $\Delta s_k > 0$. Using this in (6.14)

$$\left.\begin{aligned} &\Delta s_k < -2s_k \\ &0 < \Delta s_k < -2s_k \\ &2s_k < -\Delta s_k < 0 \end{aligned}\right\} \tag{6.16}$$

Multiplying (6.15) by s_k and (6.16) by $-s_k$,

$$-2s_k^2 < s_k\Delta s_k < 0 \tag{6.17}$$

As $\delta s_k = \frac{\Delta s_k}{T}$ the sliding condition (6.17) can be written as,

$$\frac{-2s_k^2}{T} < s_k\delta s_k < 0 \tag{6.18}$$

Remark 6.4 *The condition (6.18) clearly shows that two conditions must be satisfied for sliding to occur in discrete time system. The condition (6.18) further collapses into the familiar $\sigma\dot{\sigma} < 0$, as the sampling time $T \to 0$.*

6.4 Model Following Control

Consider the discretized continuous system (6.7)

$$\delta x_k = Ax_k + Bu_k + Be_k \tag{6.19}$$

and the sliding surface (*Ackermann and Utkin*, 1998)

$$s_k = B^T x_k + z_k \tag{6.20}$$

where

$$\delta z_k = -B^T A_m x_k - B^T B_m u_{m_k}, \quad z_0 = -B^T x_0 \tag{6.21}$$

The choice of A_m and B_m is made in such a way that

$$\delta x_{m_k} = A_m x_{m_k} + B_m u_{m_k} \tag{6.22}$$

will have desired response, like the model in a model following system.

Assumption 6.3 *The choice of model is such that it satisfies the matching condition $A - A_m = BL$ and $B_m = BM$, where L and M are known matrices of appropriate dimensions.*

From (6.20)

$$\begin{aligned}\delta s_k &= B^T \delta x_k + \delta z_k \\ &= B^T A x_k + B^T B u_k + B^T B e_k - B^T A_m x_k - B^T B_m u_{m_k} \\ &= B^T B L x_k - B^T B M u_{m_k} + B^T B u_k + B^T B e_k\end{aligned} \tag{6.23}$$

Selecting

$$u_k = u_k^{eq} + u_k^n \tag{6.24}$$

The equivalent control (u_k^{eq}) can be derived as,

$$u_k^{eq} = -[Lx_k - Mu_{m_k}] - (B^T B)^{-1} K s_k \tag{6.25}$$

where K is positive constant.

The dynamics of sliding surface can be written as,

$$\delta s_k = (B^T B)u_k^n + (B^T B)e_k - K s_k \tag{6.26}$$

Selecting $u_k^n = -\hat{e}_k$ and using $\tilde{e}_k = e_k - \hat{e}_k$ with $\hat{e}_k \cong e_k$, the dynamics in (6.26) can be written as,

$$\delta s_k = -K s_k \tag{6.27}$$

leading to

$$s_k \delta s_k = -K s_k^2 < 0 \tag{6.28}$$

Further, if $K < \frac{2}{T}$ then discrete sliding condition

$$\frac{-2s_k^2}{T} < s_k \delta s_k < 0 \tag{6.29}$$

is satisfied for arbitrarily small values of s_k.

6.4.1 Estimation of Uncertainty (e_k)

The UDE algorithm is based on the assumption that a signal can be approximated and estimated using a filter of right bandwidth. The lumped uncertainty $e(x,u,t)$ can be estimated as, $\hat{e}(x,u,t) = G_f(s)\, e(x,u,t)$, where $G_f(s)$ is a low-pass filter with unity steady state gain and sufficiently large bandwidth.

Using (6.26),

$$e_k = (B^T B)^{-1}(\delta s_k + K s_k) - u_k^n \tag{6.30}$$

Let $G_f(\gamma)$ be unity gain digital filter with unity steady state gain, where 'γ' is the transform variable as used in (*Middleton and Goodwin*, 1990).

Using the concept of UDE,

$$\hat{e}_k = e_k G_f(\gamma) \tag{6.31}$$

Now consider a digital filter given by

$$G_f(\gamma) = \frac{1 - e^{\frac{-T}{\tau}}}{1 + T\gamma - e^{-T/\tau}} \tag{6.32}$$

which is digital equivalent of continuous filter $G_f(s) = 1/(\tau s + 1)$, in δ-domain. Therefore,

$$\hat{e}_k = [(B^T B)^{-1}(\delta s_k + K s_k) - u_k^n] G_f(\gamma) \tag{6.33}$$

$$= (B^T B)^{-1}(\delta s_k + K s_k) \tfrac{G_f(\gamma)}{1 - G_f(\gamma)} \tag{6.34}$$

$$= (B^T B)^{-1} \left(s_k + \tfrac{K}{\gamma} s_k \right) \left(\tfrac{1 - e^{-T/\tau}}{T} \right) \tag{6.35}$$

6.4.2 Improvement in Estimation – 2^{nd} order UDE

The accuracy of estimation in UDE depends on the order of filter. The results with first-order filter are extended to show that error in estimation is reduced, if a second-order filter is used.

A second-order filter in delta-form *Middleton and Goodwin* (1990) is defined as,

$$G_f(\gamma) = \frac{\gamma\alpha\tau - \gamma e^{-T/\tau} + \alpha^2\tau}{\tau(\gamma+\alpha)^2} \tag{6.36}$$

where $\alpha = \dfrac{1-e^{-T/\tau}}{T}$.

The lumped uncertainty can be written as,

$$e_k = e_k G_f(\gamma) + e_k(1 - G_f(\gamma)). \tag{6.37}$$

Using (6.36) and (6.37),

$$e_k = e_k G_f(\gamma) + e_k\Big(\frac{\gamma^2\tau + \gamma\alpha\tau + \gamma e^{-T/\tau}}{\gamma^2\tau + 2\gamma\tau\alpha + \alpha^2\tau}\Big) \tag{6.38}$$

$$= e_k G_f(\gamma) + e_k\Big(\frac{\gamma^2\tau + \gamma\alpha\tau + \gamma e^{-T/\tau}}{\tau(\gamma+\alpha)^2}\Big) \tag{6.39}$$

Simplifying the above equation leads to,

$$\begin{aligned} e_k &= e_k G_f(\gamma) + e_k\Big(\frac{\gamma\alpha\tau + \gamma e^{-T/\tau} + \gamma^2\tau}{\gamma\alpha\tau - \gamma e^{-T/\tau} + \alpha^2\tau}\Big)G_f(\gamma) \qquad (6.40) \\ &= e_k G_f(\gamma)\Big(1 + \frac{\gamma\alpha\tau + \gamma e^{-T/\tau}}{\gamma\alpha\tau - \gamma e^{-T/\tau} + \alpha^2\tau}\Big) + e_k\Big(\frac{\gamma^2\tau}{\gamma\alpha\tau - \gamma e^{-T/\tau} + \alpha^2\tau}\Big)G_f(\gamma) \end{aligned}$$

The estimation of lumped uncertainty is,

$$\hat{e}_k = e_k G_f(\gamma)\ \Big(1 + \frac{\gamma\alpha\tau + \gamma e^{-T/\tau} + \gamma^2\tau}{\gamma\alpha\tau - \gamma e^{-T/\tau} + \alpha^2\tau}\Big) \tag{6.41}$$

Using (6.30) and (6.41),

$$\hat{e}_k = \Big(1 + \frac{\gamma\alpha\tau + \gamma e^{-T/\tau}}{\gamma\alpha\tau - \gamma e^{-T/\tau} + \alpha^2\tau}\Big)G_f(\gamma)((B^TB)^{-1}(\gamma+k)s_k - u_k^n) \tag{6.42}$$

Using (6.40) and (6.41),

$$\tilde{e_k} = e_k\Big(\frac{\gamma^2\tau}{\gamma\alpha\tau - \gamma e^{-T/\tau} + \alpha^2\tau}\Big)G_f(\gamma) \tag{6.43}$$

6.4.3 Control Design

The unified controller design method using a second order filter is presented here. Selecting,

$$u_k^n = -\hat{e}_k \tag{6.44}$$

Using (6.42),

$$u_k^n = -\Big(1 + \frac{\gamma\alpha\tau + \gamma e^{-T/\tau}}{\gamma\alpha\tau - \gamma e^{-T/\tau} + \alpha^2\tau}\Big)G_f(\gamma)((B^TB)^{-1}(\gamma + k)s_k - u_k^n) \tag{6.45}$$

solving for left-hand side,

$$u_k^n\Big[1 - \Big(1 + \frac{\gamma\alpha\tau + \gamma e^{-T/\tau}}{\gamma\alpha\tau - \gamma e^{-T/\tau} + \alpha^2\tau}\Big)G_f(\gamma)\Big] \tag{6.46}$$

simplifies to,

$$= \quad u_k^n\Big[1 - \frac{2\gamma\alpha\tau + \alpha^2\tau}{\gamma^2\tau + 2\gamma\alpha\tau + \alpha^2\tau}\Big] \tag{6.47}$$

$$= \quad u_k^n\Big[\frac{\gamma^2\tau}{\gamma^2\tau + 2\gamma\alpha\tau + \alpha^2\tau}\Big] \tag{6.48}$$

Simplifying right-hand side of (6.45)

$$= -G_f(\gamma)\Big(\frac{2\gamma\alpha\tau + \alpha^2\tau}{\gamma\alpha\tau - \gamma e^{-T/\tau} + \alpha^2\tau}\Big)((B^TB)^{-1}(\gamma + k)s_k) \tag{6.49}$$

with $G_f(\gamma)$

$$= -\Big(\frac{2\gamma\alpha\tau + \alpha^2\tau}{\gamma^2\tau + 2\gamma\alpha\tau + \alpha^2\tau}\Big)((B^TB)^{-1}(\gamma + k)s_k) \tag{6.50}$$

Equating (6.47) and (6.50)

$$u_k^n(\gamma^2\tau) = -(2\gamma\alpha\tau + \alpha^2\tau)(\gamma + k)((B^TB)^{-1}s_k) \tag{6.51}$$

simplifies to control law,

$$u_k^n = -(B^TB)^{-1}\Big[2\alpha + \Big(\frac{2K\alpha + \alpha^2}{\tau} + \frac{\alpha^2 K}{\gamma^2}\Big)\Big](s_k) \tag{6.52}$$

6.5 Design of Observer

A discrete observer to simultaneously estimate the states and uncertainties is designed here using UDE.

The discrete plant and model as defined in (6.7) and (6.22) are rewritten as,

$$\left.\begin{aligned} \delta x_k &= Ax_k + Bu_k + Be_k \\ y_k &= Cx_k \end{aligned}\right\} \tag{6.53}$$

$$\left.\begin{aligned} \delta x_{m_k} &= A_m x_{m_k} + B_m u_{m_k} \\ y_{m_k} &= C_m x_{m_k} \end{aligned}\right\} \tag{6.54}$$

An observer is defined as,

$$\left.\begin{aligned} \delta \hat{x}_k &= A\hat{x}_k + Bu_k + B\hat{e}_k + J(y_k - \hat{y}_k) \\ \hat{y}_k &= C\hat{x}_k \end{aligned}\right\} \tag{6.55}$$

where, $\hat{x}, J, \hat{e}_k$ are observer state vector, observer gain matrix and estimate of the lumped uncertainty respectively.

The observation error $\tilde{x}_k = x_k - \hat{x}_k$ has an exponentially convergent dynamics as,

$$\delta \tilde{x}_k = (A - JC)\tilde{x}_k + B\tilde{e}_k \tag{6.56}$$

where, $\tilde{e}_k = e_k - \hat{e}_k$.

Assumption 6.4 *This assumption is necessary to guarantee the asymptotic stability of observer.*

1. *The pair* (A, B) *is controllable*
2. *The pair* (A, C) *is observable*
3. *The triplet* (A, C, B) *has no invariant zeros, i.e. for all* $\lambda \,\epsilon\, C$

$$\mathit{Rank}\begin{bmatrix} \lambda I - A & -B \\ C & 0 \end{bmatrix} = n + 1$$

The state estimation error dynamics are derived from (6.53), (6.55) as,

$$\begin{aligned} \delta\tilde{x}_k &= (A - JC)\tilde{x}_k + B\tilde{e}_k \\ \tilde{y}_k &= C\tilde{x}_k \end{aligned} \tag{6.57}$$

The estimation of uncertainty is defined in (6.31) as,

$$\hat{e}_k = e_k G_f(\gamma) = e_k \frac{1 - e^{-T/\tau}}{1 + T\gamma - e^{-T/\tau}} \tag{6.58}$$

where $\hat{e}_k$ is estimate of uncertainty and $G_f(\gamma)$ is discrete first order low pass filter.

Therefore,

$$\hat{e}_k + \delta\hat{e}_k - e^{-T/\tau}\hat{e}_k = e_k - e^{-T/\tau}e_k \tag{6.59}$$

$$T\delta e_k = (e_k - \hat{e}_k) - (e_k - \hat{e}_k)e^{-T/\tau} \tag{6.60}$$

From (6.53) the lumped uncertainty is written as,

$$e_k = B^+(\delta\hat{x}_k - A\hat{x}_k - Bu_k) \tag{6.61}$$

$$= B^+[J(y_k - \hat{y}_k) + B\hat{e}_k] \tag{6.62}$$

$$= \hat{e}_k + B^+JC\tilde{x}_k \tag{6.63}$$

Using (6.60) and (6.61),

$$\delta\hat{e}_k = \frac{1}{T}[B^+JC\tilde{x}_k(1 - e^{-T/\tau})] \tag{6.64}$$

Subtracting both the sides of above equation from δe_k and with Assumption 6.2,

$$\delta\tilde{e}_k = -\frac{1}{T}[B^+JC\tilde{x}_k(1 - e^{-T/\tau})] + \delta e_k \tag{6.65}$$

Therefore, combining (6.58) and (6.65)

$$\begin{bmatrix} \delta\tilde{x}_k \\ \delta\tilde{e}_k \end{bmatrix} = \begin{bmatrix} (A - JC) & B \\ \dfrac{-B^+JC}{T}(1 - e^{-T/\tau}) & 0 \end{bmatrix} \begin{bmatrix} \tilde{x}_k \\ \tilde{e}_k \end{bmatrix} + \begin{bmatrix} 0 \\ 1 \end{bmatrix} \delta e_k \tag{6.66}$$

The observer dynamics can be stabilized with proper choice of J and T, if the pair (A, C) is observable. Thus $\tilde{x}_k \to 0$ and $\tilde{e}_k \to 0$ under the Assumption 6.4 and 6.2.

6.6 Stability

The error dynamics in (6.66) can be written in a compact form as,

$$\delta\tilde{d}_k = D\,\tilde{d}_k + E\,\delta e_k \tag{6.67}$$

where, $\delta\tilde{d}_k = [\,\delta\tilde{x}_k \quad \delta\tilde{e}_k\,]\ \tilde{d}_k = [\,\tilde{x}_k \quad \tilde{e}_k\,]$. p

It is possible to select the observer gains in such a way that the eigen values of D can be placed arbitrarily in a circle with center $(-1/T, 0)$ and radius $1/T$. If the observer gains are selected such that all eigen values of D have negative real parts, one can always find a positive definite matrix P such that,

$$D^T P + PD = -Q \tag{6.68}$$

where Q is a given positive definite matrix. Let λ_d be the smallest eigen value of Q.

Defining a Lyapunov function

$$V_1(\tilde{d}_k) = \tilde{d}_k^T P \tilde{d}_k \tag{6.69}$$

and calculating $\delta V_1(\tilde{d}_k)$ along (6.67)

$$\begin{aligned}
\delta V_1(\tilde{d}_k) &= \tilde{d}_k^T(D^T P + PD)\tilde{d}_k + 2\tilde{d}_k^T PE\delta^r d_k \\
&\leq -\tilde{d}_k Q\tilde{d}_k + 2\|PE\| \cdot \|\tilde{d}_k\|\,\mu \\
&\leq -\lambda_d\|\tilde{d}_k\|^2 + 2\|PE\| \cdot \|\tilde{d}_k\|\,\mu \\
&\leq -\|\tilde{d}_k\|\,(\lambda_d\|\tilde{d}_k\| - 2\|PE\|\,\mu)
\end{aligned} \tag{6.70}$$

Thus the estimation error $\|\tilde{d}_k\|$ is bounded by $\frac{2\|PE\|\mu}{\lambda_d}$. This implies,

$$\|\tilde{x}_k\| \leq \frac{2\,\|PT\|\,\mu}{\lambda_d} \qquad \text{and} \qquad \|\tilde{e}_k\| \leq \frac{2\,\|PT\|\,\mu}{\lambda_d} \tag{6.71}$$

The ratio $\frac{\|P\|}{\lambda_d}$ depends on the choice of the eigenvalues of D. The bounds on the disturbance estimation errors can be lowered by selecting larger values for the observer gains which in turn increases the sensitivity to measurement noise. Consequently, the choice of observer gains is a matter of trade-off between the desired accuracy and the quality of measurement.

The practical stability is thus proved in the sense of *Corless and Leitmann* (1981)

6.7 Application : Motion Control

Motion control is a vital requirement in many practical applications. The critical requirement in motion control is robustness; which is concerned with tracking performance in the presence of uncertainties and disturbance. The control is expected to ensure trajectory tracking, with fast convergence.

A two axis motion control using sliding mode control and neural network is reported in (*Lin and Shen*, 2006). A variety of other strategies like extended state observer (*Talole et al.*, 2010b), adaptive back-stepping (*Lin et al.*, 2008), adaptive friction compensation (*Jing et al.*, 2014) have been proposed for robust motion control. The robustness is a major concern due to backlash, coulomb friction, uneven load distribution (*Gerdes and Kumar*, 1995; *Kolnik and Agranovich*, 2012; *Aldrich and Skelton*, 2006).

6.7.1 Dynamic Model

An industrial motion control test set-up is used to validate the designed algorithm. The set-up, industrial plant emulator (*ECP220*, 2004) includes a DC brushless servo system with a PC based control platform. The system consists of two motors, one as a drive, and other as a source of disturbance, a power amplifier and an encoder for position feedback. The inertia, friction and backlash are all adjustable. A schematic is shown in Fig. 6.1.

The drive motor is coupled via a timing belt to a drive disk with variable inertia. Another timing belt connects the drive disk to the speed reduction (SR) assembly while a third belt completes the drive train to the load disk. The load and drive disks have variable inertia which may be adjusted by moving or removing brass weights. Speed reduction is adjusted by interchangeable belt pulleys in the SR assembly. Backlash may be introduced through a mechanism incorporated in the SR assembly. A disturbance motor connects to the load disk via a 4:1 speed reduction and is used to emulate viscous friction and disturbances at the plant output. A brake below the load disk may be used to introduce coulomb friction.

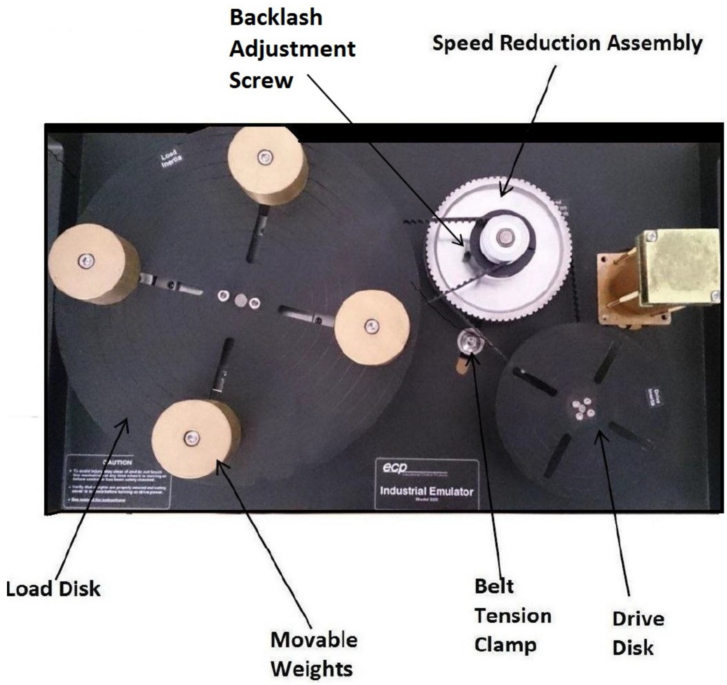

(a) Top View

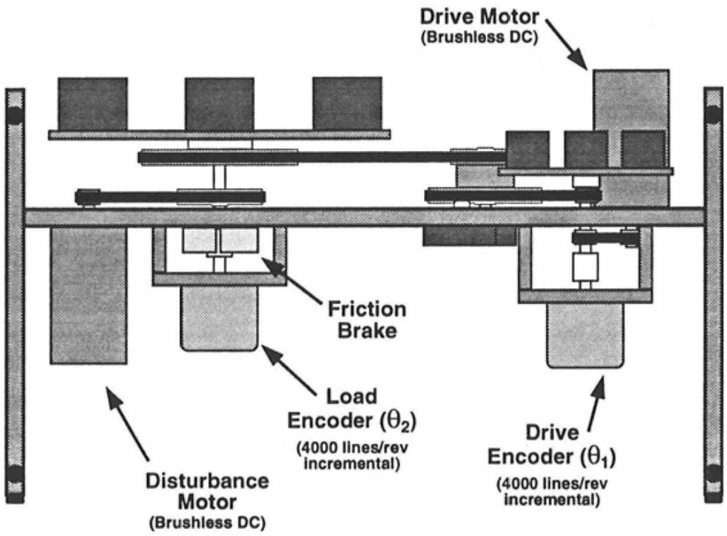

(b) Front View

Figure 6.1: ECP220 Actual Plant

In this work, a typical case is considered in which 4 brass weight, each of 500 gm is added on disturbance motor and no weight on drive motor. The gear ratio is chosen by selecting top and bottom pulley in SR assembly. In the present case the pulleys selected are with n_{pl} as 18 and n_{pd} as 72

The dynamics of industrial control test-bed can be written as in (*ECP220*, 2004),

$$J_r\ddot{\theta} + C_r\dot{\theta} \quad = \quad T_d \tag{6.72}$$

where J_r is reflected inertia at drive and C_r is reflected damping to drive. The parameter T_d is the desired torque which can be achieved suitably by selecting appropriate control voltage (u) and hardware gain (k_{hw}).

Therefore (6.72) can be rewritten as,

$$J_r\ddot{\theta} + C_r\dot{\theta} \quad = \quad k_{hw}\, u \tag{6.73}$$

The plant dynamics can be modeled in state space notation as,

$$\begin{bmatrix} \dot{x}_1 \\ \dot{x}_2 \end{bmatrix} = \begin{bmatrix} 0 & 1 \\ 0 & -\frac{C_r}{J_r} \end{bmatrix} \begin{bmatrix} x_1 \\ x_2 \end{bmatrix} + \begin{bmatrix} 0 \\ \frac{k_{hw}}{J_r} \end{bmatrix} u \tag{6.74}$$

$$y = \begin{bmatrix} 1 & 0 \end{bmatrix} \begin{bmatrix} x_1 \\ x_2 \end{bmatrix} \tag{6.75}$$

where, $[x_1 \quad x_2]^T$ are the states - position (θ) and velocity ($\dot{\theta}$), u is the control signal in volts and y is the output position in degrees.

The other parameters in (6.74) and (6.75) are,

$$C_r = C_1 + C_2\,(gr)^{-2} \tag{6.76}$$

$$gr = 6\,\frac{n_{pd}}{n_{pl}} \tag{6.77}$$

$$J_r = J_d + J_p\,(gr_{prime})^{-2} + J_l\,(gr)^{-2} \tag{6.78}$$

$$J_d = J_{dd} + m_{wd}\,(r_{wd})^2 + J_{wd_0} \tag{6.79}$$

$$J_p = J_{pd} + J_{pl} + J_{pbl} \tag{6.80}$$

$$gr_{prime} = \frac{n_{pd}}{12} \tag{6.81}$$

$$J_l = J_{dl} + m_{wl}\,(r_{wl})^2 + J_{wl_0} \tag{6.82}$$

$$J_{wl_0} = \frac{1}{2}\,m_{wl}\,(r_{wl_0})^2 \tag{6.83}$$

The details of various plant parameters are stated in Table 6.1.

Table 6.1: Parameters of industrial motion control

Symbol	Parameter	Value
C_r	Reflected damping to drive	4.08×10^{-3}
C_1	Rotary damping at load disk	0.004
C_2	Rotary damping at drive disk	0.005
gr	Drive train gear ratio	24
J_r	Reflected inertia at drive	4.63×10^{-4} kg-m²
J_d	Drive inertia	4×10^{-4} kg-m²
J_p	Inertia associated with idler pulley in SR-assembly	5.84×10^{-4} kg-m²
J_l	Load inertia	0.027125 kg-m²
$gr_{\textbf{prime}}$	Drive to SR pulley gear ratio	6
J_{dd}	Inertia of bare drive disk plus drive motor, encoder, drive disk/ motor belt and pulleys	4×10^{-4} kg-m²
m_{wd}	Weight on drive inertia	0 kg
r_{wd}	Radius of weight from middle axis of drive disk	0 m
J_{wd_0}	Inertia associated with brass weights at drive disk	0 kg-m²
J_{pd}	Drive pulley inertia	5.5×10^{-4} kg-m²
J_{pl}	Load pulley inertia	0.03×10^{-4} kg-m²
J_{pbl}	Inertia associated with backlash	0.31×10^{-4} kg-m²
n_{pd}	Number of teeth on bottom pulley of SR-assembly	72
n_{pl}	Number of teeth on top pulley of SR-assembly	18
J_{dl}	Inertia of bare load disk plus disturbance motor, encoder, load disk/ motor belt and pulleys	65×10^{-4} kg-m²
m_{wl}	Weight on load inertia	2 kg
r_{wl}	Radius of weight from middle axis of load disk	0.1 m
J_{wl_0}	Inertia associated with brass weights at load disk	6.25×10^{-4}kg-m²
r_{wl_0}	Radius of larger brass weight	0.025 m
k_{hw}	Hardware gain	5.81

6.7.2 Results

The control law is tested for model-following strategy on a industrial motion control case-study (*ECP220*, 2004). The plant dynamics are as in (6.74) with the parameters as in Table 6.1. The plant is discretized to a form as in (6.7). The structure of model to be followed is as in (6.22) with,

$$A_m = \begin{bmatrix} 0 & 1 \\ -\omega_n^2 & -2\zeta\omega_n \end{bmatrix}, \quad b_m = \begin{bmatrix} 0 \\ -\omega_n^2 \end{bmatrix} \tag{6.84}$$

The initial conditions for the plant and model are,

$$x(0) = [0 \quad 1]^T \qquad x_m(0) = [0 \quad 0]^T \tag{6.85}$$

The results are verified for model-following control with uncertainty estimated by UDE. The model parameters are $\zeta = 1$ and $\omega_n = 5$ in (6.84). The plant and model have an initial condition mismatch (6.85). The control gain is $k = 2$ and observer poles are located at $[-10 \quad -20 \quad -30]$. The reference input is a square wave of amplitude 1 and frequency 0.3 rad/sec.

Case 1: Nominal plant

The accuracy of tracking and estimation of states is illustrated in Fig. 6.2.

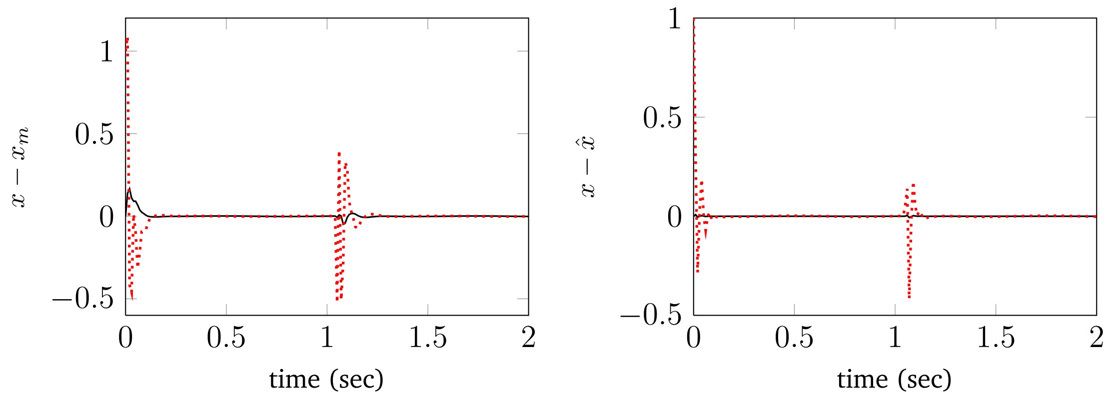

(a) model tracking error

(b) state tracking error

Figure 6.2: Model following for nominal plant

The control performance for model-following is illustrated in Fig. 6.3. The plant and model states are shown in Fig. 6.3a and 6.3a. The corresponding control effort (Fig. 6.3c) and sigma (Fig. 6.3e) are also shown..

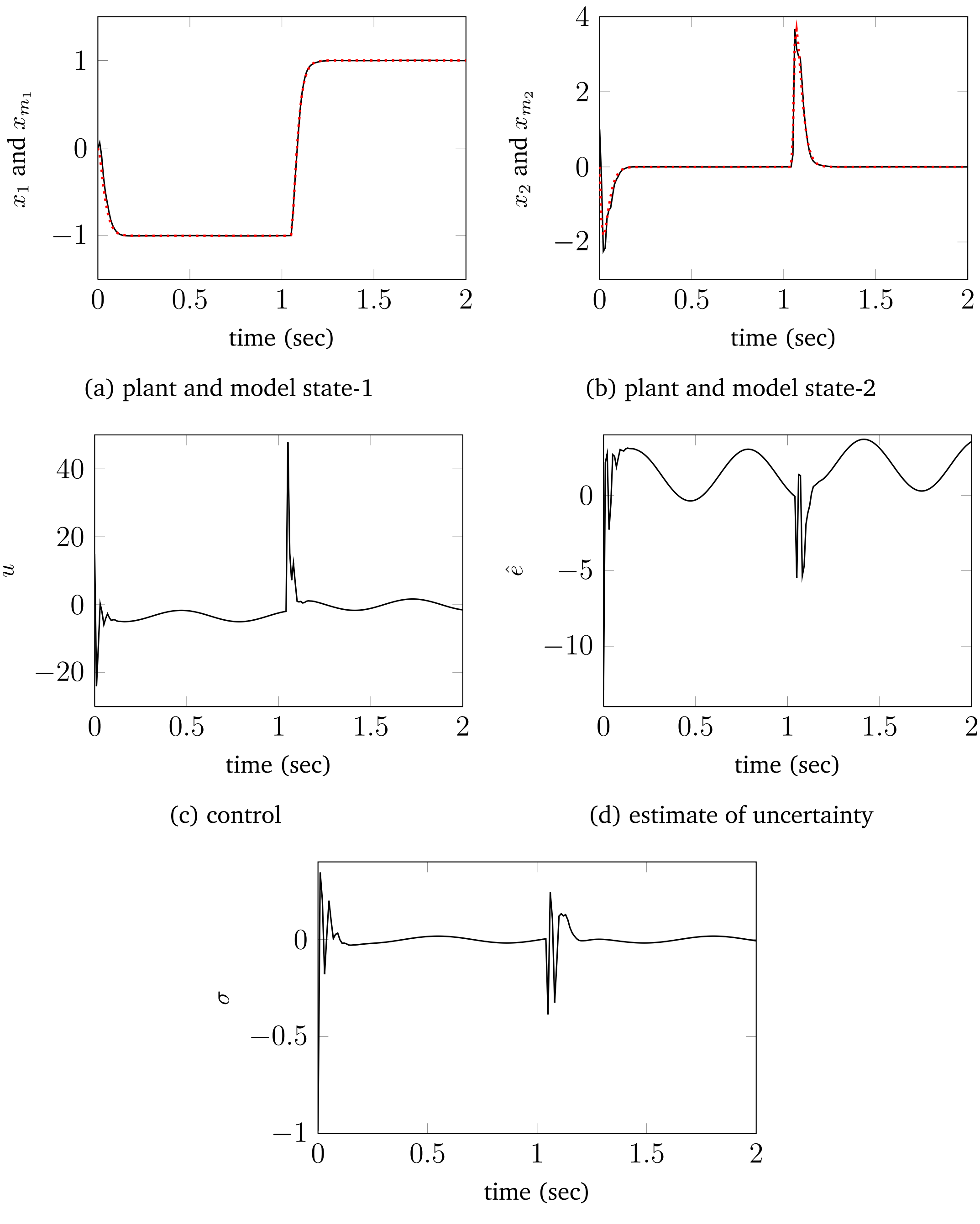

(a) plant and model state-1

(b) plant and model state-2

(c) control

(d) estimate of uncertainty

(e) sliding variable

Figure 6.3: Model following performance for nominal plant

Case 2: Effect of sampling time

The effect of sampling time is illustrated in Fig. 6.4. It is observed that the estimation and sliding width is consistent even with increase in sampling time.

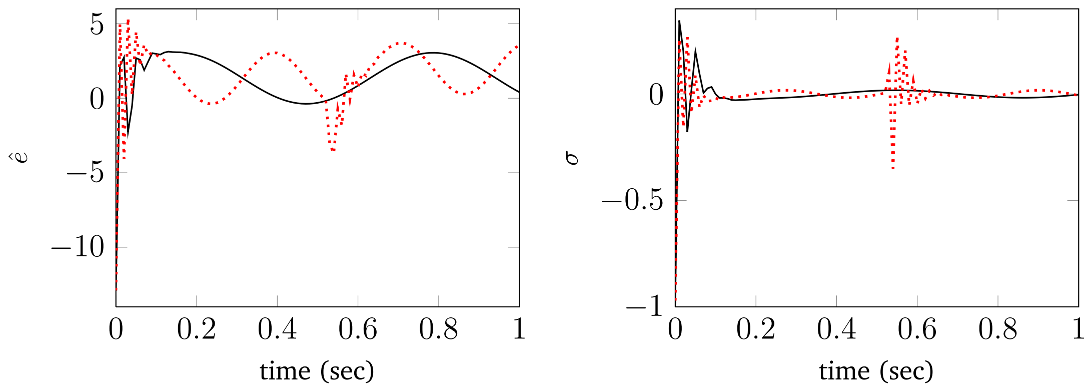

(a) estimate of uncertainty (b) sliding variable

Figure 6.4: Effect of different sampling time (10ms (solid) and 20 ms (dotted))

Case 3: Effect of filter order

The effect of filter order on estimation is illustrated in Fig. 6.5. The estimation is improved with a second order filter.

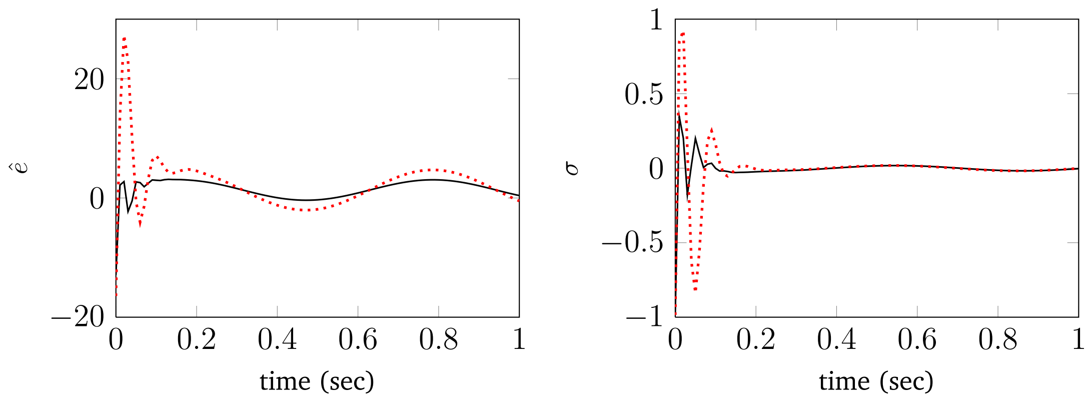

(a) estimate of uncertainty (b) sliding variable

Figure 6.5: Effect of filter order (second order (solid) and first order (dotted))

6.8 Summary

A SMC combined with UDE is extended to the discrete-time case of an uncertain system. The control law is made implementable by designing a observer to give a robust controller-observer structure in discrete domain. A notable feature of the proposed design is that, it affords control over the magnitude of the quasi-sliding for a given sampling period. The UDE enables a reduction of quasi-sliding band for a given sampling period. The sliding width is significantly reduced by using a second-order filter.

The use of δ-operator in conjunction with a new sliding condition enables complete and seamless unification of the sliding-condition, control law and UDE. It is proved that the ultimate boundedness of state estimation error, uncertainty estimation error and sliding variable is guaranteed; and the bounds can be lowered by appropriate choice of design parameters. The efficacy of design is confirmed on an application to motion control system.

Chapter 7

Conclusion

This thesis addresses some concerns and restrictions in the conventional SMC. These are tackled from theoretical as well as implementation perspective. The systems considered are all nonlinear with matched and/ or mismatched uncertainty. The estimation methods used are UDE, DO and EID.

7.1 Overall Summary

The main conclusions that result from the work presented in this thesis are broadly summarized below.

1. The method of UDE aids in mitigating the effect of chatter in conventional sliding mode. The use of UDE gives a better trade-off inside the boundary layer and this trade-off is improved by using a higher order UDE.

2. A modified sliding surface handles the problem of large initial control associated with UDE. The UDE based control enforces sliding, without using discontinuous control and without requiring any knowledge of uncertainties or their bounds.

3. The control law is made implementable by simultaneous estimation of states and uncertainties.

4. The UDE is able to compensate nonlinear uncertainty even in input vector to enable a robust SMC law. The efficacy of this design is confirmed for an inverted pendulum control.

5. The method of EID enables SMC to compensate mismatched disturbance. The integral action in conventional EID based control is avoided by the use of SMC for nominal control.

6. The method of EID is able to compensate state-dependent uncertainties. A higher-order filter facilitates improvement in the performance of EID based control.

7. The EID combined with DO can robustify the control of uncertain nonlinear systems. An extended DO is successful in improving the estimation accuracy of EID further by giving the estimate of derivatives of disturbance as well.

8. The efficacy of SMC with EID in applications for anti-lock braking system and active steering control is proved. The results prove that the system is robust to different friction models.

9. The use of δ-operator in conjunction with a new sliding condition enables complete and seamless unification of control law and UDE.

10. The UDE enables reduction of quasi-sliding band for a given sampling period. The sliding width is significantly reduced by using a second-order filter.

11. The efficacy of discrete SMC is proved for a motion control application.

12. The sliding variable, uncertainty estimation error and state estimation error are ultimately bounded in all cases. It is proved that the bounds can be lowered by appropriate choice of control parameters.

The core idea underlying all the aforementioned work is the estimation of states, uncertainty and disturbance for robust sliding mode control. The simplicity of control design supplemented by estimation capability of methods like UDE, DO and EID makes this approach an attractive proposition. The applicability of designed control to a wide range of systems shows a promise that uncertainty estimation based control techniques shall be a major topic of interest in robust control.

7.2 Recommendations for Future Work

The work in this thesis can be continued in following direction.

1. The proposed strategies need to be explored for control of under-actuated and non-minimum phase systems.

2. The proposed schemes can be designed for applications in various verticals like power converters, fuel-cells, electro-pneumatic systems, electric drives, smart structures, process control, transportation systems.

3. The proposed schemes can be further robustified by redesigning control to consider unmodeled lags, quantization effects and actuator saturation.

4. The use of nonlinear sliding surface and nonlinear DO offers interesting possibilities for applications with dual objectives.

5. The extension of proposed techniques for terminal sliding-mode and higher-order sliding mode control is also an avenue worth pursuing.

6. The implementation of proposed schemes on various digital platforms i.e. micro-controllers, digital signal processors (DSPs) and field programmable gate arrays (FPGAs) needs to be explored.

References

Acary V. and Brogliato B. Implicit euler numerical scheme and chattering-free implementation of sliding mode systems. *Systems and Control Letters*, 59(5): 284–293, 2010.

Ackermann J. and Utkin V. I. Sliding mode control design based on ackermann's formula. *IEEE Transactions on Automatic Control*, 43(2):234–237, 1998.

Aghababa M. P. and Aghababa H. P. A general nonlinear adaptive control scheme for finite-time synchronization of chaotic systems with uncertain parameters and nonlinear inputs. *Nonlinear Dynamics*, 69, 2012.

Aldrich J. B. and Skelton R. E. Backlash-free motion control of robotic manipulators driven by tensegrity motor networks. In *45th Conference on Decision and Control*, pp. 2300–2306, 2006.

Almutaitri N. B. and Zribi M. On the sliding mode control of a ball on a beam system. *Nonlinear Dynamics*, 59, 2010.

Baffet G., Charara A., and Lechner D. Estimation of vehicle sideslip, tire force and wheel cornering stiffness. *Control Engineering Practice*, 17(11):1255–1264, 2009.

Bartoszewicz A. Discrete-time quasi-sliding-mode control strategies. *IEEE Transactions on Industrial Electronics*, 45(4):633–637, 1998.

Boada B., Boada M., and Diaz V. Fuzzy-logic applied to yaw moment control for vehicle stability. *Vehicle System Dynamics*, 43(10):753–770, 2005.

Boiko I. M. Analysis of chattering in sliding mode control systems with continous boundary layer approximation of discontinous control. In *Proceedings of American Control Conference*, pp. 757–762, 2011.

Buckner G. D. Intelligent bounds on modeling uncertainty: Applications to sliding mode control. *IEEE Transactions on Systems, Man and Cybernatics - Part C: Applications and Reviews*, 32(2):113–124, 2002.

Burton J. A. and Zinobar A. S. I. Continuous approximation of variable structure control. *International Journal of Systems Science*, 17(6):875–885, 1986.

Canale M., Fagiano L., Ferrara A., and Vecchio C. Vehicle yaw control via second-order sliding mode control technique. *IEEE Transactions on Industrial Electronics*, 55(11):3908–3916, 2008.

Chan C. Y. Discrete adaptive quasi-sliding mode control. *International Journal of Control*, 72(4):365–373, 1999.

Chang J.-L. Applying discrete-time proportional integral observers for state and disturbance estimation. *IEEE Transactions on Automatic Control*, 51(5):814–818, 2006.

Chang P. H., Lee J. W., and Park S. H. Time delay observer: A robust observer for nonlinear plants. *ASME Journal of Dynamic Systems, Measurement and Control*, 119(1):521–527, 1997.

Chang P. H. and Lee J. W. An observer design for time-delay control and its application to DC servo motor. *Control Engineering Practice*, 2(2):263–270, 1994.

Chaouch D. E., Ahmed-Foitih Z., and Khelfi M. F. A self-tuning fuzzy inference sliding mode control scheme for a class of nonlinear systems. *Journal of Vibration and Control*, 18(10):1494–1505, 2011.

Chen M. S., Chen C. H., and Yang F. Y. An LTR-observer-based dynamic sliding mode control for chattering reduction. *Automatica*, 43(6):1111–1116, 2007.

Chen W. and Saif M. Novel sliding mode observer for a class of uncertain systems. In *Proceedings of American Control Conference*, Minnesota, USA, June 2006.

Chen W.-H. Nonlinear disturbance observer- enhanced dynamic inversion control of missile. *Journal of Guidance, Control, and Dynamics*, 26(1):161–166, 2003.

Chen W.-H. Disturbance observer based control for nonlinear systems. *IEEE/ASME Transactions on Mechatronics*, 9(4):706–710, 2004.

Chen W.-H., Ballance D. J., Gawthrop P. J., and OReilly J. A nonlinear disturbance observer for robotic manipulators. *IEEE Transactions on Industrial Electronics*, 47 (4):932–938, 2000.

Cheng J., Yi J., and Zhao D. Design of a sliding mode controller for trajectory tracking problem of marine vessels. *IEE Proceedings - Control Theory and Applications*, 1(1):233–237, 2007.

Choi H. H. LMI based sliding surface design for integral sliding mode control of mismatched uncertain systems. *IEEE Transactions on Automatic Control*, 52(4): 736–742, 2007.

Collins E. G. A delta operator approach to discrete-time H_∞ control. *International Journal of Control*, 72(4):315–320, 1999.

Corless M. and Leitmann G. Continuous state feedback guaranteeing uniform ultimate boundedness for uncertain dynamic systems. *IEEE Transactions on Automatic Control*, 26(5):1139–1144, 1981.

Decarlo R. A., Zak S. H., and Matthews G. P. Variable structure control of nonlinear multivariable systems: A tutorial. *Proceedings of IEEE*, 76(3):212–232, 1988.

Deshpande V. S. and Phadke S. B. Control of uncertain nonlinear systems using an uncertainty and disturbance estimator. *ASME Journal of Dynamic Systems, Measurement and Control*, 134(2):024501/1–024501/7, 2012.

Ding N. and Taheri S. An adaptive integrated algorithm for active front steering and direct yaw moment control based on direct lyapunov method. *Vehicle System Dynamics*, 48(10):1193–1213, 2010.

Drazenovic B. The invariance conditions in variable structure systems. *Automatica*, 5(3):287–295, 1969.

ECP220. *User Manual: Model 220 Industrial Plant Emulator*. Educational Control Products, Canada, 2004.

Edwards C. and Spurgeon S. *Sliding Mode Control: Theory and Applications*. Taylor & Francis, London, U.K., 1999.

Emelyanov S. V. *Theory of Variable Structure Systems*. Nauka, Moscow, 1970.

Falcone P., Tseng H. E., Borrelli F., Asgari J., and Hrovat D. MPC-based yaw and lateral stabilisation via active front steering and braking. *Vehicle System Dynamics*, 46(S1):611–628, 2008.

Fang Y. and Chow T. W. S. Chattering free sliding mode control based on recurrent neural network. In *IEEE International Conference on Systems, Man and Cybernetics*, pp. 1726–1731, 1998.

Farooq M., Wang D. B., and Dar N. U. Adaptive sliding mode hybrid/force position controller for flexible joint robot. In *Proceedings of IEEE International Conference on Mechatronix and Automation*, pp. 724–731, 2008.

Fei J. and Ding H. Adaptive sliding mode control of dynamic system using RBF neural network. *Nonlinear Dynamics*, 70, 2012.

Fridman L., Moreno J., and Iriarte R., (Eds.). *Sliding Modes after the First Decade of the 21st Century*. Lecture Notes in Control and Information Sciences, 412. Springer-Verlag, Berlin, Germany, 2011.

Fukao T., Miyasaka S., Mori K., Adachi N., and Osuka K. Active steering systems based on model reference adaptive nonlinear control. *Vehicle System Dynamics*, 42(5):301–318, 2004.

Furuta K. Sliding mode control of a discrete system. *Systems & Control Letters*, 14 (2):145–152, 1990.

Gao W., Wang Y., and Hamaifa A. Discrete time variable structure control systems. *IEEE Transactions on Industrial Electronics*, 42(2):117–122, 1995.

Gerdes J.-C. and Kumar V. An impact model of mechanical backlash for control system analysis. In *American Control Conference*, volume 5, pp. 3311–3315, 1995.

Ghorbel F., Hung H. J. Y., and Spong M. W. Adaptive control of flexible joint manipulators. *IEEE Control Systems Magazine*, 1989.

Ginoya D. L., Shendge P. D., and Phadke S. B. Sliding mode control for mismatched uncertain systems using an extended disturbance observer. *IEEE Transactions on Industrial Electronics*, 61(4):1983–1992, 2014.

Ginoya D. L., Shendge P. D., and Phadke S. B. State and extended disturbance observer for sliding mode control of mismatched uncertain systems. *ASME Journal of Dynamic Systems, Measurement and Control*, 137(7):074501–074507, 2015a.

Ginoya D. L., Shendge P. D., and Phadke S. B. Delta operator based extended disturbance observer and its applications. *IEEE Transactions on Industrial Electronics*, 62(9):5817–5828, 2015b.

Gutierrez H. M. and Rio P. I. Parametric modeling and control of a long range actuator using magnetic servo levitation. *IEEE Transactions on Magnetics*, 34(5): 3689–3695, 1998.

Gutierrez H. M. and Rio P. I. Magnetic servo levitation by sliding-mode control of nonaffine systems with algebraic input invertibility. *IEEE Transactions on Industrial Electronics*, 52(5):1449–1455, 2005.

Han J. From PID to active disturbance rejection control. *IEEE Transactions on Industrial Electronics*, 56(3):900–906, 2009.

Han M. C. and Chen Y. H. Decentralized control design: uncertain systems with strong interconnections. *International Journal of Control*, 61(6):1363–1385, 1995.

Hu B., She J.-H., and Yokoyama R. Hierarchical fault diagnosis for power systems based on equivalent-input-disturbance approach. *IEEE Transaction on Industrial Electronics*, 60(8):3529–3538, 2013.

Huang A.-C. and Chen Y.-C. Adaptive multiple-surface sliding control for non-autonomous systems with mismatched uncertainties. *Automatica*, 40(11):1939–1945, 2004.

Hung J. Y., Gao W., and Hung J. C. Variable structure control: A survey. *IEEE Transactions on Industrial Electronics*, 40(1):2–22, 1993.

Inteco. *User manual: The Laboratory Antilock Braking System Controlled from PC*, 2013.

Itkis U. *Control Systems of Variable Structure*. Wiley, New York, U.S., 1976.

Jabbari F. Lattice filters for RLS estimation of a delta operator-based model. *IEEE Transactions on Automatic Control*, 36(7):869–875, 1991.

Jia N. and Wang H. Nonlinear control of an inverted pendulum system based on sliding mode method. *Acta Analysis Functionalis Applicata*, 9(3):234–237, 2008.

Jing N., Chen Q., Ren X., and Guo Y. Adaptive prescribed performance motion control of servo mechanisms with friction compensation. *IEEE Transactions on Industrial Electronics*, 61(1):486–494, 2014.

Kanellakopoulos I., Kokotovic P. V., and Morse A. S. Systematic design of adaptive controllers for feedback linearizable systems. *IEEE Transactions on Industrial Electronics*, 36(11):1241–1253, 1991.

Kayacan E., Oniz Y., and Kaynak O. A grey system modeling approach for sliding-mode control of antilock braking system. *IEEE Transactions on Industrial Electronics*, 56(8):3244–3252, 2009.

Kiencke U. and Nielsen L. *Vehicle Modelling*. Springer, 2005.

Klier W., Reimann G., and Reinelt W. Concept and functionality of the active steering system. *SAE Paper*, 20042212:0073, 2004.

Kolhe J. P., Shaheed M., Chandar T. S., and Talole S. E. Robust control of robot manipulator based on uncertainty and disturbance estimation. *International Journal of Robust and Nonlinear Control*, 23(1):104–122, 2013.

Kolnik I. and Agranovich G. Backlash compensation for motion system with elastic transmission. In *27th Convention of Electrical and Electronics Engineers in Israel (IEEEI)*, pp. 1–5, 2012.

Koofigar H. R., Hosseinnia S., and Sheikholeslam F. Robust adaptive nonlinear control for uncertain control-affine systems and its applications. *Nonlinear Dynamics*, 56, 2009.

Krstic M., Kanellakopoulos I., and Kokotovic P. V. *Nonlinear and Adaptive Control Design*. Wiley-Interscience, New York, U.S., 1995.

Kuperman A. and Zhong Q.-C. Robust control of uncertain nonlinear systems with state delays based on an uncertainty and disturbance estimator. *International Journal of Robust and Nonlinear Control*, 21(1):79–92, 2011.

Kwon S. J. and Chung W. K. A combined synthesis of state estimator and perturbation observer. *ASME Journal of Dynamic Systems, Measurement and Control*, 125 (1):19–26, 2003.

Lee H. and Utkin V. I. Chattering suppression methods in sliding mode control systems. *Annual Reviews in Control*, 31(32):179–188, 2007.

Lei M. and Chen M.-S. Chattering reduction of sliding mode control by low-pass filtering the control signal. *Asian Journal of Control*, 12(3):392–398, 2010.

Levant A. Higher-order sliding modes, differentiation and output feedback control. *International Journal of Control*, 76(9/10):924–941, 2003.

Li S., Yang J., and Chen W. H. Generalized extended state observer based control for systems with mismatched uncertainties. *IEEE Transactions on Industrial Electronics*, 59(12):4792–4802, 2012.

Li T., Zhang S., Yang H., Zhang Y., and Zhang L. Robust missile longitudinal autopilot design based on equivalent-input-disturbance and generalized extended state observer approach. *Proceedings of IMechE, Part G: Journal of Aerospace Engineering*, 229, 2014.

Liang Y.-W., Ting L.-W., and Lin L.-G. Study of reliable control via an integral-type sliding mode control scheme. *IEEE Transactions on Industrial Electronics*, 59(8): 3062–3068, 2012.

Lin C. M. and Hsu C. F. Self-learning fuzzy sliding-mode control for antilock braking systems. *IEEE Transactions on Control Systems Technology*, 11(2):273–278, 2003.

Lin F. J., Teng L. T., and Shieh P. H. Intelligent sliding-mode control using RBFN for magnetic levitation system. *IEEE Transactions on Industrial Electronics*, 54(3): 1752–1762, 2007a.

Lin F.-J. and Shen P.-H. Robust fuzzy neural network sliding-mode control for two-axis motion control system. *IEEE Transactions on Industrial Electronics*, 53(4): 1209–1225, 2006.

Lin F.-J., Tang L.-T., and Shieh P.-H. Intelligent sliding-mode control using RBFN for magnetic levitation system. *IEEE Transactions on Industrial Electronics*, 54(3): 1752–1762, 2007b.

Lin F.-J., Shieh P.-H., and Chou P.-H. Robust adaptive backstepping motion control of linear ultrasonic motors using fuzzy neural network. *IEEE Transactions on Fuzzy Systems*, 16(3):676–692, 2008.

Liu J. K. and Sun S. F. C. Global smc with adaptive fuzzy chattering free method for nonlinear system. In *IMACS Multiconference on CESA*, pp. 541–546, 2006.

Liu R.-J., Wu M., Liu G.-P., She J.-H., and Thomas C. Active disturbance rejection control based on an improved equivalent-input-disturbance approach. *IEEE/ASME Transactions on Mechatronics*, 18(4):1410–1413, 2013.

Lu Y. S. Sliding-mode disturbance observer with switching-gain adaptation and its application to optical disk drives. *IEEE Transactions on Industrial Electronics*, 56 (9):3743–3750, 2009.

Mammar S. and Koenig D. Vehicle handling improvement by active steering. *Vehicle System Dynamics*, 38(3):211–242, 2002.

Marino R., Scalzi S., and Netto M. Nested PID steering control for lane keeping in autonomous vehicles. *Control Engineering Practice*, 19(12):1459–1467, 2011.

Middleton R. H. and Goodwin G. C. Improved finite word length characteristics in digital control using delta operator. *IEEE Transactions on Automatic Control*, AC-31(11):1015–1021, 1986.

Middleton R. H. and Goodwin G. C. *Digital Control and Estimation: A Unified Approach*. Prentice Hall, New Jersy, U.S., 1990.

Milosavljevic C. General conditions for the existence of a quasi-sliding mode on the switching hyperplane in discrete variable structure systems. *Automation and Remote Control*, 46(3):307–314, 1985.

Mirzaei A., Moallem M., Dehkordi B. M., and Fahimi B. Design of an optimal fuzzy controller for antilock braking systems. *IEEE Transactions on Vehicular Technology*, 55(6):1725–1730, 2006.

Mirzaeinejad H. and Mirzaei M. A novel method for non-linear control of wheel slip in anti-lock braking systems. *Control Engineering Practice*, 18:918–926, 2010.

Misawa E. A. Discrete time sliding mode control: The linear case. *ASME Journal of Dynamic Systems, Measurement and Control*, 119(1):819–821, 1997a.

Misawa E. A. Discrete-time sliding mode control for nonlinear systems with unmatched uncertainties and uncertain control vector. *ASME Journal of Dynamic Systems, Measurement and Control*, 119(3):503–512, 1997b.

Molero R., Roca J., Separovich D., Rojas J., Montes M., and N. Cuellar N. Nonlinear control of an electromagnetic system based on exact linerization and sliding mode control. *Mechanics Based Design of Structures and Machine*, 36:426–445, 2008.

Nam K., Oh S., Fujimoto H., and Hori Y. Estimation of sideslip and roll angles of electric vehicles using lateral tire force sensors through RLS and kalman filter approaches. *IEEE Transactions on Industrial Electronics*, 60(3):988–1000, 2013.

Oh J. H. and Lee J. Control of flexible joint robot system by back-stepping design. In *Proceedings of IEEE International Conference on Robotics and Automation*, pp. 3435–3440, 1997.

Pacejka H. *Tyre and vehicle dynamics*. Elsevier, 2005.

Pasillas-Lépine W., Loría A., and Gerard M. Design and experimental validation of a nonlinear wheel slip control algorithm. *Automatica*, 48:1852–1859, 2012.

Phadke S. B. and Talole S. E. Sliding mode and inertial delay control based missile guidance. *IEEE Transactions on Aerospace & Electronic Systems*, 48(4):3331–3346, 2012.

Potluri R. Comments on chattering free robust control for nonlinear systems. *IEEE Transactions on Control System Technology*, 20(2):562, 2012.

Poursamad A. Adaptive feedback linearization control of antilock braking systems using neural networks. *Mechatronics*, 19:767–773, 2009.

Quanser. *User manual: Rotary flexible joint*. Canada, 2008.

Rajamani R. *Vehicle Dynamics and Control*. Springer, 2011.

Rajamani R., Phanomchoeng G., Piyabongkarn D., and Lew J. Algorithms for real-time estimation of individual wheel tire-road friction coefficients. *IEEE/ASME Transactions on Mechatronics*, 17(6):1183–1195, 2012.

Rajapakse N. I., Happawana G. S., and Hurmuzlu Y. Suppression of base vibrations and tracking of the tip of an inverted pendulum using sliding mode control and quantitative feedback theory. *Proceedings of IMechE, Part I: Journal of Systems and Control Engineering*, 221(5):673–685, 2007.

Ramirez H. S. Nonlinear discrete variable structure systems in quasi-sliding mode. *International Journal of Control*, 54(5):1171–1187, 1991.

Sabanovic A. Variable structure systems with sliding modes in motion control – A survey. *IEEE Transactions on Industrial Informatics*, 7(2):212–223, 2011.

Sarpturk S. Z., Istefanopulos Y., and Kaynak O. On the stability of discrete-time sliding mode systems. *IEEE Transactions on Automatic Control*, 32(10):930–932, 1987.

She J.-H. and Xin X. Equivalent-input-disturbance method improves disturbance rejection performance: The MIMO case. In *Proceedings of the 26th Chinese Control Conference*, pp. 642–647, Zhangjiajie, Hunan, China, July 2007.

She J.-H., Xin X., and Ohyama Y. Estimation of equivalent input disturbance improves vehicular steering control. *IEEE Transactions on Vehicular Technology*, 56 (6):3722–3731, 2007.

She J.-H., Fang M., Ohyama Y., Hashimoto H., and Wu M. Improving disturbance-rejection performance based on an equivalent-input-disturbance approach. *IEEE Transactions on Industrial Electronics*, 55(1):380–389, 2008.

She J.-H., Xin X., and Pan Y. Equivalent-input-disturbance approach - analysis and application to disturbance rejection in dual-stage feed drive control system. *IEEE/ASME Transactions on Mechatronics*, 16(2):330–340, 2011.

She J.-H., Zhang A., Lai X., and Wu M. Global stabilization of 2-DOF underactuated mechanical systems - an equivalent-input-disturbance approach. *Nonlinear Dynamics*, 69(1-2):495–509, 2012.

She J.-H., Makino K., Ouyang L., Hashimoto H., Murakoshi H., and Wu M. Estimation of normalized longitudinal force for an electric cart using equivalent-input-disturbance approach. *IEEE Transactions on Vehicular Technology*, 63(8): 3642–3650, 2014.

Shendge P. D. and Patre B. M. Robust model following load frequency sliding mode controller based on ude and error improvement with higher order filter. *IAENG International Journal of Applied Mathematics*, 37(1):216–221, 2007.

Shi Z., Legate I., Gu F., Fieldhouse J., and Ball A. Prediction of antiloc braking system condition with the vehicle statinary using a model-based approach. *International Journal of Automotive Technology*, 11(3):363–373, 2010.

Slotine J. J. E. and Coetsee J. A. Adaptive sliding controller synthesis for non-linear systems. *International Journal of Control*, 43(6):1631–1651, 1986.

Slotine J. J. E. and Sastry S. S. Tracking control of nonlinear systems using sliding surfaces with applications to robot manipulator. *International Journal of Control*, 38(2):465–492, 1983.

Slotine J. J. E., Hedrick J. K., and Misawa E. A. On sliding observers for nonlinear systems. *ASME Journal of Dynamic Systems, Measurement and Control*, 109(1): 245–252, 1987.

Slotine J.-J. E. and Li W. *Applied Nonlinear Control*. Prentice Hall, New York, U.S., 1991.

Song J., Kim H., and Boo K. A study on an anti-lock braking system controller and rear-wheel controller to enhance vehicle lateral stability. *Proceedings of The Institution of Mechanical Engineers, Part D: Journal of Automobile Engineering*, 221:777–787, 2007.

Stobart R. K., Kuperman A., and Zhong Q.-C. Uncertainty and disturbance estimator-based control for uncertain LTI-SISO system with state delays. *ASME Journal of Dynamic Systems, Measurement and Control*, 133(2):024502/1–024502/6, 2011.

Talole S. E. and Phadke S. B. Model following sliding mode control based on uncertainty and disturbance estimator. *ASME Journal of Dynamic Systems, Measurement and Control*, 130(3):034501/1–034501/5, 2008.

Talole S. E. and Phadke S. B. Robust input-output linearisation using uncertainty and disturbance estimation. *Int. Journal of Control*, 82(10):1794–1803, 2009.

Talole S. E., Kolhe J. P., and Phadke S. B. Extended state observer based control of flexible joint system with experimental validation. *IEEE Transactions on Industrial Electronics*, 57(4):1411–1419, 2010a.

Talole S., Kolhe J. P., and Phadke S. B. Extended-state-observer-based control of flexible-joint system with experimental validation. *IEEE Transactions on Industrial Electronics*, 57(4):1411–1419, 2010b.

Tao C. W., Chan M. L., and Lee T. T. Adaptive fuzzy sliding mode controller for linear systems with mismatched time-varying uncertainties. *IEEE Transactions on Systems, Man and Cybernetics, Part B: Cybernetics.*, 33(2):283–294, 2003.

Tesfaye A. and Tomizuka M. Robust control of discretized continuous systems using the theory of sliding modes. *International Journal of Control*, 62(1):209–226, 1995.

Trench W. F. *Introduction to Real Analysis*. Pearson, New Jersey, 2003.

Utkin V. I. *Sliding Mode in Control and Optimization*. Springer-Verlag, Berlin, Germany, 1992.

Utkin V. I. Variable structure systems with sliding modes. *IEEE Transactions on Automatic Control*, Acc-22(2):212–222, 1977.

Utkin V. I. and Lee H. Chattering problems in sliding mode control systems. In *Proc. of IEEE Int. Workshop on Variable Structure Systems*, pp. 346–350, Alghero, Italy, 2006.

Veselic B., Perunicic-Drazenovic B., and Milosavljevic C. High-performance position control of induction motor using discrete-time sliding-mode control. *IEEE Transactions on Industrial Electronics*, 55(11):3809–3817, 2008.

Walcott B. L. and Zak S. H. Combined observer controller synthesis for uncertain dynamical systems with applications. *IEEE Transactions on Systems, Man and Cybernetics*, 18(1):88–104, 1988.

Wang W. Y., Li I.-H., Chen M. C., Su S. F., and Hsu S. B. Dynamic slip-ratio estimation and control of antilock braking systems using an observer-based direct adaptive fuzzy-neural controller. *IEEE Transactions on Industrial Electronics*, 56 (5):1746–1756, 2009.

Wen C.-C. and Cheng C.-C. Design of sliding surface for mismatched uncertain systems to achieve asymptotical stability. *Journal of the Franklin Institute*, 345 (8):926–941, 2008.

Wheeler G., Su C. Y., and Stepanenko Y. A sliding mode controller with improved adaptation laws for the upper bounds on the norm of uncertainties. *Automatica*, 34(12):1657–1661, 1998.

Won M. and Hedrick J. K. Multiple-surface sliding control of a class of uncertain nonlinear systemsm. *International Journal of Control*, 64(4):693–706, 1996.

Wu M. C. and Shih M. C. Using the sliding mode PWM method in an antilock braking system. *Asian Journal of Control*, 3(3):255–261, 2001.

Xu Y. Chattering free robust control for nonlinear systems. *IEEE Transactions on Control System Technology*, 16(6):1352–1359, 2008.

Yamaguchi Y. and Murakami T. Adaptive control for virtual steering characteristics on electric vehicle using steer-by-wire system. *IEEE Transactions on Industrial Electronics*, 56(5):1585–1594, 2009.

Yang J., Chen W. H., and Li S. Nonlinear disturbance-observer based robust control for systems with mismatched disturbances/uncertainties. *IET Control Theory Applications*, 5(18):2053–2062, 2011a.

Yang J., Li S., and Chen W. H. Nonlinear disturbance-observer based control for multi-input multi-output nonlinear systems subject to mismatching condition. *International Journal of Control*, 85(8):1071–1082, 2012a.

Yang J., Li S., and Chen W. H. Nonlinear disturbance observer-based control for multi-input multi-output nonlinear systems subject to mismatching condition. *International Journal of Control*, 85(8):1071–1082, 2012b.

Yang J., Li S., and Yu X. Sliding-mode control for systems with mismatched uncertainties via a disturbance observer. *IEEE Transactions on Industrial Electronics*, 60 (1):160–169, 2013.

Yang Y., Wang Z., and Peng W. Coordinated control of AFS and DYC for vehicle handling and stability based on optimal guaranteed cost theory. *Vehicle System Dynamics*, 47(1):57–79, 2009.

Yang Z.-J., Hara S., Kanae S., and Wada K. Robust output feedback control of nonlinear systems using a disturbance observer. *IEEE Transactions on Control Systems Technology*, 19(2):256–268, 2011b.

Yoo D. S. and Chung M. J. A variable structure control law with simple adaptation laws for upper bounds on the norm of uncertainties. *IEEE Transactions on Automatic Control*, 37(6):159–165, 1992a.

Yoo D. S. and Chung M. J. A variable structure control law with simple adaptation laws for upper bounds on the norm of uncertainties. *IEEE Transactions on Automatic Control*, 37(6):159–165, 1992b.

Youcef-Toumi K. and Ito O. A time delay controller for systems with unknown dynamics. *ASME Journal of Dynamic Systems, Measurement and Control*, 112(1): 133–142, 1990.

Young K. D., Utkin V. I., and Ümit Özgüner. A control engineers guide to sliding mode control. *IEEE Transactions on Control Systems Technology*, 7(3):328–342, 1999.

Yu X. and Yu S. Discrete sliding mode control design with invariant sliding sectors. *ASME Journal of Dynamic Systems, Measurement and Control*, 122:776–782, 2000.

Zhang H. and Wang J. Vehicle lateral dynamics control through AFS/DYC and robust gain-scheduling approach. *IEEE Transactions on Vehicular Technology*, 2015.

Zhang H., Zhang X., and Wang J. Robust gain- scheduling energy-to-peak control of vehicle lateral dynamics stabilisation. *Vehicle System Dynamics*, 52(3):309–340, 2014.

Zhang J., Shi P., and Xia Y. Robust adaptive sliding-mode control for fuzzy systems with mismatched uncertainties. *IEEE Transactions on Fuzzy Systems*, 18(4):700–711, 2010.

Zhong Q.-C. and Rees D. Control of uncertain LTI systems based on an uncertainty and disturbance estimator. *ASME Journal of Dynamic Systems, Measurement and Control*, 126(4):905–910, 2004.

Publications

[1] **Prasheel V. Suryawanshi**, P. D. Shendge, S. B. Phadke "Robust Sliding Mode Control for a Class of Nonlinear Systems using Inertial Delay Control", in *Nonlinear Dynamics: Springer*, Vol. 78, No. 3, pp. 1921-1932, 2014.

[2] **Prasheel V. Suryawanshi**, P. D. Shendge, S. B. Phadke "A Boundary Layer Sliding Mode Control Design for Chatter Reduction using Uncertainty and Disturbance Estimator", in *International Journal of Dynamics and Control: Springer*, DOI: 10.1007/s40435-015-0150-9.

[3] P. D. Shendge, **Prasheel V. Suryawanshi**, "Sliding Mode Control for Flexible Joint using Uncertainty and Disturbance Estimation", in *Proc. of the World Congress on Engineering and Computer Science*, Vol. I, pp. 216-221, San Francisco, USA, October 2011

Papers under Review

[1] **Prasheel V. Suryawanshi**, P. D. Shendge, S. B. Phadke "Improving the performance of Equivalent Input Disturbance based Control with a Higher-Order Filter", in *IEEE Transactions on Industrial Electronics*.

[2] **Prasheel V. Suryawanshi**, P. D. Shendge, S. B. Phadke "Sliding Mode Control for Mismatched Uncertain Systems using Equivalent Input Disturbance Method", in *IEEE Transactions on Control System Technology*.

[3] **Prasheel V. Suryawanshi**, P. D. Shendge, S. B. Phadke “Yaw-rate Control in Active Steering using Equivalent Input Disturbance Method”, in *IEEE Transactions on Industrial Informatics*.

[4] **Prasheel V. Suryawanshi**, P. D. Shendge, S. B. Phadke “A Robust Observer for Control of Uncertain Nonlinear Systems using Uncertainty and Disturbance Estimator”, in *Transactions of Institute of Measurement and Control*.

[5] **Prasheel V. Suryawanshi**, P. D. Shendge, S. B. Phadke “Discrete Uncertainty and Disturbance Estimator using Delta operator with Application in Sliding Mode Control”, in *International Journal of Robust and Nonlinear Control*.

Acknowledgment

Department of Instrumentation & Control Engg. where knowledge is considered as wealth and it is proved that the powers of mind are like the rays of sun; when concentrated, they illume.

First and foremost, I express my gratitude towards my advisor, Prof. P. D. Shendge who kindly consented to act as my guide, and enabled me to complete the thesis. This work would not have seen light of the day without the active involvement of our control guru, Prof. S. B. Phadke. I cannot thank both of them enough; their patience, energy, and an almost contagious positive attitude are largely responsible for a timely and enjoyable completion of this assignment. Both of them have been a pillar of great strength, motivation and commitment.

I owe my sincere gratitude to Prof. S. L. Patil and Prof. C. Y. Patil, past and present HoD for helping me in pulling out of critical situations. Their contribution is really appreciated and at times they have gone out-of-the-way to just help me. I would also like to profoundly thank Prof. V. S. Bandal for his critical comments and advice during progress presentations. I appreciate his enlightening guidance; especially his pursuit for the perfect work will help me in the long run.

I also sincerely acknowledge the inspiration and co-operation from my co-researcher, Divyesh Ginoya and other students at Advanced Control Lab. who have directly or indirectly helped me in the course of my work.

I am also grateful to Department of Atomic Energy for the funding and technical support of this research. A word of special mention to Ashitosh, who has been rock-steady for the past 3 years and has helped me focus on the task at hand, by mitigating my burden in regular chores.

I acknowledge with utmost sincerity and humility, the imperative contribution of my parent institution MITAOE Alandi in the completion of this work. A word of special thanks to our Executive Director, Dr. Sunil Karad will not be out of place for the faith he put in me and for being such a steady source of inspiration. MITAOE has provided me with a amazing group of colleagues in Aniket, Kaliprasad, Amit, Shailesh, Sandip, Ashish, Smita, Kavita, who have directly or indirectly contributed in the completion of this work.

I am appreciative of my wife, Dipti and my life, Archit who have always been around when things looked bleak, and have been very supportive through the crests and troughs in all these years. A special thanks to my parents, without whose love and support, I probably would not have reached this far.

Last but certainly not least, I would like to thank all my teachers at various levels of my education, from whom I have gained more than just academic knowledge. They have positively influenced, and shaped my ideas and made me a better person.

Prasheel V. Suryawanshi

MIS No. 131109003

A SMALL DOT CAN STOP
A BIG SENTENCE,

BUT FEW MORE DOTS .....
CAN GIVE A CONTINUITY

EVERY ENDING CAN BE A NEW
BEGINNING